Calix[4]arene modified carbon electrodes as a route to asymmetric electrochemical synthesis

By

James Peter Buttress

A doctoral thesis submitted in accordance with the requirements of the degree of Doctor of Philosophy (PhD) from the University of East Anglia, Department of Chemistry.

September 2016

I Abstract

Key words: Electrosynthesis, Calix[4]arenes, Surface modification, Enantioselective synthesis, Click chemistry.

This thesis explores a route towards the enantioselective electrochemical reduction of prochiral starting materials using glassy carbon electrodes modified with chiral calix[4]arenes. The research is divided into three chapters:

The first chapter discusses the synthesis of novel double-sided, “Janus” calix[4]arenes that have four molecular tethering sites. These allowed for the immobilisation of the macrocycle onto the electrode surface by either the upper or lower rim; whilst the opposite face of the calix[4]arene was appropriately functionalised to facilitate its decoration with a wide array of substrates.

The second chapter examines the immobilisation process required to fix the calix[4]arenes onto the electrode surface and the subsequent characterisation of these modified materials by both electrochemical and X-ray photoelectron spectroscopy analysis. This section also demonstrates the ease by which these functionalised materials can be further customised whilst immobilised onto the electrode surface.

The third and final part of this thesis describes attempts to use these tailored electrodes for the electrochemical reduction of prochiral ketones and compares these results to those obtained using unmodified surfaces.

II Acknowledgements

I have been very fortunate to have so many kind and wonderful people help me throughout my PhD, so if I have missed anyone out I am sorry but if you remind me I will happily buy you a beer!

Firstly, I would like to thank Phil Page and Gregory Wildgoose for giving me this great opportunity, for allowing me the use their laboratories and by some miracle being able to put up with me for the past four years. I would also like to thank all of the people that have worked alongside me in these laboratories and all the kind people in the chemistry department, especially those of you who have made coffee on Mondays.

I would like to thank the Wildgoose group members for all the assistance they have given me over the past years, especially when it comes to the cleaning of my dirty glassware. Robin Blagg for the wonderfully designed labels presented throughout the lab and for the writing up of the crystallographic data in section **6.8**. Elliot Lawrence for agreeing to proof read my wonderful thesis… you are welcome (but seriously thank you very much!). I would also like to thank James Courtney for always being prepared to confuse me with electrochemical theory and Ellion Bennett for the delicious array of snacks that were always available in his snack draw. I would also like to thank Francesca Kinsey and Quail Eggs (Jamie Martin) for being there for me when the chemistry got too much and a quick escape to the pub was required. A lot of gratitude also goes out to Amanda Chang who managed to keep me relatively sane throughout the later stages of my PhD, including the writing of my thesis.

These acknowledgements would not be complete without remembering Sarah Delf who would have been completing her PhD at the same time as me. Sarah was tragically taken away from us last year and her presence is sorely missed throughout the department.

Finally I would also like to thank my Mum, Dad and Sister for their constant support throughout my thesis and my life, without their guidance and friendship I would not be where I am now.

This thesis is dedicated to the memory of my Nan (Alice Buttress) and Granddad (Ernest Buttress) who I miss very dearly and will always have a place in my heart.

III Table of contents

IV List of figures

V List of schemes

VI List of tables

VII List of equations

VIII List of abbreviations

Ac	–	Acetate
AcOH	–	Acetic acid
aq	–	Aqueous
Ar	–	Aryl/Aromatic
atm	–	Atmospheric pressure
B	–	Base
BINAP	–	2,2'-Bis(diphenylphosphino)-1.1'-binaphthyl
BINOL	–	1,1'-Bi-2-naphthol
Bu	–	Butyl
BuLi	–	Butyl lithium
Cat.	–	Catalyst
ca.	–	Circa
CuAAC	–	Copper(I)-catalysed-azide-alkyne cycloaddition
COD	–	1,5-Cyclooctadiene
Cp	–	Cyclopentadienyl
d.r.	–	Diastereomeric ratio
DCM	–	Dichloromethane
DOSY	–	Diffusion-ordered NMR spectroscopy
DOPA	–	3,4-Dihydroxyphenylalanine
DMSO	–	Dimethyl sulfoxide
DMF	–	Dimethylformamide

d	–	Down
e.e.	–	Enantiomeric excess
Equiv	–	Equivalent
et al.	–	Et alii
etc.	–	Etcetera
EtOH	–	Ethanol
Et	–	Ethyl
EDTA	–	Ethylenediaminetetraacetic acid
e.g.	–	Exempli gratia
GCE	–	Glassy carbon electrode
HPLC	–	High performance liquid chromatography
HRMS	–	High resolution mass spectrometry
HCl	–	Hydrogen chloride
i.e.	–	Id est
IR	–	Infrared
IUPAC	–	International Union of Pure and Applied Chemistry
MeI	–	Iodomethane
LDA	–	Lithium diisopropylamide
MS	–	Mass spectrometry
Me	–	Methyl
NMR	–	Nuclear magnetic resonance
Nu	–	Nucleophile
ppm	–	Parts per million

PEEK	–	Polyether ether ketone
PVC	–	Polyvinyl chloride
TBDMS	–	*Tert*-butyldimethylsilyl
THF	–	Tetrahydrofuran
TBAF	–	Tetra-*n*-butylammonium Fluoride
TLC	–	Thin layer chromatography
TFA	–	Trifluoroacetic acid
u	–	Up
vs.	–	Versus
v	–	Wavenumbers (cm^{-1})
XPS	–	X-ray photoelectron spectroscopy

Electrochemical abbreviations

T	–	Absolute temperature (K)
γ_x	–	Activity co-efficient of species X
A	–	Area of electrode (cm^{-2})
ΔG	–	Change in Gibbs free energy ($J\ mol^{-1}$)
$\Delta G^{\neq}$	–	change in Gibbs free energy of activation ($J\ mol^{-1}$)
Q	–	Charge passed (C)
α	–	Charge transfer coefficient
CA	–	Chronoamperometry
C	–	Concentration ($mol\ dm^{-3}$)
[X]	–	Concentration of species X ($mol\ dm^{-3}$)

i	–	Current (A)
CV	–	Cyclic Voltammetry
D	–	Diffusion coefficient (cm^2 s-1)
φ	–	Electrical potential (V)
E	–	Electrode potential (V)
F	–	Faradays constant (96485.3 C mol^{-1})
j	–	flux (mol cm^2 s^{-1})
R	–	Gas constant (8.314 J K^{-1} mol^{-1})
G	–	Gibbs free energy (J mol^{-1})
GC	–	Glassy carbon
m	–	Gradient of Randles-Sevcik plots (A $s^{1/2}$ $V^{-1/2}$)
LSV	–	Linear sweep voltammetry
n	–	Number of electrons involved in redox event
η	–	Overpotential (V)
k_{ox}	–	Oxidative electrochemical rate constant (cm s^{-1})
i_p	–	Peak current (A)
k_{red}	–	Reductive electrochemical rate constant (cm s^{-1})
v	–	Scan rate (V s^{-1})
SCE	–	Standard calomel electrode
k^0	–	Standard electrochemical rate constant (cm s^{-1})
Γ	–	Surface concentration (mol cm^2)
t	–	Time (s)
VSR	–	Variable scan rate

IX Table of compounds

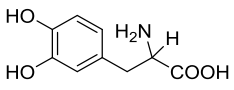

1

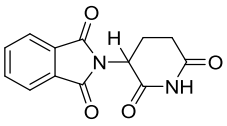

2

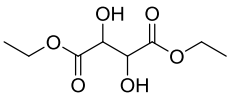

3

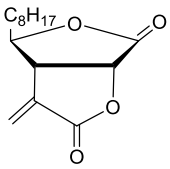

4

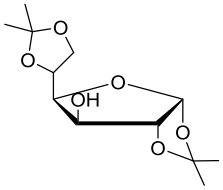

5

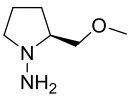

6

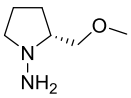

7

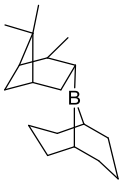

8

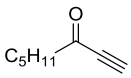

9

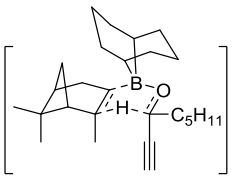

10

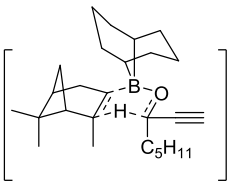

11

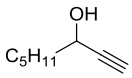

12

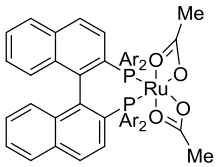

13

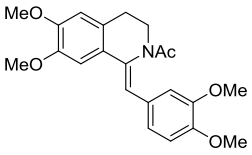

14

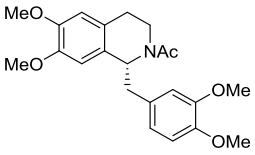

15

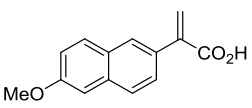

16

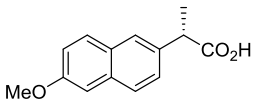

17

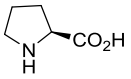

18

19

20

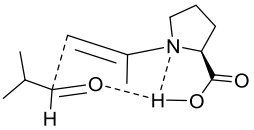

21

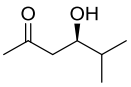

22

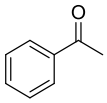

23

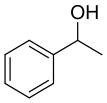

24

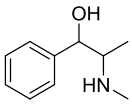

25

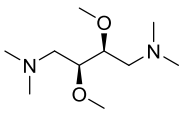

26

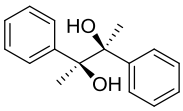

27

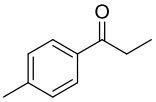

28

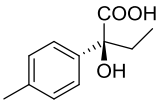

29

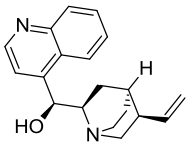

30

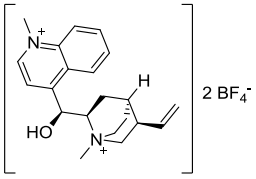

31

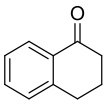

32

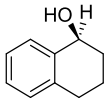

33

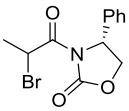

34

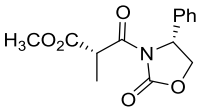

35

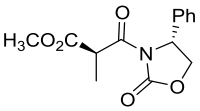

36

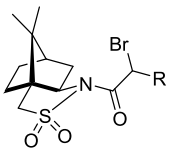

37

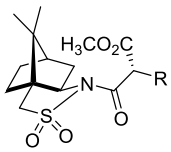

38

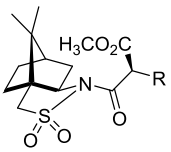

39

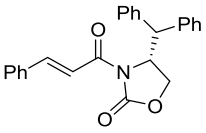

40

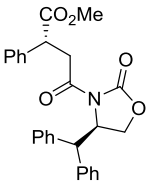

41

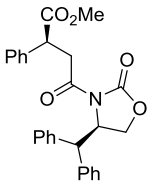

42

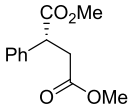

43

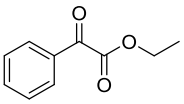

44

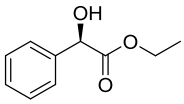

45

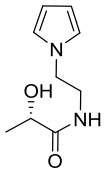

46

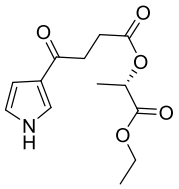

47

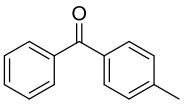

48

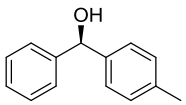

49

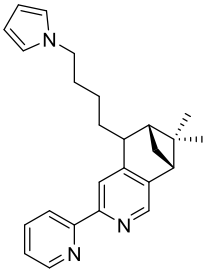

50

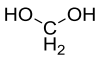

51

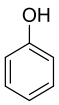

52

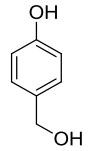

53

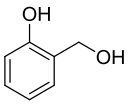

54

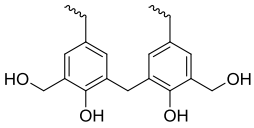

55

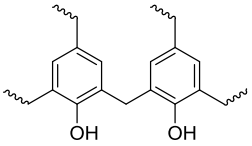

56

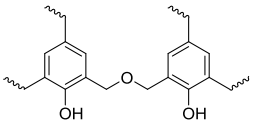

57

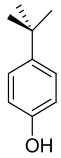

58

59

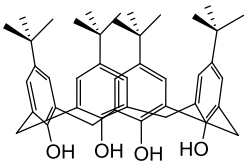

60

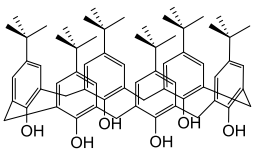

61

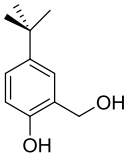

62

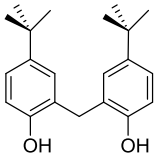

63

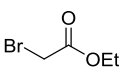

64

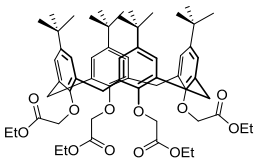

65

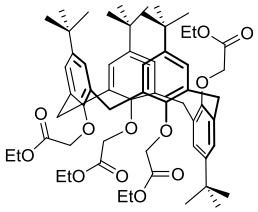

66

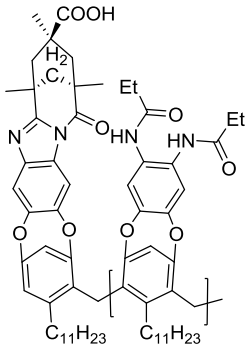

67

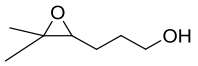

68

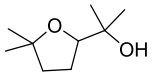

69

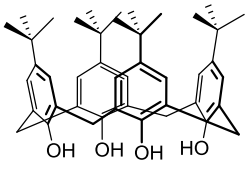

70

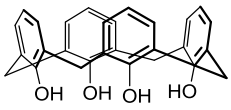

71

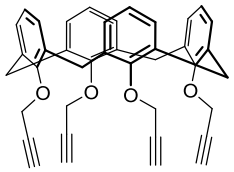

72

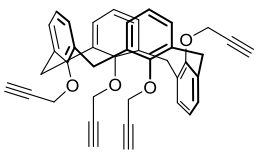

73

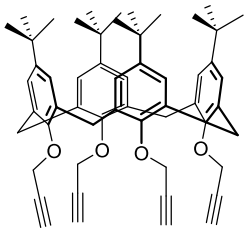

74

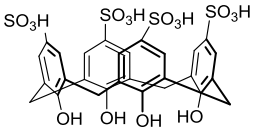

75

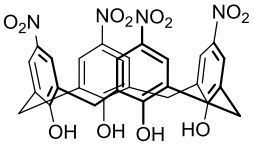

76

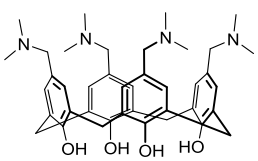

77

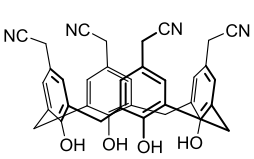

78a

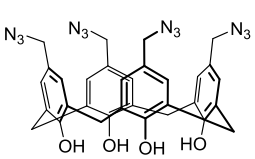

78b

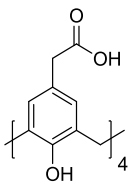

79

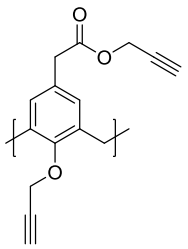

80

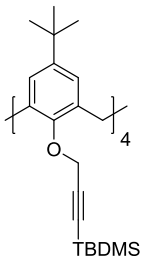

81

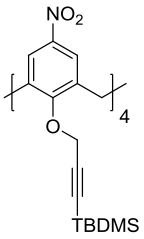

82

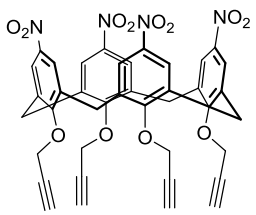

83

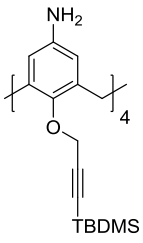

84

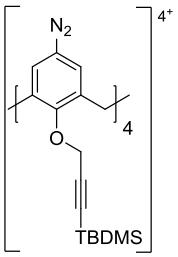

85

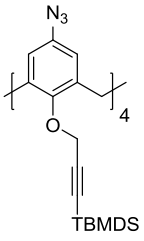

86a

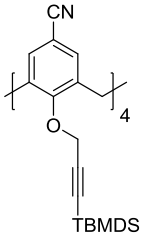

86b

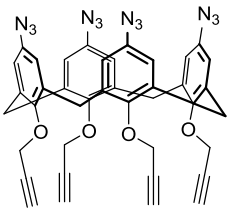

87

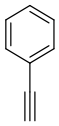

88

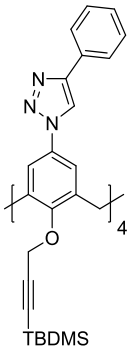

89

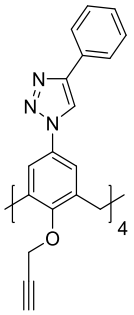

90

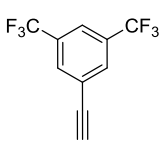

91

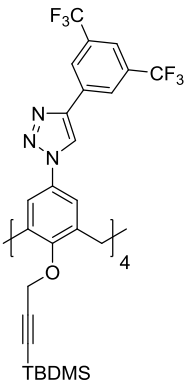

92

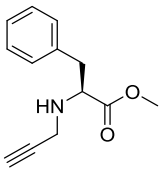

93a

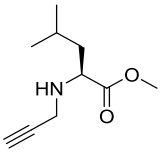

93b

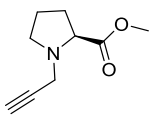

93c

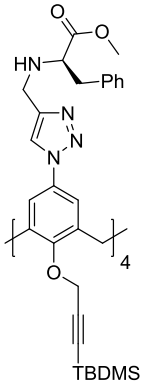

94a

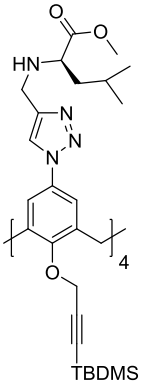

94b

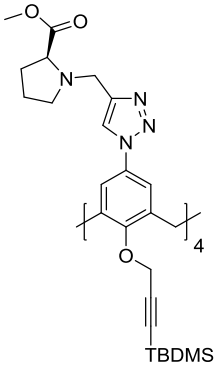

94c

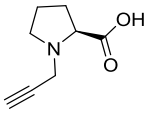

95

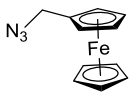

96

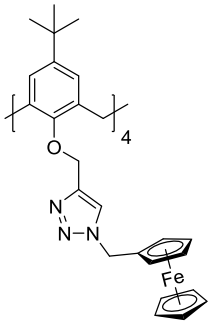

97a

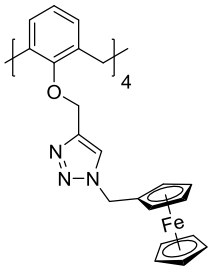

97b

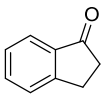

98

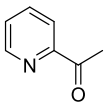

99

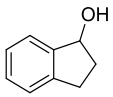

100

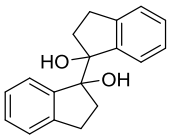

101

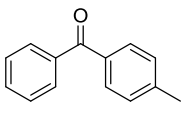

102a

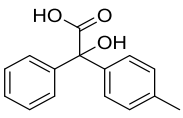

103

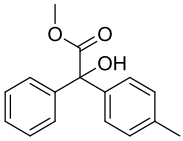

104

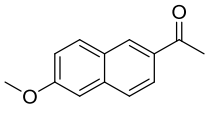

105

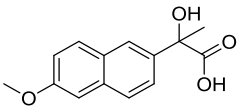

106

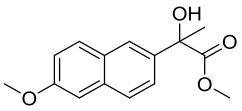

107

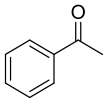

108

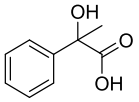

109

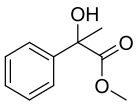

110

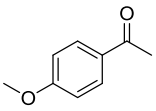

111

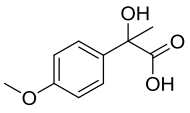

112

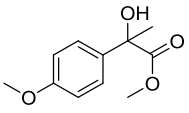

113

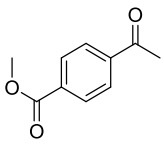

114

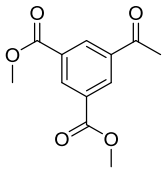

115

X Table of modified surfaces

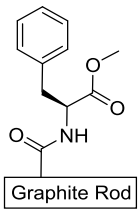

S1

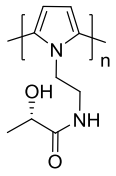

S2

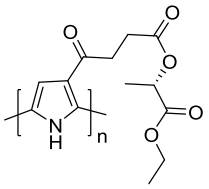

S3

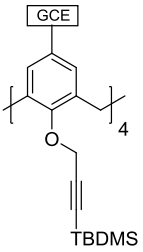

S4

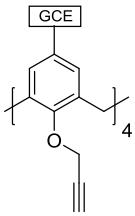

S5

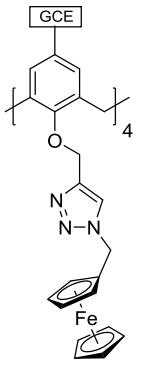

S6

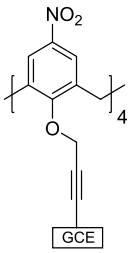

S7

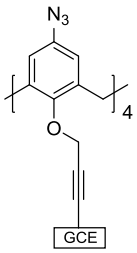

S8

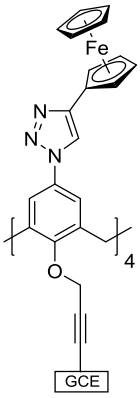

S9

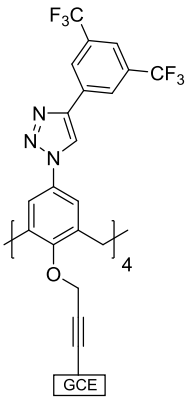

S10

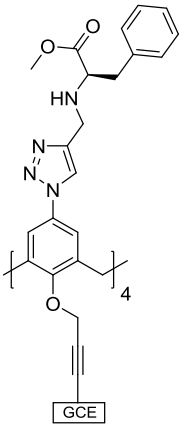

S11a

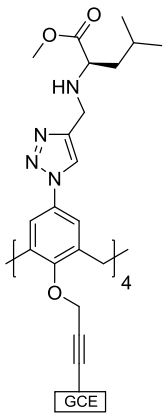

S11b

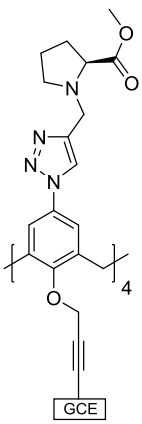

S11c

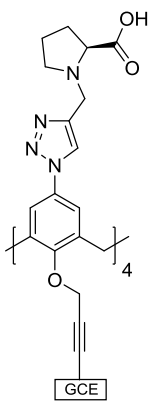

S11d

Chapter 1

Introduction

1.1 The importance of asymmetric synthesis

Asymmetric synthesis is an important topic in synthetic organic chemistry that is used in both academic and industrial laboratories. The subject matter is a major challenge in an extremely fertile field of research that is commonly utilised in the development of new agrochemicals and pharmaceuticals. As shown in Figure 1, the number of publications focussing on the asymmetric synthesis of organic compounds has increased year on year from 2,637 in 2004 to 4,144 in 2015.

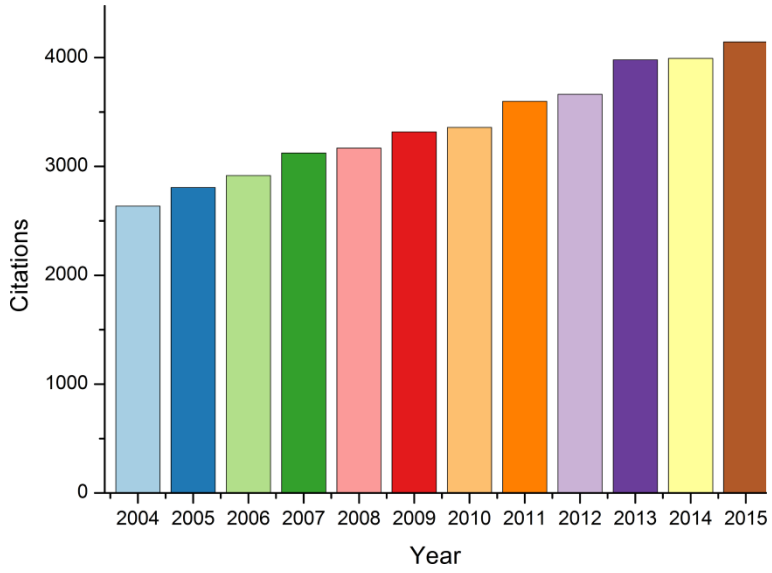

Figure 1: Citations per year for the search term "Asymmetric synthesis" supplied by Web of Science™ (accessed 08/08/2016)

The importance of being able to synthesise enantiomerically pure compounds is of great significance, especially for agrochemical and pharmaceutical applications as in biological systems, enzymes and other biological receptors are able to discriminate between different enantiomers of a chiral compound and may interact with them in different ways.[1] Although it is important to note that two enantiomers of the same drug may have very similar effects, such as making the drug marginally less effective, to completely different effects, such as promoting an entirely different physiological response, within the subject.[2] A couple of interesting examples include the differences in activity between *L*-DOPA *L*-**1** and *D*-DOPA *D*-**1** as well as the change in biological activity observed between the enantiomers of thalidomide **2**.

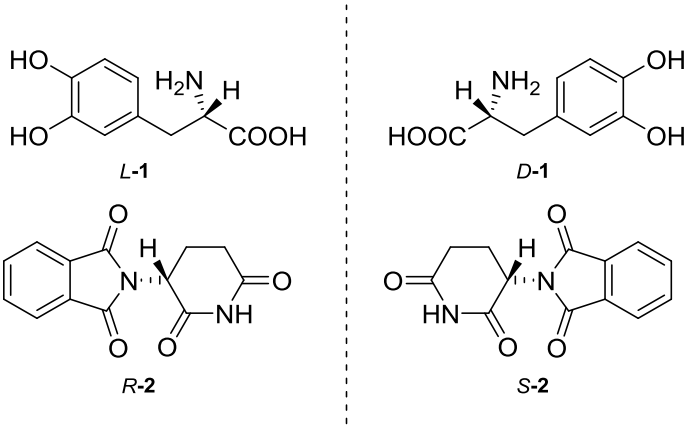

Figure 2: Chemical structures of the two enantiomers of DOPA and thalidomide

DOPA is a commonly used pro-drug, a biologically inactive compound that is metabolised in the body to produce the active drug, for the treatment of Parkinson's disease. To become biologically active the compound needs to pass through the blood-brain barrier where it is decarboxylated by an enzyme catalysed reaction to the biologically active achiral compound dopamine. Unfortunately the decarboxylase enzyme which catalyses the decarboxylation of the pro-drug is able to discriminate between the two enantiomers of DOPA and therefore only the *L*-DOPA is converted into the active drug. It is therefore essential to administer *L*-DOPA in its enantiomerically pure form otherwise *D*-DOPA may accumulate in the human body leading to possible adverse side-effects.[3,4,5]

The use of thalidomide in the late 1950s is a devastating example that highlights how the differences in chirality of a drug compound can alter the biological effect that it has on the subject. The drug was being used as a sedative and anti-nausea agent to help pregnant females suppress "morning sickness" but the adverse side effects attributed to this compound caused an estimated 10,000 infants to be born with deformities world-wide.[6] The problem arose because the drug molecule was being administered in its racemic form and one of the enantiomers was very harmful to the foetus due to some very potent teratogen effects.[7] It was later discovered that the *R*-isomer **2** was the active sedative and did not appear to cause any deformities whereas the *S*-isomer **2** was found to be the cause of the potent teratogen effects.[8]

There has been a large drive in both academic and pharmaceutical laboratories to develop a "tool box" of techniques that can be utilised in organic synthesis to aid the formation of one

enantiomer of a chiral organic molecule. These methods of asymmetric synthesis can be split into four generations and will be discussed briefly.[9]

1.1.1 First generations of chiral synthesis: chiral starting materials

The use of readily available, naturally occurring enantiomerically pure starting materials from what is commonly referred to as the "chiral pool" is a simplistic way of forming optically active compounds. It is important to note that virtually all known methods of asymmetric synthesis find their origin from the chiral pool. An example of this is the famous catalyst utilised in the Sharpless epoxidation that finds its source of chirality from the naturally occurring tartaric acid **3**,[10] which is formed by the fermentation of sugars using yeast.[11] These naturally occurring compounds are commonly used as cheap starting materials in the synthesis of a much more valuable natural product. For instance in the synthesis of avenaciolide **4** Fraser and co-workers used diacetone *D*-glucose **5** as their starting material due to the large degree of overlap between the sugar and their target molecule (structures shown in Figure 3).[12] However this strategy is not without limitation as it requires the desired structure to bears a close resemblance to a compound within the chiral pool otherwise a difficult synthesis involving multiple steps and large losses in yield is required. Furthermore the use of chiral starting materials relies on the preservation of the stereogenic centre(s) during each synthetic transformation which can be problematic.

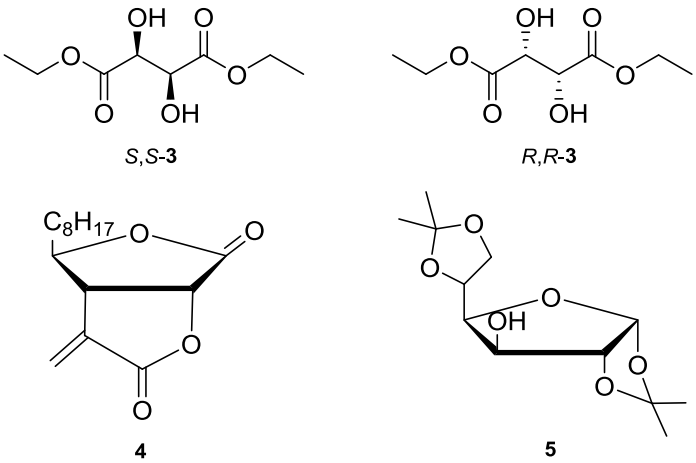

Figure 3: Showing the structures of tartaric acid, diazcetone *D*-glucose and avenaciolide.

1.1.2 Second generation of chiral synthesis: chiral auxiliaries

A chiral auxiliary is an enantiomerically pure compound that can be temporarily attached to a prochiral substrate to direct the reaction resulting in the formation of an optically-active compound, once the auxiliary is removed. [13,14] This methodology is effective because the relative energies of the diastereomeric transition states that are formed during the reaction are not equivalent and therefore one enantiomer will be formed preferentially. Furthermore, the diastereomeric products that are formed while the chiral auxiliary is still attached are not chemically equivalent and as such can be purified by flash chromatography. [15]

Two examples of chiral auxiliaries that are commonly used in asymmetric synthesis are (*S*)-amino-2-methoxymethylpyrrolidine **6** and (*R*)-amino-2-methoxymethylpyrrolidine **7**, both of which are synthesised from naturally occurring amino acids;[16] the use of these molecules in asymmetric alkylations was originally developed by Enders and Corey.[17,18] The pathway in which **6** and **7** impart chirality onto the substrate is shown in Scheme 1.[19]

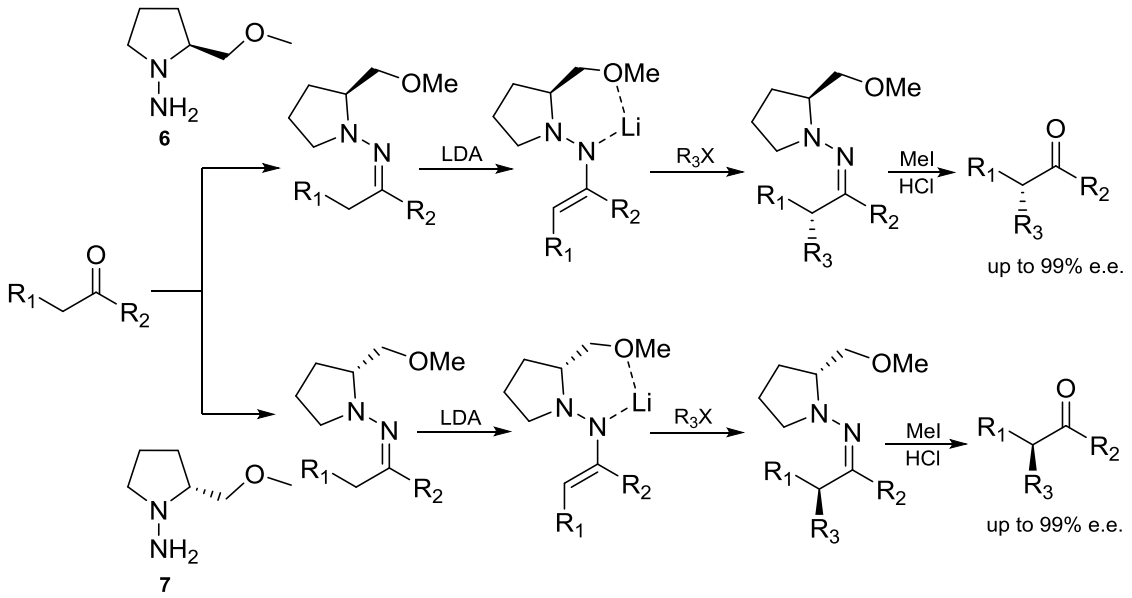

Scheme 1: Reaction pathway using 6 and 7 in the alkylation of a prochiral starting material

As is highlighted in Scheme 1 the reaction pathway follows three steps; first the chiral auxiliary reacts with the prochiral ketone to form an imine and then de-protonation at the alpha position is conducted using LDA to form an aza-enolate intermediate. The anionic intermediate is stabilised by the lithium cation which is co-ordinated between the negatively

charged nitrogen atom and the ether.[20] The alkylating agent then attacks the least hindered face of the intermediate to form a diastereomerically enriched species which, after removal of the chiral auxiliary, yields the desired (*R*) or (*S*) product with an enantiomeric excess (e.e.) of up to 99%.

1.1.3 Third generation of chiral synthesis: asymmetric reagents

Asymmetric reagents are chiral molecules that are used to impart chirality upon a prochiral starting material through an intermolecular process. Usage of these reagents is advantageous over the use of chiral auxiliaries because the two extra steps required for the attachment and subsequent removal of the auxiliary are no longer necessary. This makes the use of these reagents a very attractive technique but unfortunately effective asymmetric reagents currently only exist for a small range of reactions.[9]

An example of an asymmetric reagent is Alpine-Borane® **8**, which is commonly used in the stereoselective reduction reaction known as the Midland reduction.[21,22] This reaction involves the reduction of prochiral starting materials, such as ketone **9**, and follows the reaction pathway described in Scheme 2. The chirality induced from this reaction can be predicted by considering the boat like transition state of the possible intermediates, **10** and **11**. The intermediate with the least-hindered side group occupying the axial-like position is favoured; this leads to preferential formation of the *R* isomer in the example shown in Scheme 2.[23]

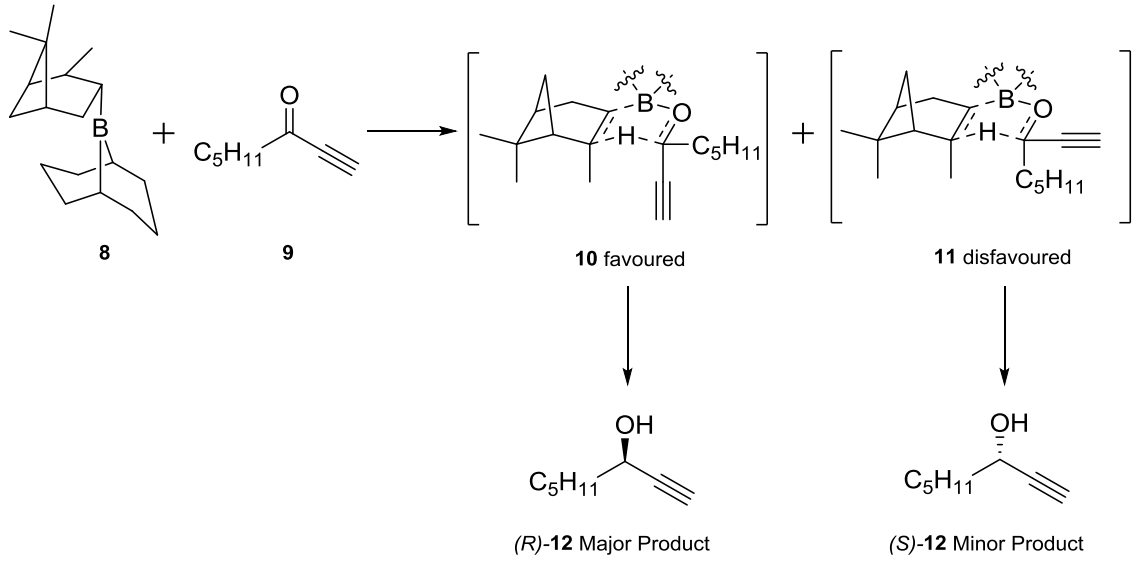

Scheme 2: Midland reduction of compound 9 showing boat like transition states

1.1.4 Fourth generation of chiral synthesis: asymmetric catalysts

Chiral catalysts are very important in asymmetric synthesis because, unlike when using a chiral reagent, only a catalytic quantity of the chiral compound is required for stereocontrol of the reaction. This is essential, especially in industrial processes: if only a small amount of the catalyst is required the cost of the asymmetric reaction is kept relatively low, even when using precious metal catalysts. Furthermore, the catalyst can normally be recovered from the reaction, once the synthetic transformation is complete, and used again in future reactions.

Asymmetric catalysts can generally be split into two categories; metal catalysts with chiral ligands that are used to control the chirality, such as the Noyori's asymmetric hydrogenation using 2,2'-bis-1,1'-binaphthalene (BINAP)-Ru **13**, or more recently organic asymmetric catalysts such as (*L*)-Proline **18**.

1.1.4.1 Metal asymmetric catalysts

This section of chemistry describes the use of metal catalysts that are bound to chiral molecules to create a complex that can be utilised in the synthesis of optically active compounds. An example of this type of catalyst can be found in the work reported by Noyori and Takaya into the metal catalysed asymmetric hydrogenation of achiral starting materials.[24] The chiral ligands that were used in their catalysts were BINAPs synthesised from either racemic or enantiomerically pure samples of 1,1'-bi-2-naphthol (BINOL)[25,26]. Interestingly these

compounds do not possess point chirality, as in they do not have a stereogenic centre, instead they exhibit axial chirality wherein the axis on which the substituents are held is trapped in a specific spatial arrangement and as such the enantiomers of this molecule are non-superimposable.

These catalysts are prepared by the treatment of [$RuCl_2COD$] with (*R*)-or (*S*)-BINAP in toluene followed by reaction with sodium acetate to afford catalysts (*R*) or (*S*)-**13**.[27,28] It was found by Takaya that 0.5 mol% of (*R*)-**13** could be used in the asymmetric hydrogenation of enaminde **14** to form the enantiomerically pure (>99.5% e.e.) product **15,** with a quantitative yield.[29] Meanwhile the (*S*) enantiomer of **13** has been used effectively in the asymmetric synthesis of the nonsteroidal anti-inflammatory drug Naproxen **17**, which was synthesised from prochiral alkene **16** by Noyori and co-workers,[27] using 0.5 mol % of the catalyst they achieved a yield of 92% and an enantiomeric excess of 97%. Both of these reactions and the structures of the catalysts used are shown in Scheme 3.

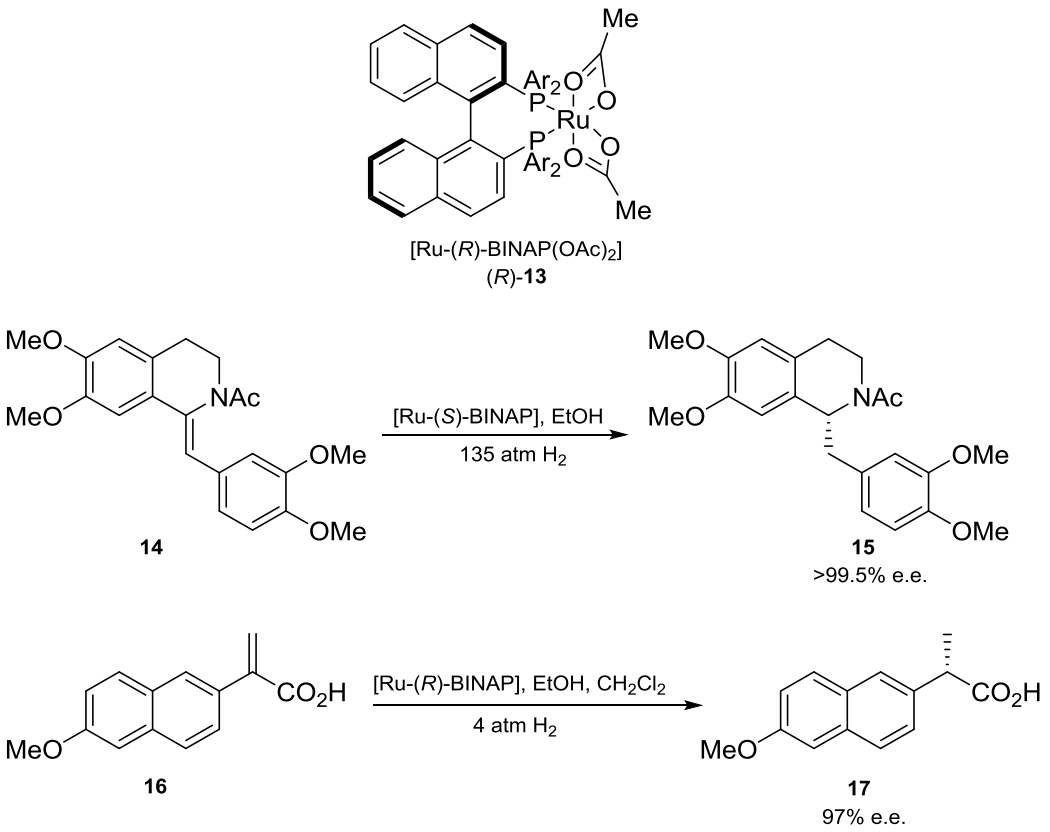

Scheme 3: Asymmetric reductions of prochiral starting materials using 13

1.1.4.2 Organic asymmetric catalysts

The realisation that small molecules such as *L*-proline **18** could be used as asymmetric catalysts sparked a renewed interest in the field of asymmetric synthesis, as it demonstrated that these transformations were not limited to metal complexes and enzymes.[30] This strategy was first brought to light by the Hajos-Parrish-Eder-Sauer-Wiechert reaction which involves the proline-catalysed intramolecular aldolisation.[31,32] However, it wasn't until the early 2000s that the first examples of asymmetric intermolecular aldol reactions were published by Gröger and co-workers.[33] Their work showed that small organic molecules could provide promising alternatives to reactions that were commonly catalysed using either enzymes or metallic catalysts. They believed that these systems would have several advantages over their enzyme driven counter parts in that the organic catalysts would have:

- Both enantiomers readily available at a comparable price (due to availability of most compounds from the chiral pool).
- Relatively low molecular weight (so high atom efficiency).
- Ease of separation
- And simplistic recovery of the catalyst after workup

Scheme 4 depicts the direct asymmetric aldol reaction of 2-propanone **19** and isobutyraldehyde **20** catalysed by **18** resulting in the formation of the (*R*)-enantiomer of **22** with a yield of 97% and an e.e. of 96%. It is important to note that this reaction does not proceed through the normal aldol reaction pathway. Instead, it is speculated that the enamine intermediate **21** is formed by the reaction of **18** with **19** and this intermediate then attacks the aldehyde **20** on the least hindered face (the re face); subsequent hydrolysis of the resulting iminium with water affords the desired product **22** as the *R* enantiomer.

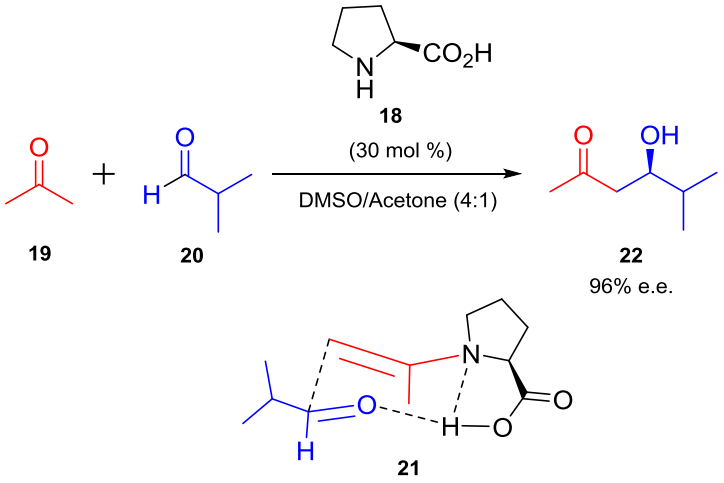

Scheme 4: Asymmetric aldol reaction catalysed by *L*-Proline

This was an important discovery as it showed that small chiral molecules can mimic enzymes. For instance in the case described in Scheme 4 the *L*-proline is behaving as an aldolase type I enzyme mimic.

1.1.5 The hunt for a fifth generation of asymmetric catalysis: enzymes

Enzymes or biological devices are at the forefront in the "hunt" for another generation of asymmetric techniques. They have proven to be able to drastically accelerate the rate of reactions, be extremely selective in the formation of enantiomerically pure compounds, and be subject to regulation (as the catalytic activity of the enzyme is strongly influenced by the concentration of substrates, products or other species).[34,35] Enzyme-catalysed reactions are frequently used to provide a rich source of chiral starting materials as they are able to selectively generate chiral materials from prochiral compounds with high optical purities.[36] An example of this is shown in the work reported by Gu and co-workers wherein they describe the selective reduction of both ketones and di-ketones using either baker's yeast (*Saccharomyces cerevisidae)* to form the *S* enantiomer or *Geotrichum* sp. 38 to yield the *R* enantiomer of the product, with enantiomeric excesses of up to 99% (as shown in Scheme 5).[37,38]

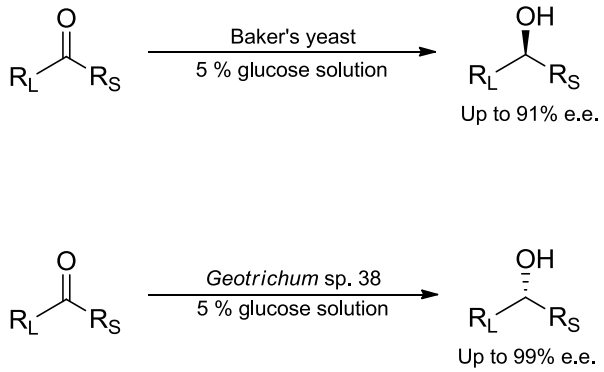

Scheme 5: Asymmetric reduction of prochiral ketones using baker's yeast and *Geotrichum* sp. 38

Enzymes are also used routinely in the asymmetric formation of C-C bonds. The example I am going to talk about is the enantioselective formation of cyanohydrins. Cyanohydrins are an important class of starting materials as they can be readily converted to a wide range of desirable functionalities such as α-amino acids, α-hydroxy acids and vicinal diols. The asymmetric synthesis of these compounds is already well established using chiral catalysts such as cyclic dipeptides[39] or chiral complexes containing aluminium,[40] titanium[41] or boron[42] as the reactive metal centre. However these reactions can also be conducted using a class of enzymes called hydronitrilases (or oxynitrilases) which are obtained from plant sources. The origin of the enzyme is of upmost importance because hydronitrilases isolated from bitter almonds (*prunus amygdalus*) have been shown to be selective towards the *R* enantiomer[43] whereas oxynitrilases isolated from the leaves of *hevea brasiliensis* are shown to be selective towards the formation of the *S* enantiomer.[44] Both of these enzymes are able to catalyse the addition of the cyanide ion onto a range of different aromatic or alkyl aldehydes to afford the desired cyanohydrins with e.e. of up to 99%, Scheme 6.

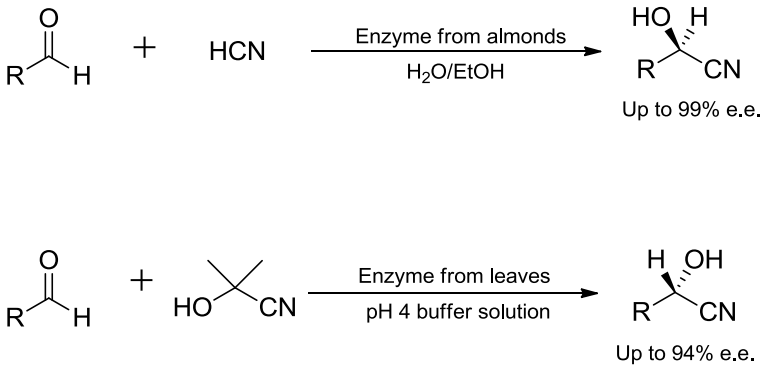

Scheme 6: Asymmetric C-C bond formation using hydronitrilases

Although extremely useful these biological machines do not come without limitations, the largest of which include:

- The narrow range of substrates that the enzymes can effectively catalyse.
- The majority of enzymes require aqueous systems to operate which is problematic as many organic compounds are sparingly soluble in water.
- And that they are very sensitive to different reaction conditions such as changes in pH and temperature.

Enzymes with narrow substrate specificity are normally very efficient at catalysing a reaction using their natural substrate; however this property becomes a problem when trying to develop a catalytic system that will be effective towards a wide range of unnatural substrates. Fortunately many enzymes have now been found to be synthetically useful towards unnatural materials and are commercially available, although it is important to note that there are many bond formations that are required in organic chemistry that enzymes are unable to create.[45–49]

1.1.6 The hunt for a fifth generation of asymmetric catalysis: electrosynthesis

Since the discovery of the Kolbe reaction in 1854 electrosynthesis is becoming more and more important in synthetic organic chemistry.[50] The reaction was one of the first organic reactions that was conducted using electrolysis and it showed that the electron itself could be used as the worlds simplest chemical reagent.[51] This opened up a new avenue of green chemistry that could be used to perform reductive reactions at room temperature, without

toxic solvent systems, with high energy and atom efficiency, using an electrode as the source of electrons opposed to toxic reagents. [52]

It took until the late 1960s before the first asymmetric electrosynthetic reduction (to my knowledge) was reported by Horner and Degner.[53] Using both enantiomers of ephedrine as a chiral inducer, in the electrochemical solution, they were able to selectively reduce acetophenone **23** to phenylethanol **24** with optical purities of up to 5%. Interestingly using (-)-ephedrine (-)-**25** formed the *R* isomer of **24** whereas using (+)-**25** preferentially created the (*S*) enantiomer, as shown in Scheme 7.

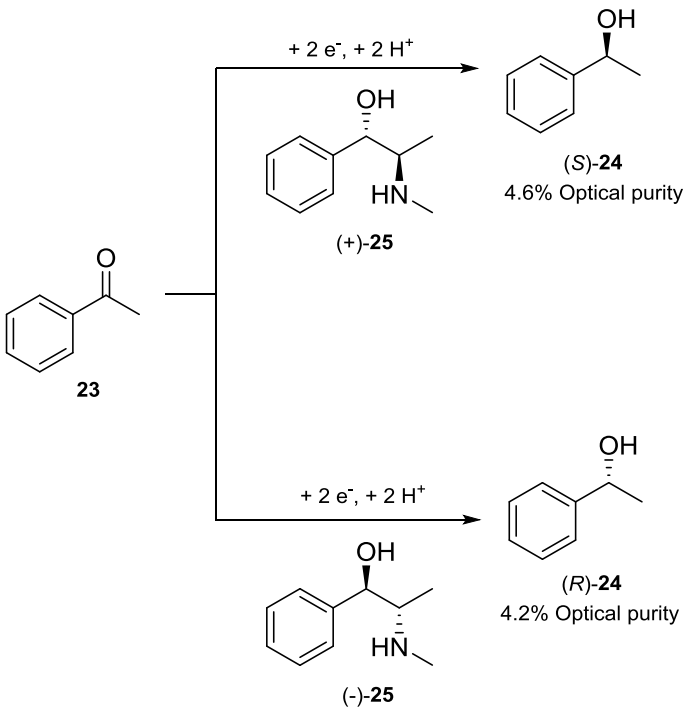

Scheme 7: The first reported example of an asymmetric electrochemical reduction

The asymmetric electrochemical reduction of prochiral starting materials has been developed since the 1960s, with considerable progress in both the application and the theory surrounding the technique. This field of research can be split into several categories separated by the method in which chirality is induced upon the products, each of these categories will be described in the following sections with a couple of examples for each.

1.1.6.1 Chiral additives

A similar system to the one described in Scheme 7 was reported by Oei and Seebach in 1975; they investigated the asymmetric reduction of acetophenone **23** in the presence of chiral additives (+)- and (-)-2,3-dimethoxy-1,4-bis(dimethylamino)butane **26**.[54] In their research the main product from the reduction was not the alcohol but pinacol **27**, which was formed as the *R*,*R* diastereoisomer (shown in Scheme 8).

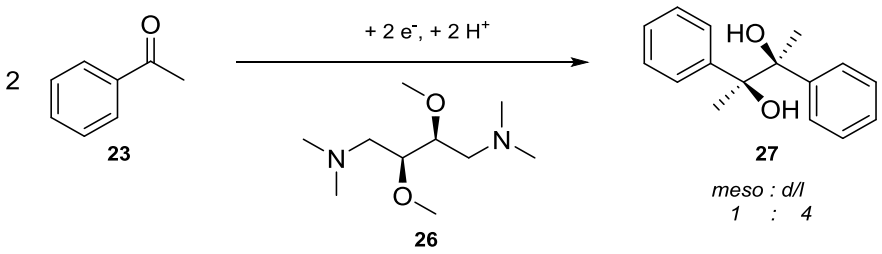

Scheme 8: Selective pinacol formation

It is important to note that the electrochemical reduction of ketones can result in the formation of alcohols or pinacols; selective formation of one product is complicated, and this was one of the problems encountered in my research (section **4.2**). The formation of the alcoholic product requires two one–electron reductions to first the radical anion and then to the alcohol, after protonation at each step. On the other hand, to make the pinacol product the ketone has to be reduced to the radical anion but then, instead of being reduced again by another electron, the radical undergoes bimolecular termination with another radical resulting in the formation of the pinacol, as shown in Scheme 9.[55] Results reported by Lu and co-workers suggest that increasing the water content of the electrochemical system promotes the formation of the alcoholic product stating that "a rich proton source is more conductive to the reduction of the intermediate carbonyl radical, because the resulting anion is protonated faster".[56]

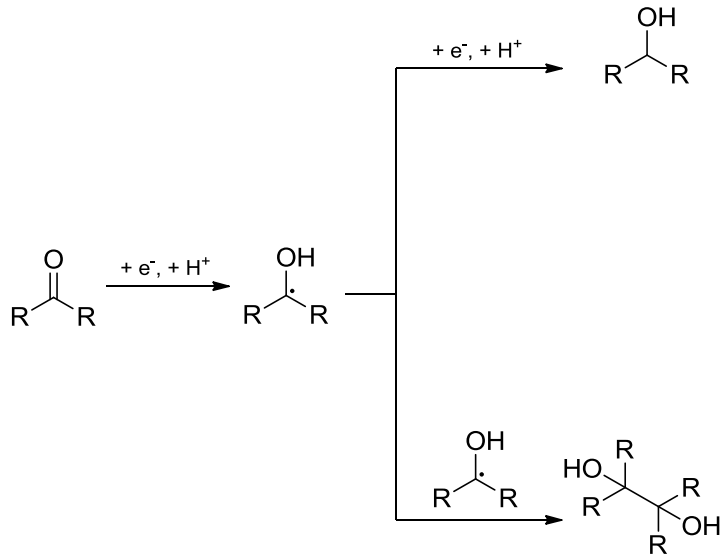

Scheme 9: The formation of alchols and pinacols from the electrochemical reduction of ketones.

A more recent example of asymmetric electrosynthesis was reported by Wang and co-workers. They performed the electrocarboxylation of 4-methylpropiophenone **28** in the presence of alkaloids that were used to induce chirality upon the product, note that *n*-butanol was used as a co-catalyst to re-protonate the alkaloids after the chiral induction step.[57] Using this technique (*S*) α-hydroxycarboxylic acid **29** was formed with an e.e. of 33%, achieved while using 5 mol % cinchonine **30** as the chiral inducer and a stoichiometric amount of *n*-butanol (Scheme 10).[58]

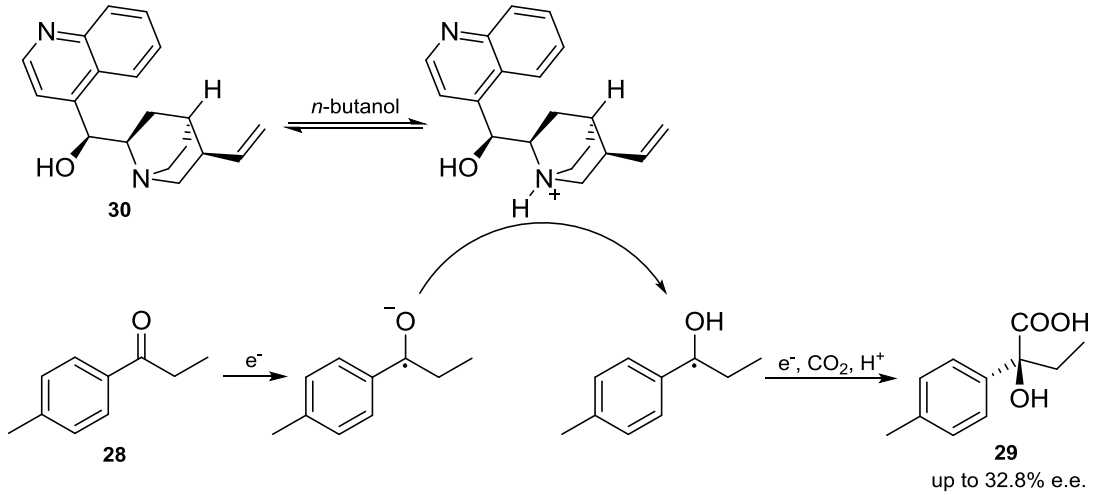

Scheme 10: The asymmetric reduction of 28 using cinchonine as a chiral inducer

A much improved e.e. was obtained by Yadav and co-workers by reducing prochiral ketones in the presence of (-)-*N*,*N*'-dimethylquininium tetrafluoroborate **31** at a mercury pool working electrode.[59,60] Using 25 mol% of **31** they reduced ketone **32** to the corresponding alcoholic product **33** with a yield of 80% and an e.e. that was 66% selective towards the *S* enantiomer, as shown in Scheme 11. It is believed that the high e.e. obtained under these conditions is caused by **31** being strongly adsorbed onto the cathodic working electrode surface and therefore being able to rapidly protonate the reduced anionic intermediate, as described in similar systems.[61,62] Although a moderate e.e. is achieved, it is unfortunate that the use of a toxic mercury electrode is required as it counteracts with the green and clean synthetic advantages afforded by the use of electrosynthetic techniques.

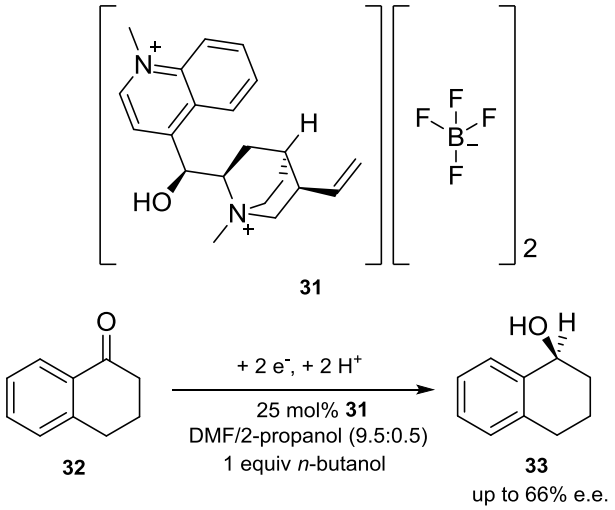

Scheme 11: Electrochemical reduction of 32 in the presence of chiral inducer 31

1.1.6.2 Intrinsic optical substrate conformation

This section will describe the technique of asymmetric synthesis using a combination of electrochemistry and chiral auxiliaries. This method is largely unexplored with, to the best of my knowledge, only three accounts of this method in the literature – all reported by Feroci and co-workers. The first asymmetric procedure they described demonstrated the use of an Evans' chiral auxiliary in the electrocarboxylation of *N*-(2-bromopropionyl)-4-(*R*)-phenyloxazolidin-2-one **34** to achieve the selective formation of the methylmalonic ester (*S*,*S*) **35** over the (*S*,*R*) **36** with a diastereoisomeric ratio of 60:40 (**35** : **36**), as shown in Scheme 12.[63] Interestingly when the reaction was extended to a wider range of substrates the more abundant diastereomer was always the (*S*,*R*) species, presumably due to preferential formation of the "non-Evans" conformation of the intermediate.[64] Furthermore molecules **35** and **36** could be easily isolated as pure compounds using flash chromatography.[63] Although not mentioned in their research, Evan's chiral auxiliary can be cleaved from the substrate under basic conditions to yield the chirality enhanced carboxylic acid.

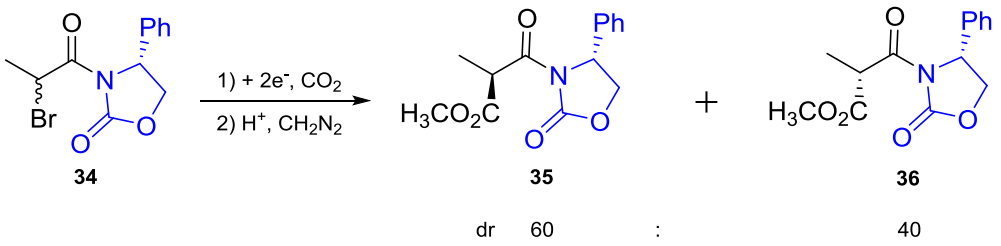

Scheme 12: Asymmetric electrosynthesis using Evan's chiral auxiliary. Evan's chiral auxiliary while attached onto the substrate is drawn in blue.

They later reported in a full paper the effects that different chiral auxiliaries had on the reaction yield, formation of side products and diastereoisomeric ratio. The most impressive of which was the use of Oppolzer's camphor sultam as a chiral auxiliary that while bound onto the substrate resulted in yields of up to 80% with recovery of 19% of the starting material **37** (showing there to be very minimal formation of side products) and with very good diastereoselectivity of up to 98:2 in favour of isomer **38** (shown in Scheme 13).[65] This experiment was then repeated with several different substrates with increasingly sterically hindered alkyl chains after the bromine (ethyl, butyl and iso-propyl) and they showed that an increase in steric bulk made very little difference to the overall yield or selectivity of the reaction. [65] Again, although not mentioned in their research, the sultam can be easily removed to yield the unprotected carboxylic acid under reductive or hydrolytic conditions.[66]

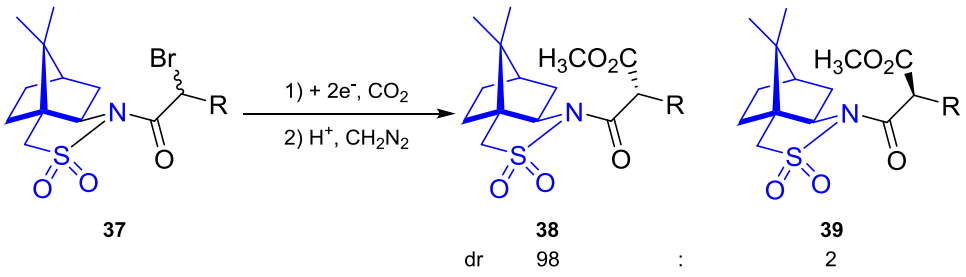

Scheme 13: Asymmetric electrochemical reduction using Oppolzer's camphor sultam. Oppolzer's camphor sultam while attached to the substrate is drawn in blue

Similar reactions were conducted using chiral cinnamic acid derivatives, such as compound **40**, that when exposed to the electrocarboxylation conditions resulted in the

preferential formation of 2-phenyl succinic ester **41** with a diastereomeric ratio of 70:30 and a yield of 48%, as shown in Scheme 14. Subsequent removal of the chiral auxiliary with lanthanum(III) iodide formed the *R*-enantiomer **43** with an enantiomeric excess of 40%.[51]

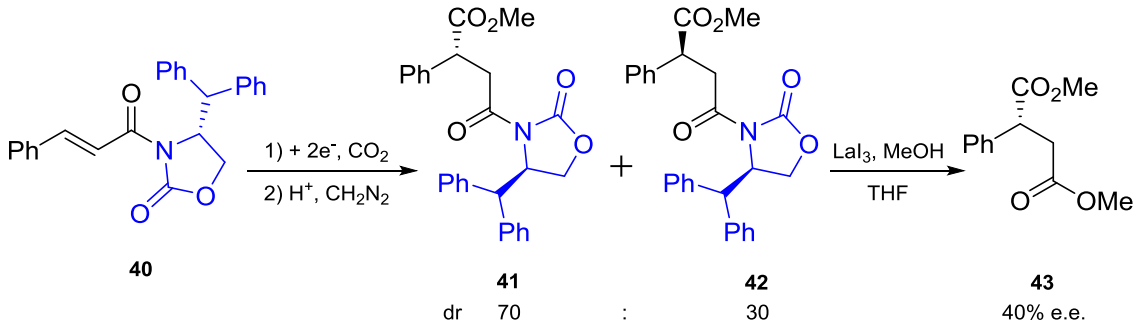

Scheme 14: Asymmetric reduction of 40 using Evan's chiral auxiliary and removal of the auxiliary using LaI_3. While attached to the compound the chiral auxiliary is drawn in blue

1.1.6.3 Chiral electrodes

The advantages of using chirally modified electrode surfaces to induce stereocontrol in electrochemical synthesis are similar to the advantages afforded in the use of heterogeneous catalysis over homogeneous methods. In that the chiral additives can be easily separated from the reaction mixture once the reaction is complete and while less of the chiral inducer is required, it remains highly concentrated at reaction centre.[67] In this way the cost of the reaction is drastically lowered as the modified electrode can be reused in future reactions and less resources are required during the purification to remove the chiral inducers.[68]

An early example of asymmetric electrochemical synthesis being conducted using a chiral electrode was reported by Miller and co-workers in 1975. They modified graphite rods with chiral substituents by first baking them in air to introduce acidic groups onto the surface of the electrode. These “acidified” surfaces were then treated with thionyl chloride to facilitate the reaction with (*S*)-phenylalanine to form chiral surface **S1**.[69]

Ethylbenzoylformate **44** was reduced using modified surface **S1** in a 50:50 mix of ethanol and acetate buffer solution that resulted in the formation of **45** with a high yield of 94% and a moderate e.e. of 10%, as shown in Scheme 15. They also demonstrated that the origin of the chiral induction came from the amino acid whilst bound onto the surface of the electrode and

not from electrode material that had been leeched off during the reaction. This was demonstrated when a racemic mixture of products was obtained by repeating the experiment using an unmodified graphite electrode in a solution containing 0.015 M of (*S*)-phenylalanine as a chiral inducer.[70]

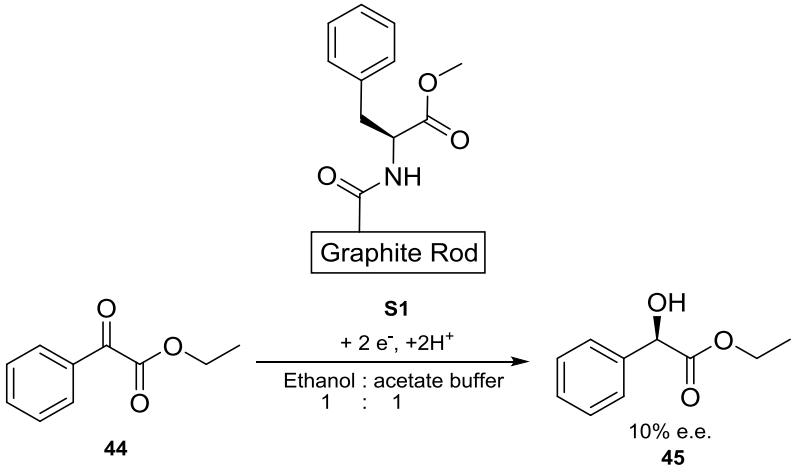

Scheme 15: Asymmetric reduction of 44 using chiral surface S1

Another report made by Pleus and co-workers describes the polymerisation of chiral pyrroles onto a platinum surface resulting in the formation of a chiral electrode, which was then used in the enantioselective reduction of prochiral starting materials.[71] In their systems the enantioselectivity was shown to depend on the electrolyte that was used during the electropolymerisation. It was suggested by Pleus that the use of polymer modified electrodes may be advantageous over the use of a monomolecular layer due to their being a much larger amount of the chiral species on the surface of the electrode.[72] The polymer electrodes were created by the polymerisation of monomers **46** and **47** to form surfaces **S2** and **S3** respectively.[71,73] These modified materials were then used in electrochemical systems to reduce compound **48** to **49** under anhydrous conditions. The best optical yields were obtained when using modified electrodes **S2** and **S3** that were fabricated while using $LiClO_4$ as the electrolyte during the polymerisation step. The reduction reactions that were performed using these surfaces formed optically active products with enantiomeric excesses of up to 17%, as shown in Scheme 16. The absolute configuration of the major enantiomer was determined to be the *R* isomer, based on the sign of the optical rotation compared to literature results.[72]

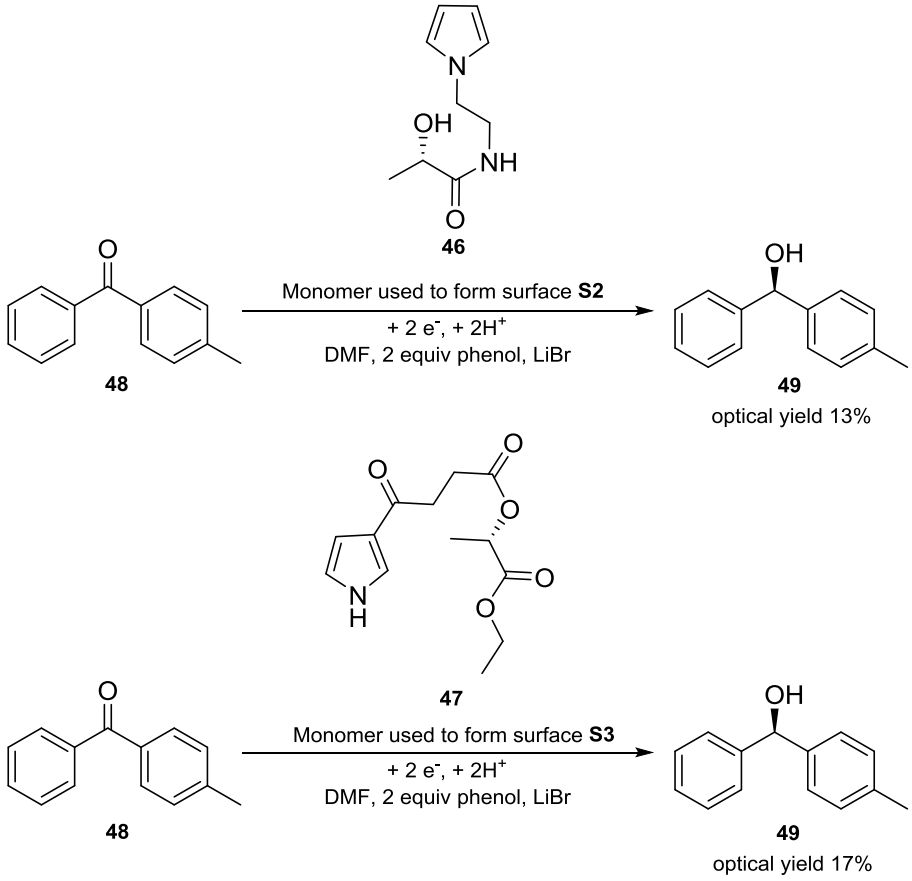

Scheme 16: Asymmetric reduction of 48 using chiral surfaces S2 and S3

The last example I would like to discuss is the use of immobilised chiral metal complexes in the asymmetric reduction of prochiral starting materials. The pioneers in this field of research are Moutet and co-workers who reported the immobilisation (by polymerisation) of rhodium(III) complexes containing chiral polypyridyl ligands, such as **50**, onto carbon felt electrodes. These surfaces were shown to be effective in the asymmetric reduction of prochiral ketones, as shown in Scheme 17.[74] The electrochemical reduction is believed to form a Rh(I) complex on the surface of the electrode that is then able to use water as a hydrogen donor resulting in the formation of a rhodium(I) hydride species on the surface of the electrode.[75] This hydride is the active species in these electrochemical reactions and the electrons used in this process do not directly reduce the prochiral substrates but instead regenerate the active Rh(I) complex. This was determined by attempting to electrolyse the prochiral ketones in the absence of the Rh complexes under the same experimental conditions but when using these blank electrodes no conversion of the starting material was observed.

This suggests that the rhodium is acting as a catalyst in these systems by lowering the potential at which the reduction reactions are able to proceed.[76]

Using these systems the asymmetric reduction of acetophenone **23** was achieved with an enantiomeric excess of up to 12% (in favour of the *S* isomer), a current efficiency of 61% and a catalytic turnover of 140-180 (mol of product formed/mol of the immobilised complex). It was interesting that they investigated the effect that the thickness of the polymer film had on enantioselectivity and they found that the best optical purities were obtained while using the smallest amount of the chiral complex. They observed that while using only 1.3 mmol of the complex an e.e. of 12% was achieved whereas when using 3 mmol of the complex an e.e. of 7% e.e was attained.[76] They reasoned that the increase in current density during the electrolysis reaction, caused by the increased amount of the electrochemically active rhodium complex on the surface, was the source of the reduced selectivity. These findings were also reported by Fujihira and co-workers who worked with similar systems utilising chiral tartaric acid modified Raney nickel electrodes.[77]

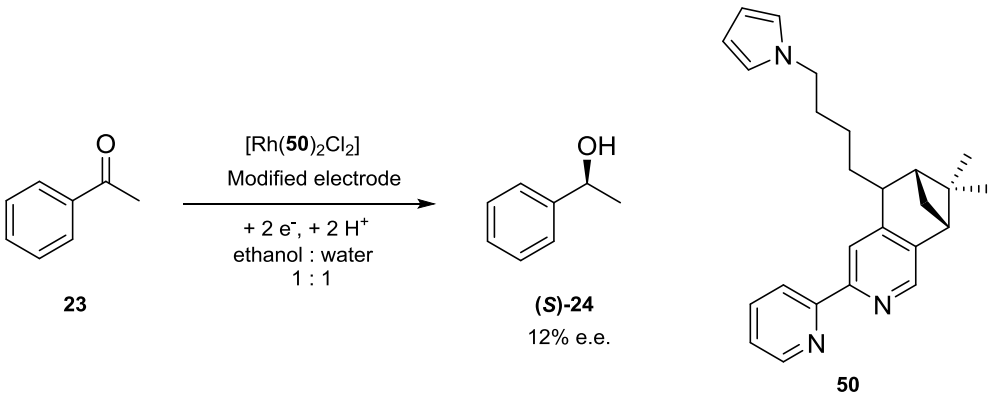

Scheme 17: Electrochemical reduction of 23 using Rh modified electrode

In the research conducted in this thesis I attempted to formulate a methodology that would allow for the functionalisation of a carbon electrode surface with a monolayer of calixarenes. These modified surfaces were to be used as a scaffold on which would be attached an array of chiral inducers that could be utilised in asymmetric electrochemical reductions to stereoselectivity reduce prochiral ketones, such as **23**. It was believed that due to the hydrophobic core of the calixarene with adequate decoration of the upper rim it would be

possible to create a chiral environment on the surface of the electrode that would mimic that of an enzyme.[78,79]

To further introduce these topics the rest of this introduction will be focussed towards a brief history of calixarenes and their synthesis and then a description of the electrochemical techniques that were used throughout my research.

1.2 Calixarenes

The discovery of calixarenes began with an investigation, conducted by Baeyer in 1872, into the reaction of phenols, such as benzene-1,2,3-triol, and formaldehyde in the presence of strong acids.[80,81] In his papers he commented on the formation of a "kittartige substanz" (a hard cerement-like substance) and this was the beginning of a new field of phenol-formaldehyde chemistry. Unfortunately, he was unable to isolate any pure compounds from these reactions and was therefore unable to propose any feasible structures. It wasn't until twenty years later that Lederer and Manasse independently discovered the base catalysed dehydration reaction between the hydrated form of formaldehyde **51** and phenol **52** which resulted in the formation of *p*-hydroxymethylphenol **53** and *o*-hydroxymethylphenol **54**, these compounds were isolated as crystalline solids as shown in Scheme 18.[82,83] The success of this reaction, which was later coined the Lederer-Manasses reaction, depended on the use of mild well-controlled reaction conditions because under harsher conditions the base-induced reaction forms an ill-defined resinous tar, similar to that observed by Baeyer under strong acidic conditions.

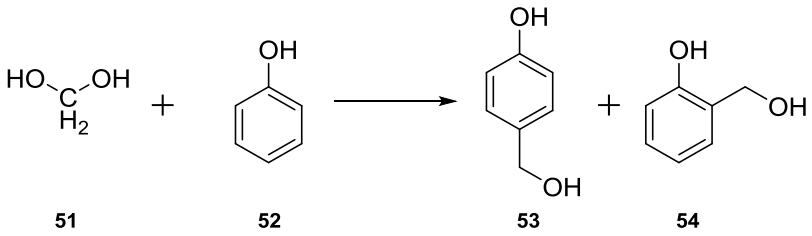

Scheme 18: Reaction between formaldehyde monohydrate 51 and phenol 52 in the presence of a base

Over the next century several research groups attempted to find a practical use for the resinous tars that were being formed under the harsh reaction conditions, but it wasn't until 1907 that a product with marketable qualities was discovered by Baekeland and co-workers.[84] Following on from the research conducted by Baeyer, wherein the formation of a hard

cerement-like substance was discovered, Baekeland demonstrated that with a small controlled amount of base the formation of a commercially viable plastic, now known as Bakelite, was possible.[85] As was already predicted by Baeyer, the main linkages between the aromatic rings in these structures were found to contain either methylene or ether functionalities. The molecular structure of these resins are dominated by diaryl moieties such as (shown in Figure 4) resoles **55**, novolaks **56** and dibenzyl ethers **57**. It is important to note that during the "curing" process, heat treatment results in the conversion of resole **55** structures into novalak **56** structures.[86]

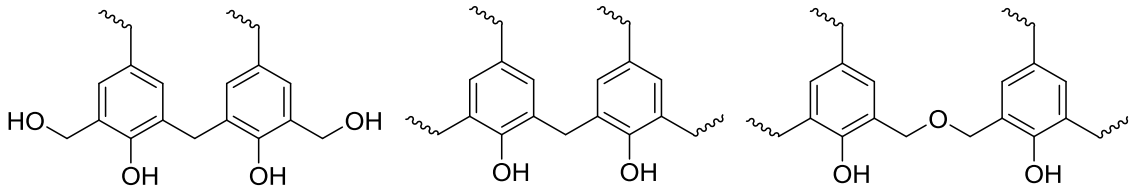

55 **56** **57**

Figure 4: Structures of resoles, novalaks and dibenzyl ethers

It was from an investigation into this "curing" process that caused Zinke and Ziegler to examine the condensation of *p*-substituted phenols in an attempt to simplify the reaction. When unsubstituted phenol is used, the ring can react at both the *ortho* and *para* positions. However in the *p*-substituted phenol example, reaction can only occur at the *ortho*- positions. This simplification was predicted to lead to the formation of a linear chain polymer of phenols;[87] it wasn't until a report three years later that Zinke postulated that these compounds may in fact have cyclic structures,[88] although it was just a speculation at this point in time and was based on no experimental data. It wasn't until 1952, when another publication provided more evidence, that the formation of the cyclic phenol structures become more widely accepted.[89] Absolute proof of the structure was determined by Hayes and Hunter wherein they conducted the stepwise "rational" synthesis of a "cyclic tetranuclear *p*-cresol novolak" (calixarene) confirming the structure that Zinke's predicted.[90]

Thirty-five years after their initial conception, these cyclic tetramers were finally given a name by Gutsche, who in 1978 coined the term "calixarene". This name was derived from the Greek word "calix" meaning a vase or chalice corresponding to the cup like shape of the macrocycle and arene corresponding to the presence of the aryl subunits connected by the methylene

bridges.[91] It is important to note that the number in the square brackets after calix e.g. calix[n]arene, corresponds to the number (n) of aryl subunits present in the macrocycle.

Furthermore, since vases normally stand upright on their smaller face, and the name calixarene comes from the Greek word meaning vase, Gutsche named the rim normally functionalised by the hydroxyl groups (the *endo* face) the lower rim and accordingly named the larger opposite larger face the upper rim (the *exo* face), as shown in Figure 5

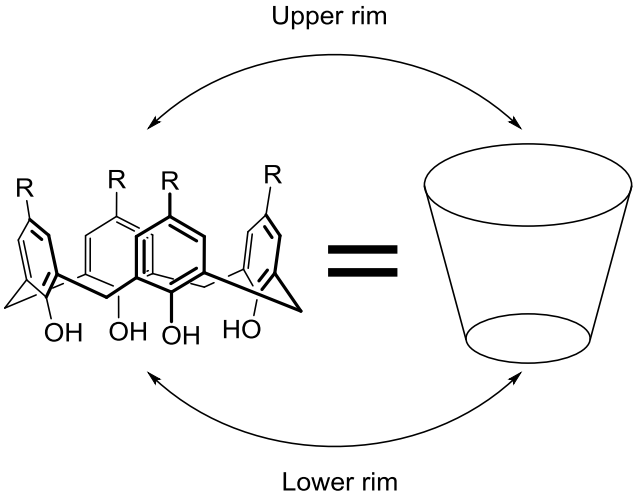

Figure 5: Depicting the upper and lower rims of a calix[4]arene

1.2.1 Synthesis of calixarenes

For a long time the preparation of *p-tert*-butylcalix[4]arene **60** was extremely difficult with most research groups reporting low yields or unquantifiable yields.[86] It wasn't until careful investigation into the reaction conditions by Zinke,[88] Cornforth[92] and later Gutsche,[93] that a reliable experimental procedure for the one-pot base-catalysed synthesis of calix[4]arene was determined.

It was found that the optimal amount of base, sodium hydroxide, required to produce calix[4]arene **60** was around 0.03-0.04 equivalents, for each mole of phenol **58**. When less base was added, the yield of the reaction began to rapidly decrease; if too much base was added, the yield also began to decrease due to the formation of calix[6]arene **61**. Note that when 0.3 or more equivalents of sodium hydroxide were used the cyclic hexamer became the

main product and could be isolated with a reasonable yield.[94] These reactions are shown in Scheme 19.

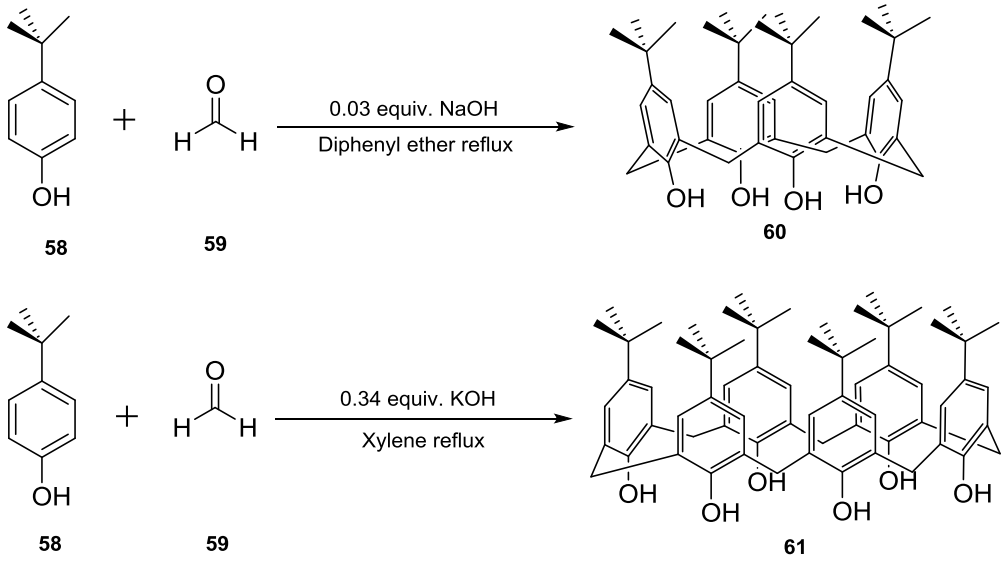

Scheme 19: Formation of *p-tert*-calix[4] and *p*-tert-calix[6]arene

These two calixarenes along with calix[8]arene are generally considered to be the "major" calixarenes, due to them all being readily available and easy to make on a large scale in the laboratory. However many more calixarenes can be synthesised, such as calix[5]arene,[95] calix[7]arene,[96] calix[9]arene[96] and calix[10]arene,[97] to name a few. These calixarenes are much harder to synthesise than the major calixarenes, and the reaction yields are significantly lower, making them less readily available.

The reaction pathway of the base-catalysed reaction between phenol **58** and formaldehyde **59** is initiated by de-protonation of the phenol to form a phenoxide intermediate, which is then able to attack the highly reactive formaldehyde, resulting in the formation of intermediate **62** (shown in Scheme 20). Under mild conditions, the reaction can be terminated at this point and **62** can be isolated and characterised, as shown by Ullmann and Brittner.[98]

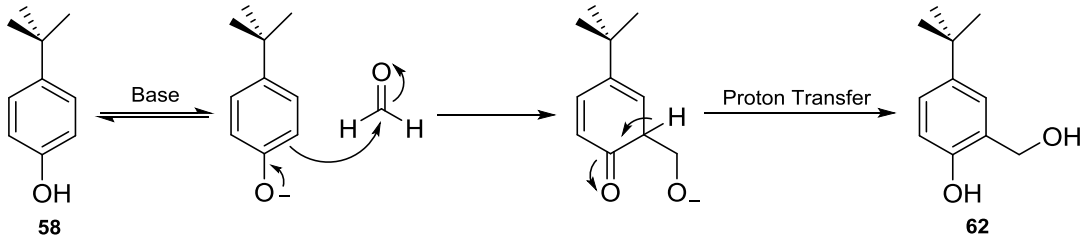

Scheme 20: Base catalysed formation of 62

Under harsher reaction conditions **62** reacts further to give compound **63**, which is comprised of two aryl subunits connected by a methylene bridge. This reaction presumably goes through the *o*-quinone methide intermediate which is able to react with the phenoxide species, Scheme 21. This results in the formation of dimer **63**, which has been isolated by Zinke and co-workers by reaction of *p-tert*-butylphenol with aqueous formaldehyde in the presence of sodium hydroxide at 50°C.[89] These dimers can then undergo condensation reactions when heated, to form linear oligomers (a linear of chain of phenol groups attached by methylene linkers) and, depending on the precise reaction conditions used, these precursors can cyclise to give calix[4-10]arene. The precise pathway in which these oligomers cyclise to form calix[4]arene is unknown, with the precursor containing over forty different compounds, as determined by mass spectrometry.[86] Although it is speculated that calix[8]arene is formed first and then "pinches off", resulting in the formation of two molecules of calix[4]arene. This was demonstrated by Gutsche and co-workers when a pure sample of calix[8]arene was refluxed in diphenyl ether to form calix[4]arene in the presence of a catalytic amount of sodium hydroxide.[99]

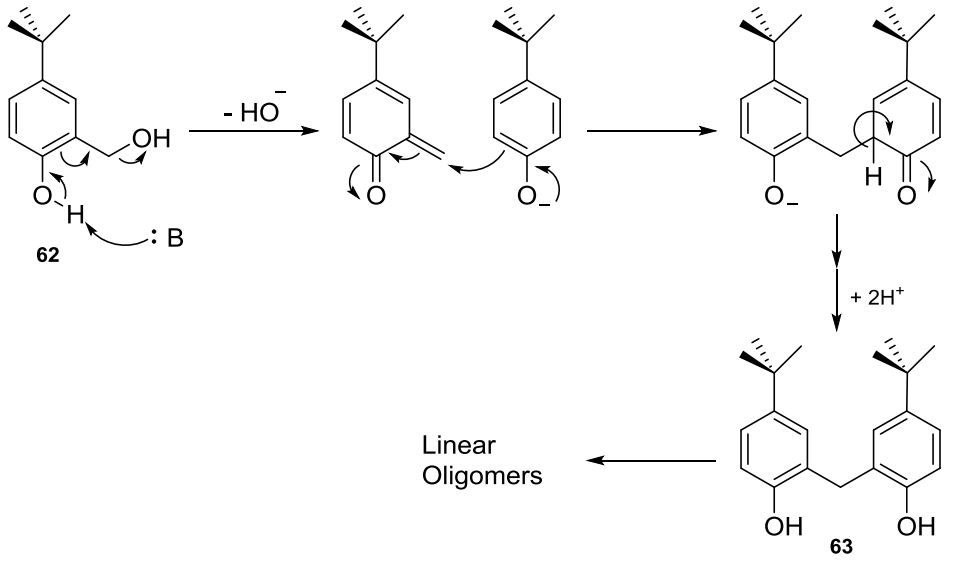

Scheme 21: Base catalysed formation of 63

1.2.2 Conformations of calix[4]arene

It was first proposed by Cornforth and co-workers that the calix[4]arenes could exist as four different diastereoisomers if the phenolic groups were unable to rotate about the methylene bonds that joined them.[92] The phenyl groups are normally considered to be pointing downwards (d) or upwards (u) relative to the plane described by the methylene bridges. These four conformations were later named by Gutsche as the cone conformation (u, u, u, u), the partial cone conformation (u, u, u, d,), the 1,3-alternate (d, u, d, u) and the 1,2-alternate (u, u, d, d) as shown in Figure 6.[100]

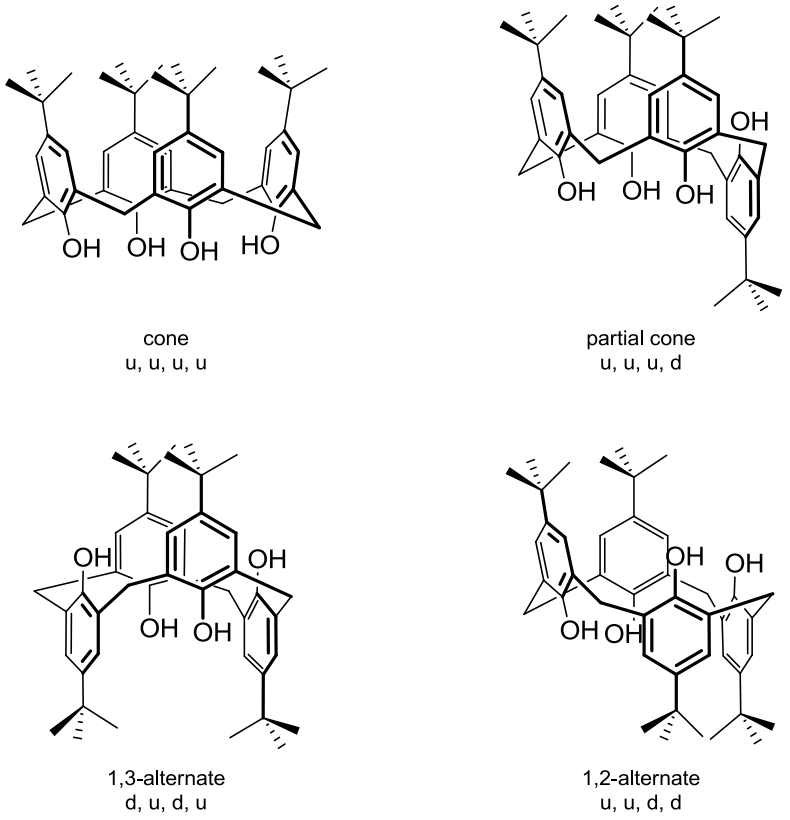

Figure 6: The four different conformations of calix[4]arene

It is important to note that all calix[4]arenes, before modification at the lower rim, are considered to be conformationally mobile when in solution, as the hydroxyl groups are able to rotate through the middle of the cavity, although the ease at which the aryl subunits can rotate does vary from one ring system to another. The rate of rotation is dependent on the reaction conditions such as the temperature, solvent and which base is used for the de-protonation. For instance, in polar solvents the energy required for the change in conformation is lowered, presumably due to the solvent interfering with the intramolecular hydrogen bonding, resulting in destabilisation of the conical strucutre.[101,102]

Thankfully it is possible to lock the conformation of the calixarene by replacement of all four of the –OH groups with sufficiently bulky alkyl chains. During the alkylation of the hydroxyl groups, the base employed for the de-protonation step is of upmost importance as the use of different bases can determine which conformation the calixarene will be locked into. For instance, alkylation of *p-tert*-calix[4]arene **60** with ethyl bromoacetate **64** using Na_2CO_3 as the base produces the tetraakylated calixarene in the cone conformation **65**. However, when

Cs_2CO_3 is used, the predominant product is the calixarene in the partial cone conformation **66** (shown in Scheme 22).[103,104]

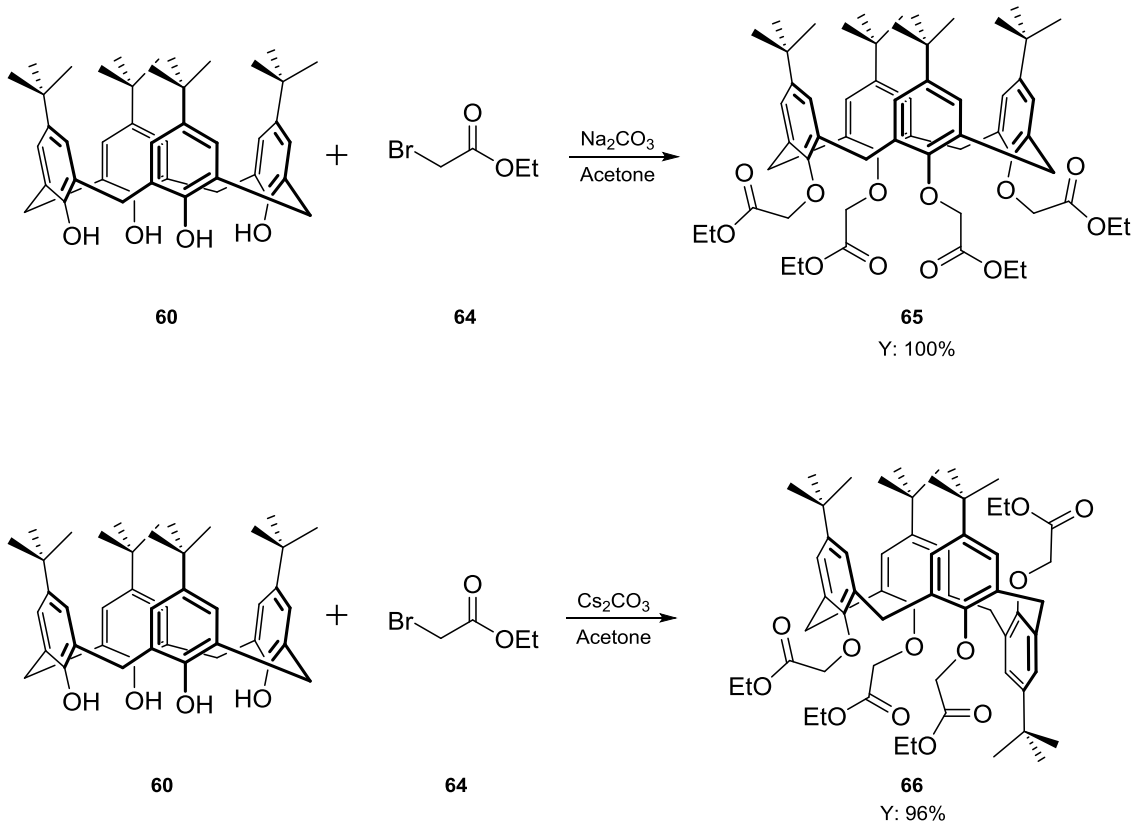

Scheme 22: Locking of the conformation of calix[4]arene by alkylation at the lower rim

1.2.3 Calixarenes as molecular baskets

The use of calixarenes as molecular vesicles is one of the properties that I will attempt to utilise in my research, so it seemed fitting that I mentioned this property in the introduction. It has long been known that even the most simple of calixarenes, such as **60**, can form very strong complexes in the solid state with small hydrophobic molecules such as chloroform, benzene, toluene, xylene and anisole. These calixarenes hold onto their guest molecules extremely tightly and as a result the guest compounds are still present within the macrocycle even after prolonged periods of heating under vacuum [105,106]

This ability of calixarenes to act as host molecules in non-aqueous solvent systems has been investigated by Aoyama and co-workers. They found that a resorcinol-derived calixarene was able to selectively complex neutral organic compounds and this property was utilised for the

organic extraction of D-ribose, riboflavin, vitamin B_{12} and haemin into carbon tetrachloride from an aqueous solution also containing glycerol and D-glucose.[107]

More recent usage of the calixarene cavity can be found in the work described by Rebek and co-workers in 2008 where they used a resorcin[4]arene, a calixarene made from resorcinol, scaffold modified with peptide moieties and Kemp's triacid to catalyse the regioselective cyclisation of epoxy alcohols, such as compound **68**. The host molecule **68** was shown to bind into the cavity of calixarene **67** by NMR studies, and then was presented with an inwardly directing carboxyl group, highlighted in red, that initiated the cyclisation of the substrate selectively to the five membered ring product **69**, as shown in Scheme 23.[108,109] This elegant work highlights the possibility that calix[4]arenes can be utilised as artificial enzyme mimics for use in organic synthesis.

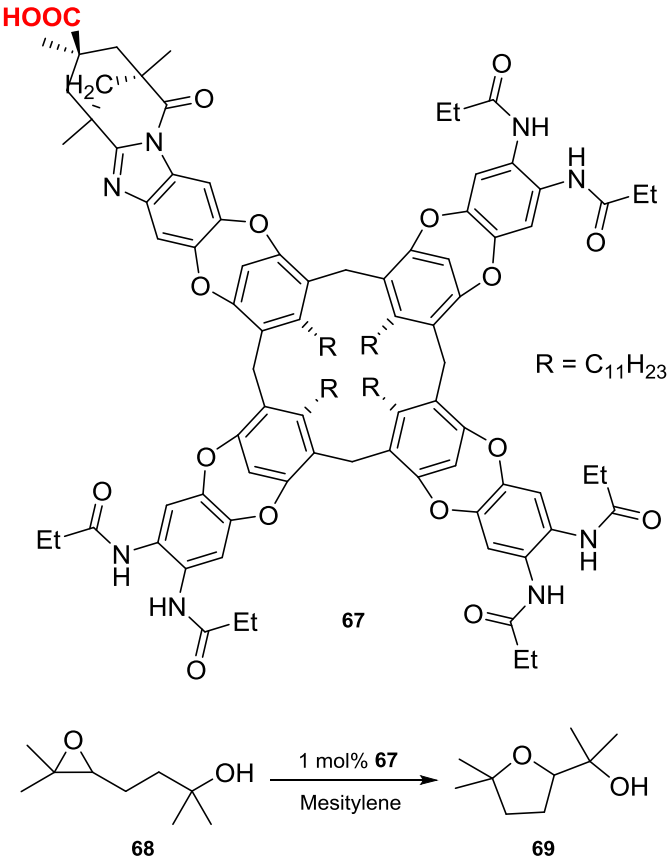

Scheme 23: Regioselective cyclisation of 68 catalysed by calixarene 67

1.2.4 Calixarenes as electrochemically active compounds

Calixarenes with sufficient modification at either the upper or lower rim have found applications in electrochemistry as molecular sensors. An example of this comes from the work conducted by Gupta and co-workers wherein they formed PVC-based membranes of a calixarene modified with tertiary butyl groups at the upper rim and carbamoylmethoxy groups at the lower rim. This electrochemically active surface was then used as a potentiometric sensor to determine the concentration of phosphate ions in agricultural field samples.[110] Another example comes from the work described by Diamond and McKervey wherein they investigated the properties of a range of different calixarenes for use in solution for both environmental and biomedical sensing.[111–113]

Calixarenes with the appropriate decoration at the upper rim, i.e. functionalised with peptide or sugar groups, have been shown to act as enzyme mimics, as described in section **1.2.3**.[78,79] As these macrocycles have also proven to be electrochemically active and effective in asymmetric synthesis it was hoped that these systems could be adapted for use in asymmetric electrosynthetic reactions.[114,115]

1.3 Electrochemistry

Chemically–modified electrodes was a term that was first introduced by Murray and co-workers in 1975, and is a field of research that has been expanding every year since its inception.[116,117] Since then, these modified surfaces have found a plethora of different uses ranging from studies of electrochemically active attached molecules,[118] catalysis,[119] inhibition of electrochemical processes[117], sensing[120,121] and even use in asymmetric electrosynthesis (see section **2.1.5.4**).[68,72,77,122,123] In this section I will introduce some of the basic electrochemical techniques and theories that feature throughout this thesis.

1.3.1 Electrosynthesis

Before discussing the more theoretical aspects of electrochemistry, I thought it would be fitting to include a couple of examples where electrosynthesis is utilised in the real world. An example of this is the electrolytic process that is used on a large industrial scale in the production of chlorine and sodium hydroxide from concentrated brine.[124] This technology uses an electrolysis cell that is divided into two sections by a cation–permeable membrane. This facilitates the transfer of sodium ions from one side of the electrochemical cell to the other. At the anode the chloride ions are oxidised to chlorine gas, which is then isolated as it “bubbles” out of the solution, whereas at the cathode water is being reduced to hydrogen and hydroxyl anions that go on to form the sodium hydroxide (as illustrated in Figure 7).[125]

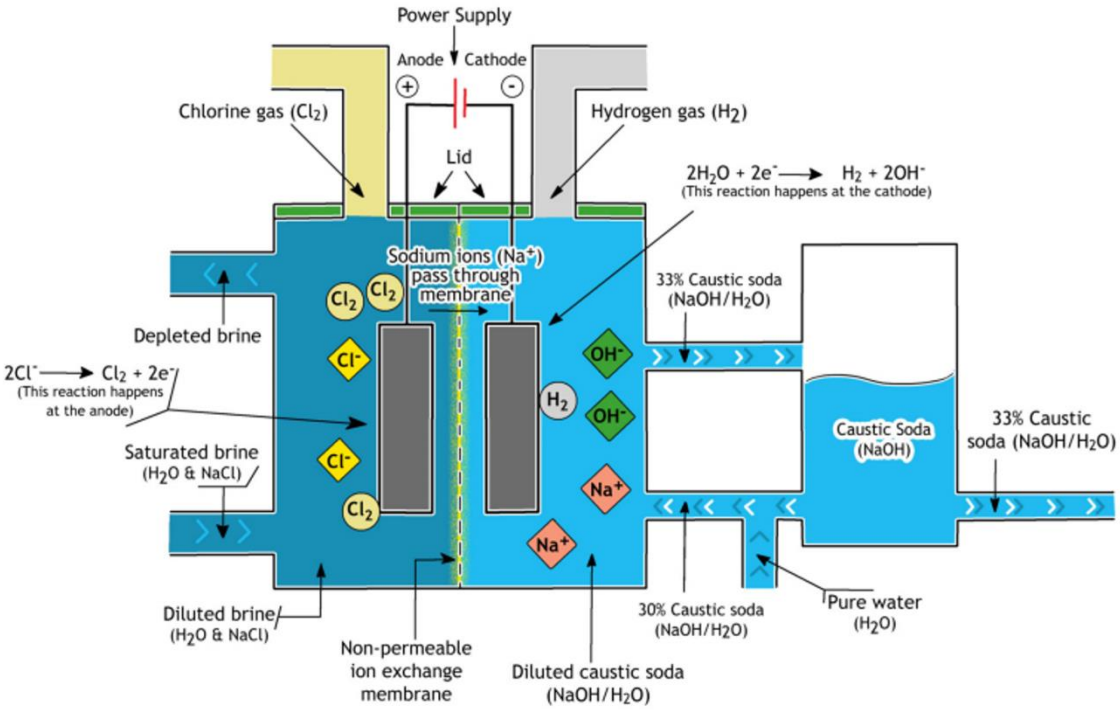

Figure 7: Schematic of a membrane cell system used in the electrochemical chloralkali process. Image reproduced from reference.[126]

It has been shown that the use of modified electrodes in electrochemical synthesis can catalyse electrolysis reactions. The work conducted by Dong and co-workers demonstrated that a polyaniline film electrode doped with cobalt phthalocyanine could be used to catalyse the reduction of dioxygen to hydrogen peroxide. The use of the modified GCE significantly shifts the potential of the redox process to a more positive voltage compared to performing the same reduction at an unmodified GCE, this ability to reduce the overpotential required to drive the synthetic reaction is a key aspect in this type of research.[119]

1.3.2 Electrochemical equilibria and electrochemical potentials

A simple example of an electrochemical equilibrium is described by an aqueous solution containing $[Fe(CN_6)]^{3-}$ (depicted as reagent **A**) and $[Fe(CN_6)]^{4-}$ (depicted as reagent **B**), Scheme 24. When an electrode, such as platinum wire, is added to this system the solution now has a source or sink of electrons and an electrochemical equilibrium is established at the surface of the electrode. The formation of this equilibrium is responsible for the difference in

charge between the solution and the electrode surface, this difference is known as the electrode potential ($\varphi_m - \varphi_s$).

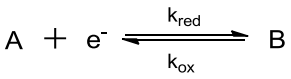

Scheme 24: Electrochemical equilibrium between $[Fe(CN_6)]^{3-}$ (depicted as reagent A) and $[Fe(CN_6]^{4-}$ (depicted as reagent B) in the presence of an electrode

Unfortunately it is impossible to measure the electrode potential of a single electrode-solution interface. For a measurement to be made possible, another electrode must be added into the system and the difference in the potential of these two electrodes can then be measured to give the "measured electrode potential" (*E*), described in Equation 1. This additional electrode is known as the reference electrode $(\varphi_m - \varphi_s)_{ref}$ and is assigned an arbitrary value.

$$E = (\varphi_m - \varphi_s)_{Pt} - (\varphi_m - \varphi_s)_{ref}$$

Equation 1: The measured electrode potential (*E*) using a platinum working electrode *vs*. a reference electrode.

In the systems discussed in this thesis the aqueous electrochemistry is referenced against a standard calomel electrode (SCE) which has a constant potential of +0.242 V *versus* the standard hydrogen electrode. The SCE is comprised of a column of liquid mercury coated with an insoluble layer of mercury(I) chloride (traditionally know as calomel). Both of these species of mercury are submerged in an aqueous solution saturated with potassium chloride, as illustrated in Figure 8. Non-aqueous systems are referenced to a silver wire. This is not a fixed thermodynamic reference electrode as it only constitutes one redox half-reaction rather than a pair of redox reactions and hence is called a "*pseudo*-reference electrode". Unfortunately the potential of this pseudo-reference electrode is subject to drift and therefore must be referenced internally to a standard redox couple, in this work the $Cp_2Fe^{0/+}$ redox couple is used (where possible) following IUPAC recommendations.[127]

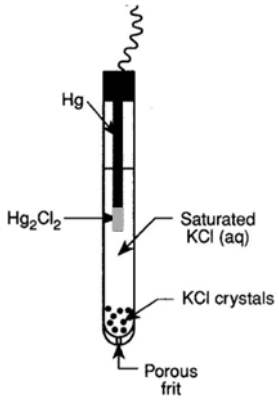

Figure 8: Schematic of a calomel reference electrode. Image adapted from reference.[128]

A change in the concentration of ions at the surface of the electrode results in a change of the electrode potential. This relationship is described by the Nernst equation, which can be derived from the Gibbs free energy Equations 2-4. It is important to bear in mind that all useful work conducted in an electrochemical cell is electrical work (provided the redox process describes a reversible electrochemical reaction at constant temperature and pressure) which is attributed to the movement of charges and therefore Gibbs free energy in such systems is equal to the electrical work done (Equation 3).

$$\Delta G = \Delta G^{\circ} + RTlnK$$

Equation 2: Relating change in Gibbs free energy (Δ*G*) to change in Gibbs free energy under standard conditions (Δ*G*°). *R* is the ideal gas constant (8.314 J K^{-1}), *T* is the temperature (K) and *K* is the equilibrium constant of Scheme 24

$$\Delta G = -nFE = W_{electrical}$$

Equation 3: Showing the relationship between the electrical work done ($W_{electrical}$) and the change in Gibbs free energy. *n* is the number of moles of electrons passed, *F* is Faradays constant (96485 C mol^{-1}) and *E* is the cell potential.

$$\Delta G^\circ = -nFE^\circ$$

Equation 4: Shows relationship between ΔG° and standard electrode potential E°

Substitution of equations 2 and 3 into 4, after rearrangement, yields the Nernst equation (Equation 5). This equation relates the observed reduction potential of the cell to the standard reduction potential and the concentration of A and B at the surface of the electrode. This is purely a thermodynamic relationship and does not contain any information about the kinetics of the system. In rigorous treatments, the concentrations of A and B are not used in the Nernst equation due ion-ion and solvent-ion interactions. Instead, concentrations are replaced by the activities of the relevant species by using the activity co-efficient *γ*. In an ideal system the activity coefficients will approach unity.

$$E = E^\circ - \frac{RT}{nF}\ln\left(\frac{\gamma_A[B]}{\gamma_B[A]}\right)$$

Equation 5: The Nernst equation. [A] is the concentration of A (mol dm^{-3}), [B] is the concentration of B (mol dm^{-3}), γ_x is the activity co-efficient of A or B. *F* is Faraday's constant, *R* is the universal gas constant and *n* is the number of electrons transferred in the redox event.

1.3.3 Kinetics of a one–electron transfer

It is important to remember that although the Gibbs free energy (or electrode potential) can determine if a reaction is favoured, it does not yield any information about the kinetics or rate of the reaction.

To illustrate this, first consider the simple electrolysis reaction depicted in Scheme 24. If a potential, that is not equal to the potential at equilibrium, is applied to this electrochemical system, then an electrochemical reaction can be driven to force the net oxidation of B or the net reduction of A and, in doing so, cause a current to flow between the electrode and the solution. The magnitude of this current, *i*, for the electrode reaction is directly proportional to the area of the electrode surface, *A*, and the flux, *j*, as shown in Equation 6.

$$i = nAFj$$

Equation 6: Current of the electrochemical oxidation of species B. *i* is the current attributed to the oxidation process (B), *n* is the number of electrons transferred during the redox event, *F* is Faraday's constant and *j* is the flux (mol cm^{-2} s^{-1}).

It is important to note that during electrolysis, the concentration of the bulk solution is not equal to the concentration at the electrode surface. By assuming that the transfer of electrons at the electrode is much faster than the rate of mass transport, we can consider the net flux to be equal to the relative rates of the oxidative and reductive electrochemical reactions, approximated as first order processes (Equation 7). Note that at equilibrium the relative rates of the oxidative and reductive reactions are equal.

$$j = j_{ox} - j_{red} = k_{ox}[B] - k_{red}[A]$$

Equation 7: Overall rate equation

The overall current is therefore equal to the sum of the currents passed during the reductive and oxidative processes, shown in Equation 8. By convention i_{ox} is positive and i_{red} is negative giving rise to the minus sign.

$$i = nFA(j_{ox} - j_{red})$$

Equation 8: Current passed at electrode surface

By substitution of Equation 7 into Equation 8 we arrive at Equation 9 that relates the current passed during the electrolysis to the concentration of A and B at the surface of the electrode.

$$i = FA(k_{ox}[B] - k_{red}[A])$$

Equation 9: Relating the current at the electrode surface to the concentration of A and B at the electrode surface.

Changing the applied potential away from that of the standard (equilibrium) potential by an amount, Δ*E*, lowers the Gibbs free energy attributed to either the oxidised (A) or reduced species (B). This extra driving force from the change in potential is called the overpotential (η) and is described in Equation 10. The effect of this is that as the potential is increased, the Gibbs energy associated with the oxidised species (A) is decreased relative to that of the reductive species (B), and this drives the reaction towards the formation of the oxidised species (A). Furthermore, it is important to note that although the Gibbs free energy of the oxidised species is decreased by *F*Δ*E*, the activation barrier only changes by a fraction of this energy difference. The fraction that the activation barrier energy changes relative to the applied potential reflects the symmetry of the transition state. This is accounted for by the charge transfer coefficient (α) and represents a $(1-\alpha)F\Delta E$ decrease in the activation energy for an oxidation process – but represents an $\alpha F\Delta E$ increase in activation energy for a reduction process. When α approaches 0 the transition state is said to resemble the reactant; alternatively, when α approaches 1 the transition state resembles the product. This allows the change in the Gibbs free energy of activation to be defined in terms of the applied potential, as shown in equations 11 and 12.

$$\eta = E - E^0$$

Equation 10: Definition of the overpotential (η)

$$\Delta G_{red}^{\neq} = \Delta G_{red}^{\neq 0} + \alpha F(\eta)$$

Equation 11: Relating the Gibbs energy of activation of the reductive process at an applied potential to the free energy of activation under standard conditions.

$$\Delta G_{ox}^{\neq} = \Delta G_{ox}^{\neq 0} - (1-\alpha)F(\eta)$$

Equation 12: Relating the Gibbs energy of activation of the oxidative process at an applied potential to the free energy of activation under standard conditions.

The observed rate constants k_{red} and k_{ox} can be expressed in the form of Arrhenius equations 13 and 14 and are used to relate the applied potential, *E*, to the rate constant. Note this requires the assumption that the activation energy (E_A) is approximate to Gibbs free energy of activation.

$$k_{red} = A_{red}\exp\left(-\frac{\Delta G_{Red}^{\neq}}{RT}\right)$$

Equation 13: Arrhenius equation relating the rate constant of the reductive process to the Gibbs free energy of activation

$$k_{ox} = A_{ox}\exp\left(-\frac{\Delta G_{ox}^{\neq}}{RT}\right)$$

Equation 14: Arrhenius equation relating the rate constant of the oxidative process to the Gibbs free energy of activation

Substitution of equations 11 and 12 into equations 13 and 14**,** respectively, yields the Arrhenius type equations 15 and 16 as shown below.

$$k_{red} = A_{red}\exp\left(-\frac{\Delta G_{red}^{\neq o}}{RT}\right)exp\left(-\frac{\alpha F\eta}{RT}\right)$$

Equation 15: Arrhenius equation relating the rate constant of the reductive process to the Gibbs free energy of activation and the over potential

$$k_{ox} = A_{ox}\exp\left(-\frac{\Delta G_{ox}^{\neq o}}{RT}\right) exp\left(\frac{(1-\alpha)F\eta}{RT}\right)$$

Equation 16: Arrhenius equation relating the rate constant of the oxidative process to the Gibbs free energy of activation and the over potential

It is apparent that equations 15 and 16 are made up of two sections: the first is independent of the applied electrochemical potential and is known as the standard electrochemical rate constant (k^0), the second half of these equations is dependent on the applied electrode potential. This information allows for the simplification of equations 15 and 16 to equations 17 and 18 by substitution of the electrochemical rate constant**.**

$$k_{red} = k^0 exp\left(-\frac{\alpha F}{RT}\eta\right)$$

Equation 17: Simplification of Arrhenius equation 15

$$k_{ox} = k^0 exp\left(\frac{(1-\alpha)F}{RT}\eta\right)$$

Equation 18: Simplification of Arrhenius equation 16

When equations 17 and 18 are substituted into equation 9 we arrive at a form of the Butler-Volmer equation (shown in Equation 19). The Butler-Volmer equation describes the fundamental relationship between the current passed in an electrochemical system and the potential applied.

$$i = FAk^o \left\{ [B] exp\left(\frac{(1-\alpha)F\eta}{RT}\right) - [A] exp\left(-\frac{\alpha F\eta}{RT}\right) \right\}$$

Equation 19: A form of the Butler-Volmer equation

1.3.4 Cyclic Voltammetry

Cyclic voltammetry is a common technique utilised in electrochemistry. It is used to characterise the electrochemical processes occurring at the interface between the electrode and the electrolyte solution. This method involves applying a potential to the working electrode that changes linearly over time as shown in Figure 9A, the rate at which the potential changes is called the voltage scan rate (ν). The potential of the working electrode starts at potential E_1 and then either increases or decreases in potential to E_2 at which point the sweep direction is reversed and the potential starts decreases or increasing until the stop potential E_3 is reached; at this point the experiment is normally stopped. Note that in most experiments E_1 is the same as E_3 but this does not need to be the case. While the experiment is running the flow of current through the working electrode is recorded as a function of the applied potential; this plot is known as a "cyclic voltammogram" and is shown in Figure 9B.

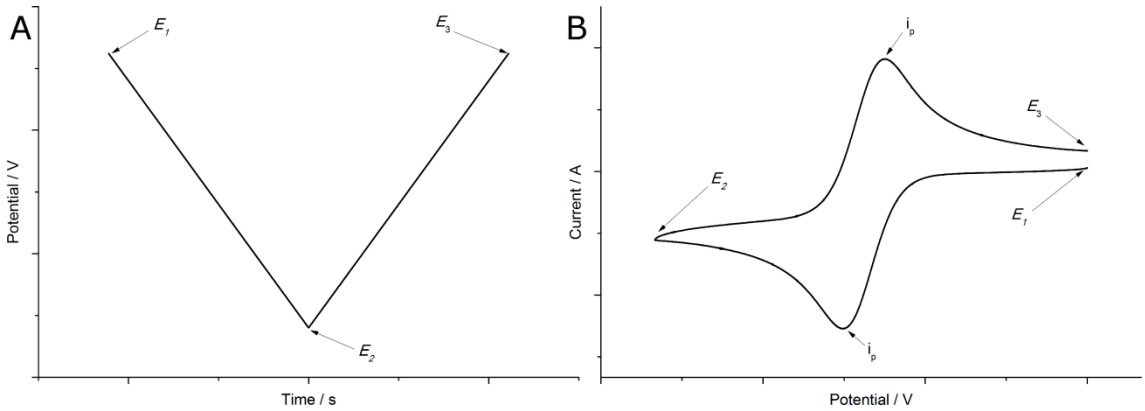

Figure 9: (A) Graph depicting the potential over time applied during a CV. (B) Typical cyclic voltammogram of a reversible species. (i_p is the peak current)

In reversible systems where the analyte is dissolved in the electrochemical solution (i.e. not immobilised onto the electrode) the wave shape shown in Figure 9B is typical. The

reason for this is that as the potential approaches i_p the current caused by the electrolysis increases and should, in theory, keep rising exponentially, as described by the Butler-Volmer equation. In reality, however, the concentration of the analyte at the surface of the electrode decreases as the reactants are consumed. A drop in the current passed is then observed when the rate of the electrolysis becomes dependent on the rate that fresh analyte is able to diffuse from the bulk solution to the electrode surface (resulting in the current being limited by mass transport).

The peak current is described by the Randles-Sevcik equation (Equation 20), which shows that in a diffusion-controlled system the peak potential is proportional to the square root of the voltage scan rate. This is because at faster scan rates the diffusion layer is smaller and therefore the driving force (concentration gradient) for the diffusion of fresh analyte to the electrode surface is greater, resulting in a larger current. At slower scan rates, the diffusion layer is larger and therefore diffusion of fresh analyte to the electrode surface is slower, resulting in a smaller current. Note that stirring the electrochemical solution has the effect of compressing the size of the diffusion layer and therefore increasing the current response.

$$i_p = 268600 n^{\frac{3}{2}} A D^{\frac{1}{2}} C v^{\frac{1}{2}}$$

Equation 20: The Randles-Sevcik equation for a reversible system under standard conditions. *n* is the number of electrons passed in the redox event, *A* is the area of the electrode (cm^2), *D* is the diffusion coefficient ($cm^2 s^{-1}$), *C* is the concentration of the analyte (mol cm^{-3}), *v* is the scan rate (V s^{-1}).

Conversely, in systems where the analyte is absorbed onto the electrode surface the peak current is directly proportional to the voltage scan rate, as shown in Equation 21. As all of the redox active species are constantly present on the electrode surface, mass transport effects are not relevant.

$$i_p = \frac{F^2}{4RT} \nu A \Gamma$$

Equation 21: Equation describing the peak current (i_p) of an absorbed analyte. *F* is Faraday's constant, *R* is the ideal gas constant, *v* is scan rate (V s^{-1}), *A* is the area of the electrode (cm^{-2}) and *Γ* is the surface coverage of the analyte (mol cm^2).

1.3.5 Chronoamperometry

Chronoamperometry is an electrochemical technique where, unlike in cyclic voltammetry, the potential of the working electrode is held at a constant voltage throughout the experiment, as shown in Figure 10A, and the change in the current is recorded against time, as shown in Figure 10B.

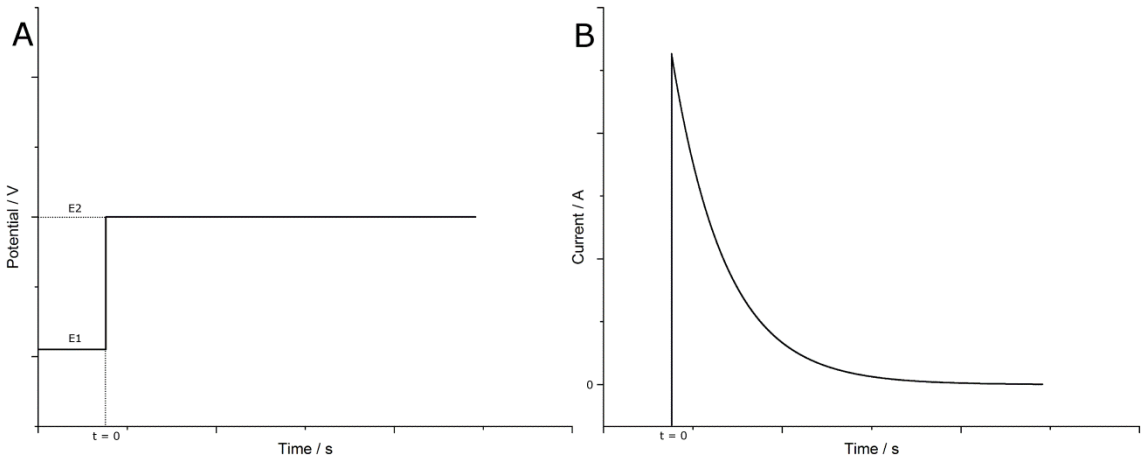

Figure 10: (A) Graph depicting the potential over time applied during a CA. (B) Typical chronoamperometry of a electrochemical analyte

At the beginning of the experiment the potential is held at E_1 until t=0 at which point the potential is stepped up (or down) to E_2. While the potential is held at E_2 the change in current over time is recorded. The large initial spike in the current consists of both Faradaic and non-Faradaic components. The non-Faradaic component arises from the capacitive charging of the system caused by the migration of electrolyte to the electrode surface to match the build-up of charge on the electrode upon an instantaneous change in voltage at the electrode surface. The capacitive charging current rapidly decays exponentially over a short period of time

(typically 10-20 µs). The rate at which the Faradaic component of the current that is associated with the electron transfer redox reactions decays at a macrodisk electrode is much slower and is described by the Cottrell equation (Equation 22).

$$i = \frac{nFACD^{\frac{1}{2}}}{\sqrt{\pi t}}$$

Equation 22: The Cottrell equation. *i* is the current passed. *n* is the number of electrons passed during the redox event, *F* is Faraday's constant, *A* is the area of the electrode (cm^2), *C* is the concentration of the analyte, *D* is the diffusional coefficient ($cm^2\ s^{-1}$) and *t* is time (s).

The Faradaic current passed is once again controlled by the rate at which the analyte is able to diffuse into the electrode double layer and decays to zero with infinite time. Stirring the solution has the effect of decreasing the size of this diffusion layer surrounding the electrode, improving mass transport of analyte and resulting in a steady-state current (until the supply of analyte in the solution is completely exhausted).

A related technique commonly utilised in electrolysis is chronopotentiometry wherein the cell demands a constant current and the change in voltage over time is recorded.

In this research, chronoamperometry will be used to reduce analytes on a scale that will significantly change their concentration in the bulk solution. To calculate the number of moles of product formed in these electrolysis reactions, Faraday's constant can be used as shown in Equation 23. Furthermore, due to significant changes in the concentration of the bulk solution, the resting potential or Nernst potential of the electrochemical cell will also change during the course of the electrosynthetic reactions.

$$\frac{C}{F} = n$$

Equation 23: Calculating the number of moles of electrons passed during an electrolysis reaction (*n*). *C* is the charge passed during the electrolysis (coulombs), *F* is Faraday's constant.

Unfortunately Equation 23 does not take into account any additional charge that is passed due to non-Faradaic processes and therefore the Faradaic yield is quoted as a percentage of the

number of moles of isolated product (times by the number of electrons required to form the product) against the number of moles of electrons passed during the electrolysis.

1.4 Aims

My primary goal is to develop a chiral calixarene electrode surface that could be used in the enantioselective electrolysis of simple prochiral compounds. It had been shown by other research groups that an electrode functionalised with chiral peptide chains can be used in electrosynthetic reductions of achiral starting materials to form optically active compounds, albeit with less than desirable optical purity. [70,72] It was hypothesised that immobilised calixarenes when sufficiently decorated with amino acids would be able to encourage binding of substrates sufficiently close to the upper rim of the macrocycle to allow for electron transfer between the chemisorbed calixarenes and the substrate. The peptido-calix[4]arenes have shown promise as enzyme mimics and have been utilised in the literature in asymmetric reactions due to their ability to bind substrates, through strong hydrogen bonding interactions, around the deep hydrophobic cavity [108,129,130] This property of the calixarenes will be exploited in an attempted to impart chirality onto the electrosynthetic products.

To test this hypothesis the synthesis of a calixarene that could be tethered to an electrode surface is required. Ideally the macrocycle could be attached by either the upper or lower rim to determine if access to the hydrophobic cavity was of importance in the asymmetric reductions (Figure 11). The opposite face of the calixarene are required to be functionalised by a wide array of different substrates, either in solution before the immobilisation of the macrocycle or while the calixarenes are bound onto the electrode. This can then be later used to fine tune the properties of the modified surfaces.

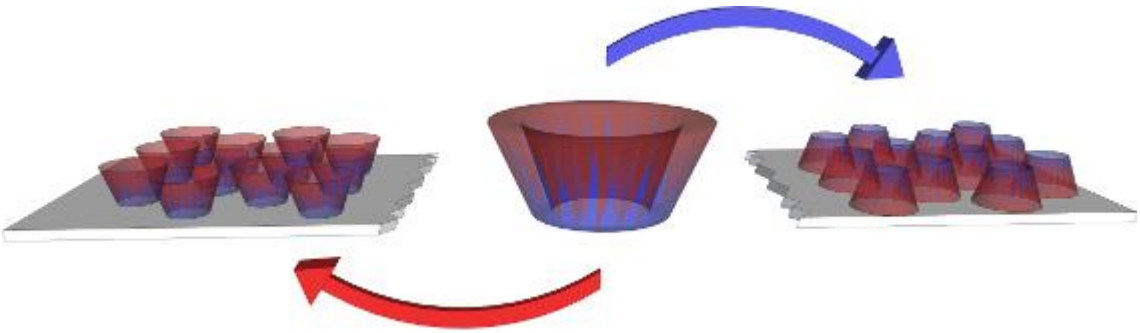

Figure 11: A cartoon showing the fabrication of an electrode surface by either the upper or lower rim of a calixarene. The blue side of the conical shape represents the lower rim and the red side of the cone represents the upper rim.

Initially, to demonstrate that attachment of the macrocycles was successful the calixarenes are modified with electrochemical labels to facilitate their detection and characterisation by electrochemical techniques. Note that the synthesis and surface attachment of these compounds has been published by the author.[131] The final chapter of this thesis is dedicated to the formation of the chiral calixarenes surfaces and their use in the electrosynthetic reduction of prochiral starting materials, and is compared to the same reduction reactions conducted using an unmodified GCE.

Chapter 2

Results and discussion

Synthesis of Calix[4]arenes

2.1 Overview

Within this chapter I will discuss the synthesis of several novel calixarenes that were used in the functionalisation of glassy carbon electrodes (GCEs). The calixarenes were designed to allow for attachment to the electrode by one rim and the other rim could then be modified with a variety of substrates to allow for tuning of the surfaces in later work. It is important to note that these surfaces were required to be stable under strongly reductive conditions as they would be used for electrosynthetic reductions in later research. Throughout the synthesis of these molecules, maintaining the conical conformation of the macrocycles was essential as the intention was to utilise this structure to aid in the formation of chiral environments upon the electrode surface.

The first attachment protocol considered was an advancement of the work described by Lagrost and co-workers in 2012,[132] wherein they modified the upper rim of a calix[4]arene with four amino groups that were then converted to diazonium salts using $NaNO_2$. These salts were then electrografted onto an electrode surface using a reductive potential. In their research the exposed face of the calixarene was functionalised with four phenol groups to allow for modification of the immobilised surface by ester linkers. Due to the electrosynthetic applications, my research required a linker that would be stable under strongly reductive conditions and therefore esters were not appropriate. Instead the lower rim of the calixarene was functionalised with alkynyl groups to allow for attachment of a variety of substrates via an electrochemically stable triazole linkage.

This route was also attempted for the attachment of calixarenes to an electrode surface by the lower rim, but the synthesis of a calixarene core functionalised with four aryl amines at lower rim was unsuccessful so another route was required. I was inspired by the work first presented by Geiger and co-workers in 2013 wherein they developed a method for the immobilisation of porphyrins to an electrode surface using the electrochemical oxidation of pendant alkynyl groups.[133] This required the synthesis of a calix[4]arene functionalised with four propargyl ethers at the lower rim to allow for attachment of the molecule to the electrode surface. Furthermore, to facilitate the modification of the immobilised surfaces, the upper rim of the calixarene was functionalised with four azido groups that could be reacted with a variety of substrates using the copper(I) catalysed-azide-alkyne cycloaddition (CuAAC) reaction.

2.2 Synthesis of central calix[4]arene cores

The most common method used for the synthesis of calix[4]arene **60** is the base-catalysed condensation reaction that was first reported by Zinke in 1941,[134] this protocol has

since been refined by Cornforth[92] and Gutsche.[135] The synthesis involves the condensation of *p-tert*-butylphenol **58** and formaldehyde **59** in the presence of a catalytic amount of sodium hydroxide to yield calix[4]arene **60**, shown in Scheme 25.

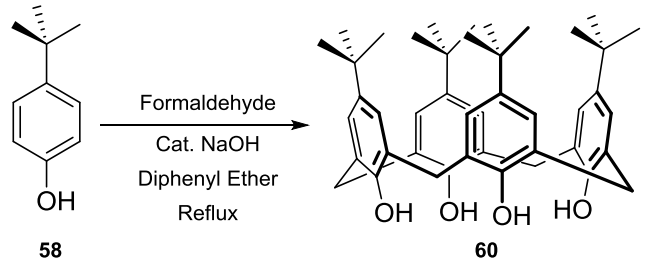

58 **60**

Scheme 25: Synthesis of calixarene 60

Calix[4]arene **60** was used as the main starting material, since it is relatively cheap and easy to synthesise on a large scale using the reaction conditions shown in Scheme 25. In spite of this, the synthesis of calix[4]arene from *p*-nitrophenol was attempted, to afford calixarene **76** directly from the condensation reaction. However, without the steric effects of the *t*-butyl groups the condensation of formaldehyde with *p*-nitrophenol lacked control and yielded a complex mixture of linear and cyclic oligomers, meaning any structural modification of the calixarene required post-funcationalisation of **60** as the structure of the monomer could not be varied. So functionalisation of the upper rim was conducted by removal of the *t*-butyl by the treatment of **60** with $AlCl_3$ to give **71**, using a modified procedure first reported by Gutsche and co-workers in 1982,[136] conditions shown in Scheme 26.

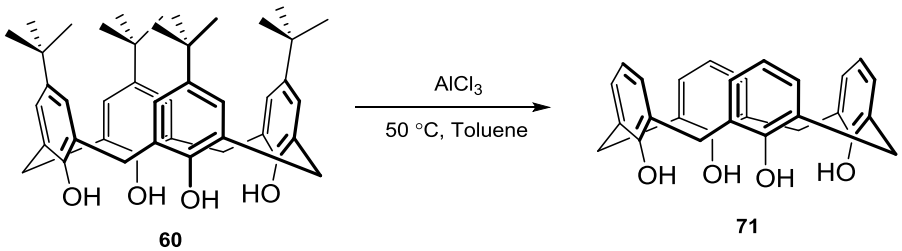

60 **71**

Scheme 26: Dealkylation of calixarene 60

It was important that the calix[4]arenes maintained the cone conformation, as the conical shape of the macrocycles was to be utilised in the formation of nano-reactor sites on

the electrode surface. Both calixarenes **60** and **71** have a mobile conformation in solution, as they contain free OH groups on the lower rim, allowing the phenol subunits to rotate around the methylenes. As such, they are able to interchange between any of the calix[4]arene conformations, including the desired cone shape. The degree of mobility varies from one ring system to another; this was observed when alkylating molecules **60** and **71.** Retention of the cone configuration of calixarene **71** required the use of a base with a small counter ion, such as sodium hydride (resulting in the formation of **72**), since the conformational stabilising effect of the coordinating counter ions has been shown to have a descending effect in the order of Li^+> Na^+ > K^+.[137] Otherwise, when attempting to alkylate **71** using a larger base, such as potassium carbonate, the main product was the calixarene in the partial cone conformation **73**. On the other hand, due to the bulky *t*-butyl groups on the upper rim of calixarene **60,** the alkylation of this compound using potassium carbonate in refluxing acetonitrile maintained the cone conformation **74**; reaction conditions shown in Scheme 27.

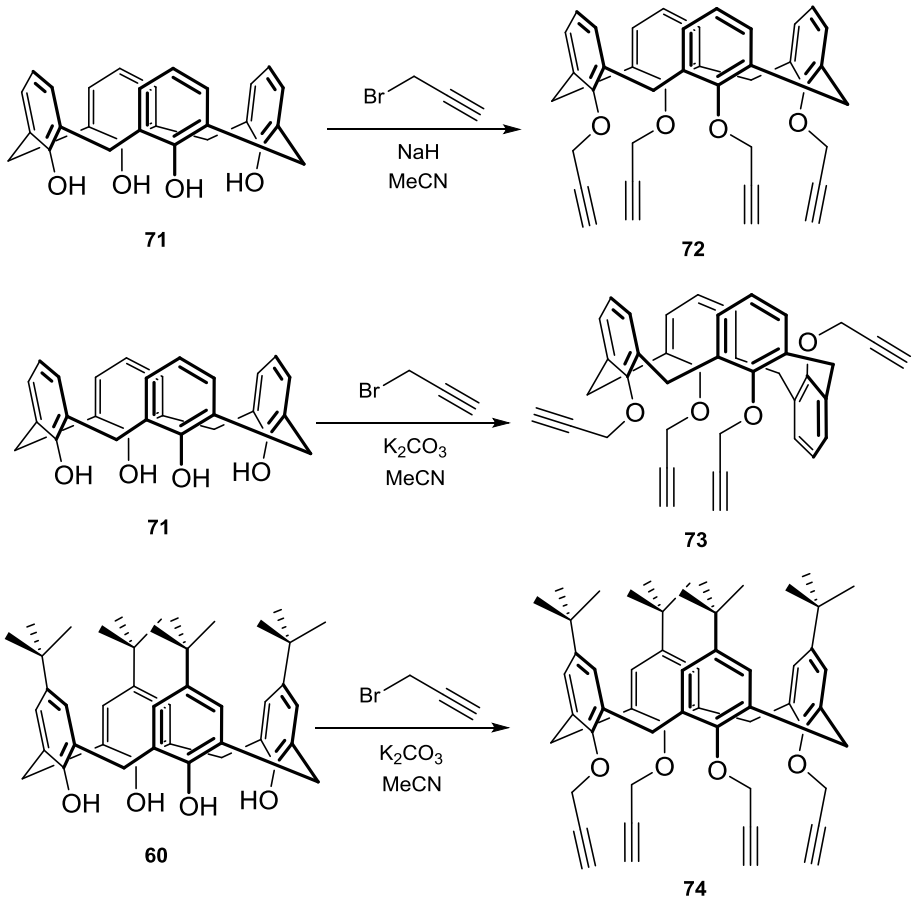

Scheme 27: Alkylation of calixarenes 60 and 71

2.3 Modification at the upper rim of calix[4]arenes before alkylation

One of the methods used to attach calixarenes to an electrode surface was a continuation of the work first presented by Geiger in 2013.[138] They described a method that allowed for the immobilisation of ferrocene moieties onto an electrode surface using pendant alkynyl groups as linkers. I wanted to adapt this methodology for the attachment of calix[4]arenes to an electrode surface, while using the upper rim of the calixarene to fine tune the modified surfaces both sterically and electronically. Initially, I attempted to modify the upper rim of the calixarene and then perform the alkylation with propargyl bromide on the lower rim.

2.3.1 Formation of *p*-nitrocalix[4]arene 76

Introduction of amino groups to the upper rim of calixarene **71** was attempted so that further functionalisation would be possible by peptide coupling reactions. This route required the formation of *p*-tetranitrocalix[4]arene **76** which could then be reduced to yield the *p*-tetraaminocalix[4]arene. The first reported synthesis of **76** (Scheme 28) was reported by Shinkai *et al*.[139] They showed a two-step synthesis from the *p-H*calixarene **71** to the product that included a sulfonation reaction using sulfuric acid followed by an *ipso*-nitration using a solution of nitric acid and sulfuric acid.

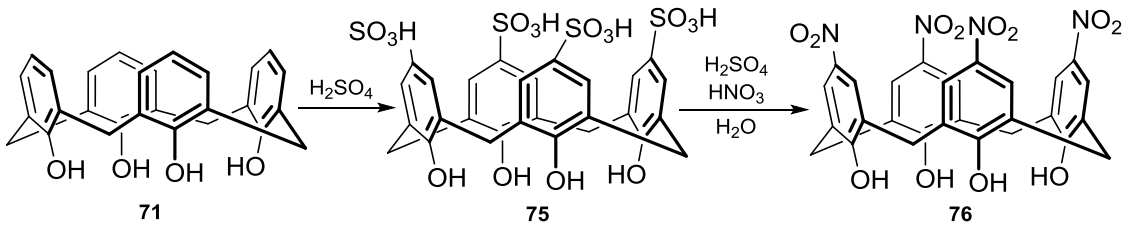

Scheme 28: Shinkai's synthesis of *p*-nitrocalixarene 76

I repeated the route described above but achieved a greater yield using a method described by Yong wherein calixarene **71** was dissolved in chloroform and nitrogen dioxide gas, generated from copper powder and nitric acid, was bubbled through the reaction mixture. After five minutes the reaction was complete and the product precipitated out of the solution as a yellow solid, which was then isolated by filtration. Unfortunately, functionalisation at the lower rim of *p*-tetranitrocalixarene **76** by nucleophilic alkylation with propargyl bromide was unsuccessful. This could be due to the electron withdrawing properties of the nitro functionalities reducing the nucleophilicity of the phenolic alcohols.

2.3.2 Modification at the upper rim pre-alkylation

Another method commonly employed for adding functionality to the upper rim of calixarene **71** is a pathway first described by Gutsche *et al* in 1998.[140] Molecule **71** is reacted with formaldehyde and dimethylamine under acidic conditions to form calix[4]arene **77**. In this reaction the ketone and secondary amine react to form an iminium intermediate that is then attacked by the aryl ring of the calixarene forming **77**. The Mannich base groups are then methylated by methyl iodide to form the corresponding quaternary ammonium salts. These act as good leaving groups and under basic conditions are eliminated from the calixarene to

form the *p*-quinonemethide intermediate. This is then able to react with a wide array of nucleophiles (Scheme 29) providing a particularly short route to a wide variety of functionalised calix[4]arenes, such as molecules **78a** and **78b**. Unfortunately, as this reaction proceeds through the quinonemethide intermediate the phenolic groups could not be alkylated prior to this reaction and so the cone conformation of the calixarene is not fixed at this point.

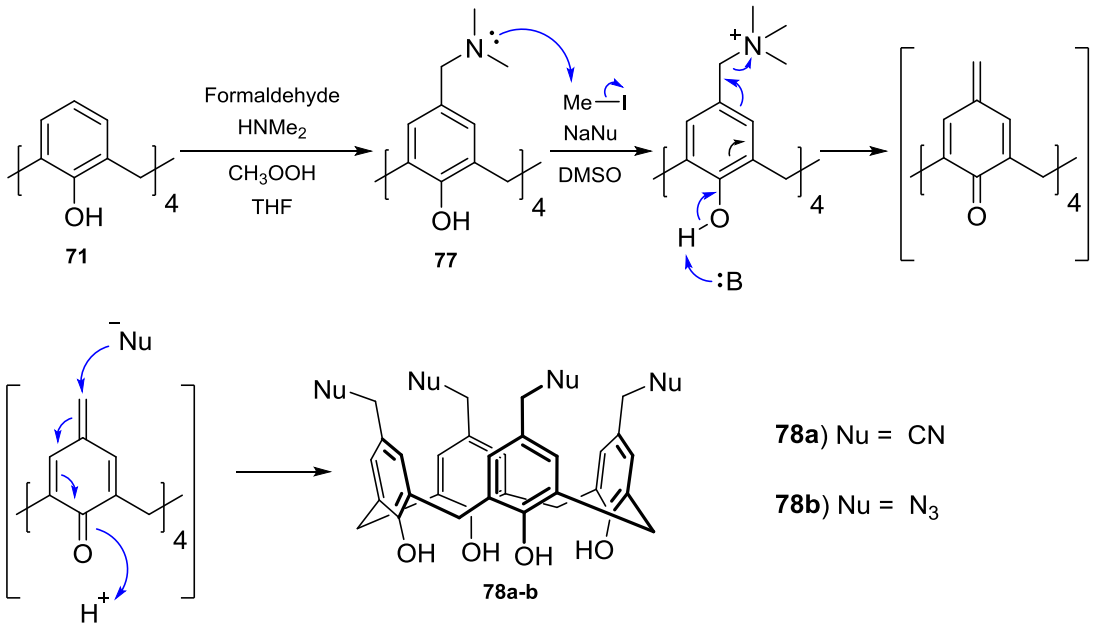

Scheme 29: Formation of calixarene 77 and mechanism of *p*-quinonemethide reactions

Alkylation at the lower rim of calix[4]arene **78a** was attempted using propargyl bromide in a range of different conditions but no conversion was observed. So hydrolysis of the cyano groups was conducted following a procedure reported by Gutsche,[141] wherein calixarene **78a** was reacted with sulfuric and acetic acid in the presence of water to form **79**. The alkylation was then attempted on molecule **79**, using propargyl bromide and sodium hydride, but the carboxylate groups on the upper rim of **79** also reacted with the propargyl bromide and formed propargyl esters, yielding **80**.The hydrolysis of the ester groups to the desired carboxylic acid functionalities, using both acid and base catalysed conditions, did not proceed as expected and I was unable to isolate any recognizable calixarenes.

Alkylation of calix[4]arene **78b** was also conducted using propargyl bromide and either NaH or K_2CO_3 as the base, but no formation of product was observed. For this reaction it was a

concern that the acidic protons on the terminal positions of the alkynes were affecting the reaction, so they were protected using silyl groups before the alkylation, but still no conversion was observed.

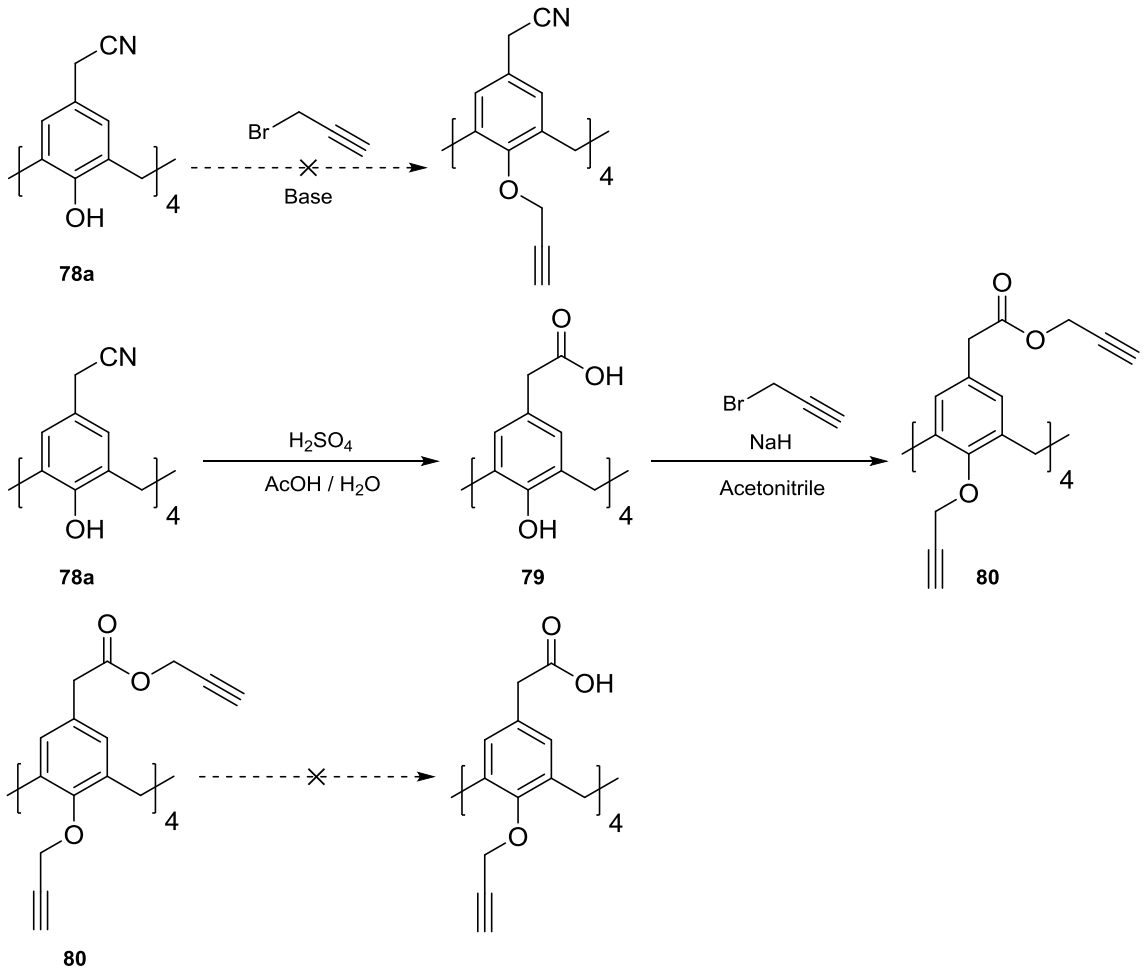

Scheme 30: Attempted modifications of molecule 78a

2.4 Modification at the upper rim post-alkylation

As discussed at the beginning of this chapter the synthesis of **72** by reaction of **71** with NaH and propargyl bromide proceeded in good yield. I then attempted to functionalise the upper rim of **72** with aldehydes using the Duff reaction;[142] these groups could then be oxidised to carboxylic acids allowing for further functionalisation by peptide coupling or condensation reactions. Unfortunately, although this reaction had been utilised for similar molecules in the literature[143] bearing propyl ethers on the lower rim of the calixarenes, the introduction of the

more reactive propargyl ether groups adversely affected the reaction, and no product formation was observed.

As the Duff reaction was unsuccessful I designed another route that would allow for functionalisation of the upper rim of calixarene **74** with amino groups. This route involved the *ipso* nitration of molecule **74** (i.e. with propargyl ether groups already incorporated onto the lower rim) and the subsequent reduction of the nitro groups to form amine functionalities. The nitration of calixarenes bearing simple alkyl ether at the lower rim has been reported previously in the literature[144] but never for calixarenes functionalised with propargyl ethers. Unfortunately, the nitration reaction of **74** proved to be very low yielding and unreliable. I hypothesised that this problem was due to the presence of reactive, unprotected alkynyl groups on the lower rim of the calixarene. Exposure of these alkyne groups to the harsh conditions of the nitration reaction could result in either their hydrolysis, or the electron-rich alkynes could be attacked by the electrophilic nitronium ion, as first reported by Bernardi and co-workers.[145]

To enable calixarene **74** to undergo nitration, the alkynyl groups needed to be protected by bulky silyl groups, *tert*-butyldimethylsilyl (TBMDS).The use of large silyl groups was important as they provided steric protection whilst ensuring that they were not cleaved under the harsh conditions used in the nitration reaction. The protection of the alkynes was conducted using a strong base, lithium bis(trimethylsilyl)amide, to remove the terminal alkynyl proton, and then TBDMSCl was added slowly at -78 °C, as shown in Scheme 31. Once isolated, the silyl-protected product **81** was then able to be nitrated to form calixarene **82**.

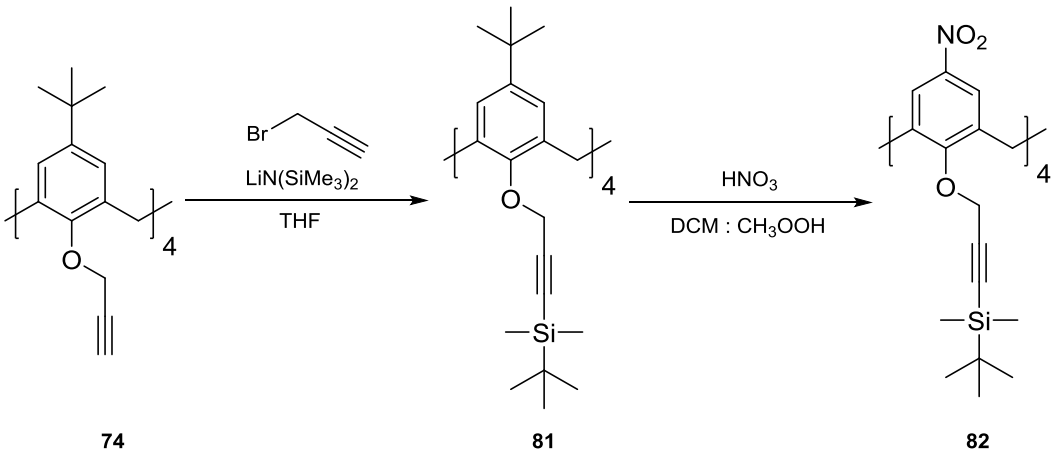

Scheme 31: Protection of calixarene 74 and the subsequent *ipso*-nitration

Although the TBDMS groups aided in the nitration reaction they needed to be removed from the molecule before it could be attached to an electrode surface. Removal of the silyl protecting groups was conducted using a solution of tetrabutylammonium fluoride (TBAF) in THF at room temperature which, after purification by flash chromatography, yielded calixarene **83**. This was the first calixarene that I chemisorbed onto a GCE surface (more details in chapter 3) and due to the electrochemically active nitro substituents on the upper rim this molecule could be detected while immobilised on the electrode. This allowed for characterisation of the modified surface using electrochemical techniques.

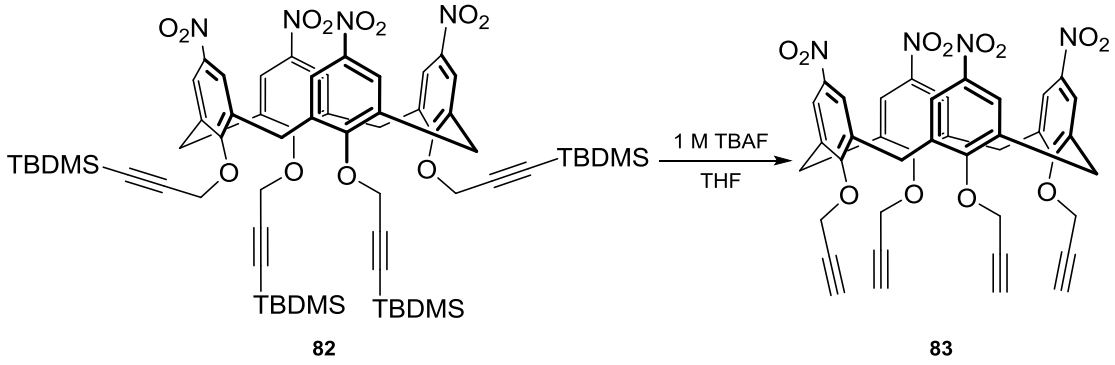

Scheme 32: Deprotection of 82 using TBAF

The importance of maintaining the conical conformation of the calixarenes has been highlighted throughout this chapter. The structure of **83** was determined both in the liquid and the solid state by NMR and X-ray crystallography respectively. In the NMR data of calixarene **83** two doublets at 4.72 and 3.49 ppm are observed. These signals are attributed to the bridging methylene protons between the aryl subunits, and this splitting pattern is diagnostic of a calixarene that is fixed into the cone conformation.[100,146] Furthermore, the crystallographic structure (shown in Figure 12) clearly reveals that the calixarene is in the conical conformation in the solid state.

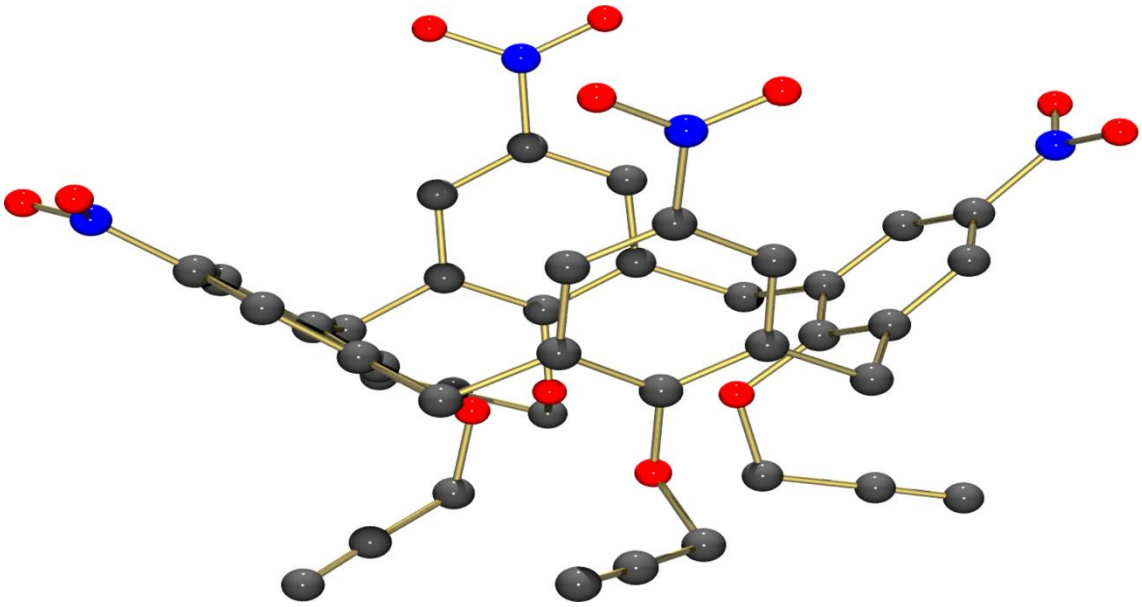

Figure 12: X-ray crystallographic structure of compound 83

Although I was able to attach molecule **83** to an electrode surface and observe its electrochemical response, a system was required that would allow for the immobilised calixarene to be functionalised by an array of substrates. This was attempted by chemically reducing the nitro groups to amino groups to allow for modification of the calixarenes by peptide coupling reactions. The reduction was originally attempted using standard conditions such as palladium on carbon with hydrogen or hydrazine but these conditions proved to be too harsh for the alkynyl groups on the lower rim. So milder, more selective conditions were required such as the method first described by Bellamy *et al.* in 1984; this reaction involved dissolving the calixarene in a solution of degassed ethanol containing 5 equivalents of $SnCl_2(H_2O)_2$. The mixture was then refluxed for 48 hours (Scheme 33).[147] This gave good

conversation of molecule **82** to **84** but isolation of the desired product proved to be problematic, due to the amount of tin required to force the reaction to completion. This was an issue because the tin formed an insoluble salt that could not be removed by aqueous extraction alone. I overcame this problem by concentrating the reaction mixture under vacuum and stirring the residue in 2 M sodium hydroxide for 30 mins. This hydrolysed the tin salts to $NaSn(OH)_3$ which are water soluble and therefore easily removed by aqueous extraction, yielding **84** as a pure beige powder.

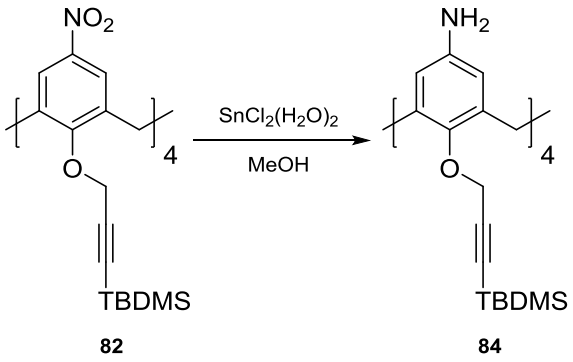

82 **84**

Scheme 33: Reduction of calixarene 82 using $SnCl_2(H_2O)_2$

The upper rim of calixarene **84** was to be modified with amino acids by a peptide bond. Unfortunately, after trying to optimise the conditions and using numerous different coupling reagents I was unable to form a peptide bond at the upper rim of the calixarene. Instead, the amino groups were converted to azido functionalities as this would allow for modification of the upper rim by the copper(I)-catalyzed azide-alkyne cycloaddition (CuAAC) reaction. Conversion of the amino groups was conducted using the Sandmeyer reaction wherein molecule **84** was dissolved in trifluoroacetic acid at 0°C before an aqueous solution of sodium nitrite was slowly added to form the diazonium salt. This was then either isolated by aqueous extraction and used as a crude intermediate or used *in situ* and reacted with sodium azide or sodium cyanide to afford molecules **86a** and **86b** respectively (Scheme 34). It is important to note that for reaction with sodium cyanide the diazonium salt first needed to be isolated as the reaction could not be conducted in the acidic conditions required for the salt formation, since this would protonate the sodium cyanide. The cyano groups on molecule **86b** could then be hydrolysed to carboxylate functionalities. Molecules **86a** and **86b** offered two possible routes to functionalise the upper rim of the calixarene core; however, I decided to

focus on applying the CuAAC reaction to molecule **86a** as it had several advantages over the peptide coupling reactions such as its ease of formation and stability in strongly reductive conditions.

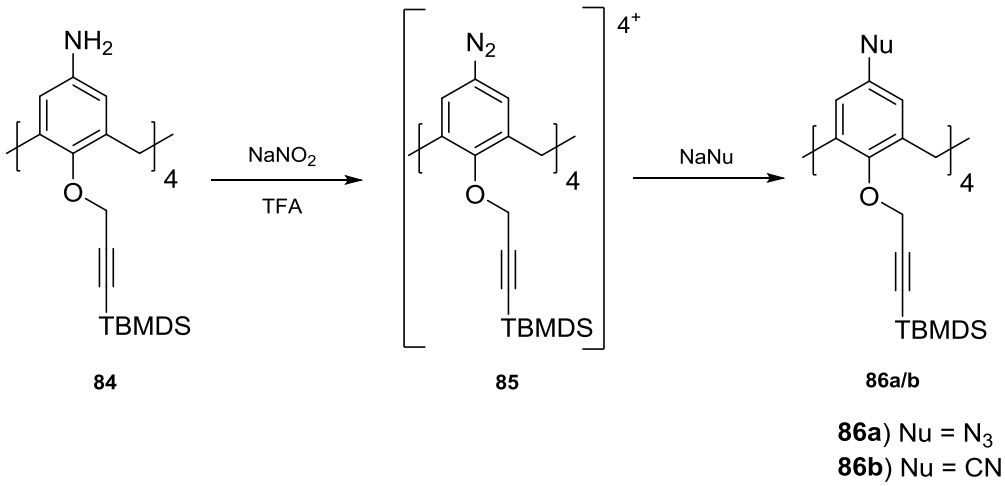

Scheme 34: Sandmeyer reaction of calixarene 84

Furthermore, before compound **86a** could be attached to an electrode surface the TBDMS groups needed to be cleaved using a 1 M solution of TBAF in THF resulting in the formation of compound **87**, shown in Scheme 35.

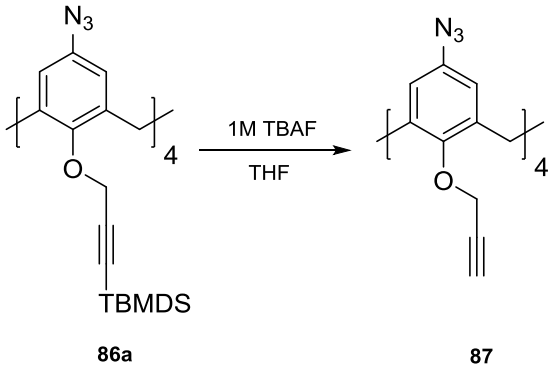

Scheme 35: Remove of TBDMS groups from molecule 86a

2.5 Modification of Calixarenes using the CuAAC reaction

Before electrografting the calixarenes onto an electrode surface some preliminary work was required to investigate the effectiveness of the CuAAC reaction on compound **86a**. The CuAAC reaction is one of the most commonly employed reactions in a set of "click" reactions as originally described by Barry Sharpless and co-workers in 2001.[148] Describing a set of reactions that are both high yielding and proceed under mild non-toxic conditions, the CuAAC reaction fits this description so well it has even been described as "cream of the crop" by Sharpless himself. The first CuAAC reaction attempted on molecule **86a** was with phenylacetylene **88** in the presence of a catalytic amount of Cu(I), made *in situ* by reaction of copper sulfate and sodium ascorbate. Initially, there were some difficulties with this reaction caused by the solubility of the calixarene in the water and alcohol solvent mixtures commonly employed for the reaction. This was addressed by adding a small amount of DCM to create a biphasic mixture and with rapid stirring the reaction was able to proceed to completion and converted all four of the azide functionalities to triazole groups, yielding molecule **89**. After functionalization of the upper rim, the TBDMS groups were then cleaved off the alkynes using similar conditions as those described for molecule **82**, shown in Scheme 32. These steps describe a route to synthesise a novel calixarene that is readily functionalised using the CuAAC reaction while maintaining the conical core of the calixarene.

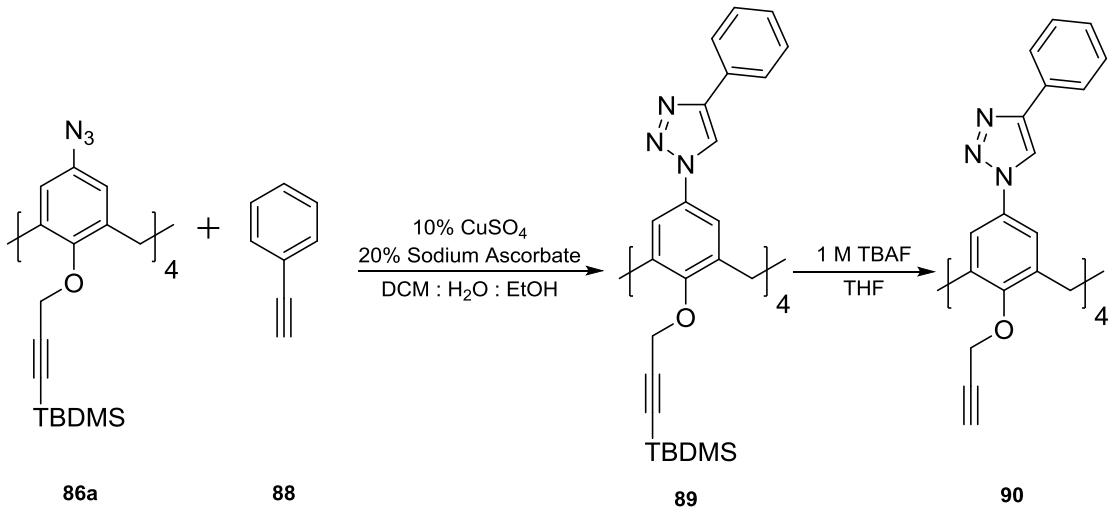

86a **88** **89** **90**

Scheme 36: Initial CuAAC reactions and subsequent deprotection

This initial research proved very promising in providing a method to allow for the formulation of an array of modified calixarenes. Now a procedure to observe the immobilised calixarenes on the electrode surface was required as well as a way of utilising the conical structure of the molecules to form chiral pockets, for the enantioselective reductions. It is important to note that molecules **94a-c** and **97b** were never directly bound onto the electrode surface. Instead calixarenes **87** and **85** were bound to the electrode by either oxidation of the lithio-activated alkynyl groups or reduction of the diazonium salts respectively. These surfaces were then further functionalised by the CuAAC reaction to tune the properties of the calixarene modified electrodes. We made a variety of different modifications to the immobilised calixarenes, making them electrochemically active, easily observable by XPS or chiral. Models of the immobilised calixarenes that were to be formed on the electrode surface (calixarenes **92, 94a-c** and **97b**) were synthesised in solution to demonstrate that their construction on the electrode was feasible and to confirm that they maintained the cone conformation after the CuAAC reaction.

I functionalised the upper rim of calixarene **86a** using 1-ethynyl-3,5-bis(trifluoromethyl)benzene **91** in the presence of a catalytic amount of Cu(I); conditions shown in Scheme 37. This afforded fluorine labelled compound **92** that would be readily detectable by XPS analysis when bound onto a GCE.

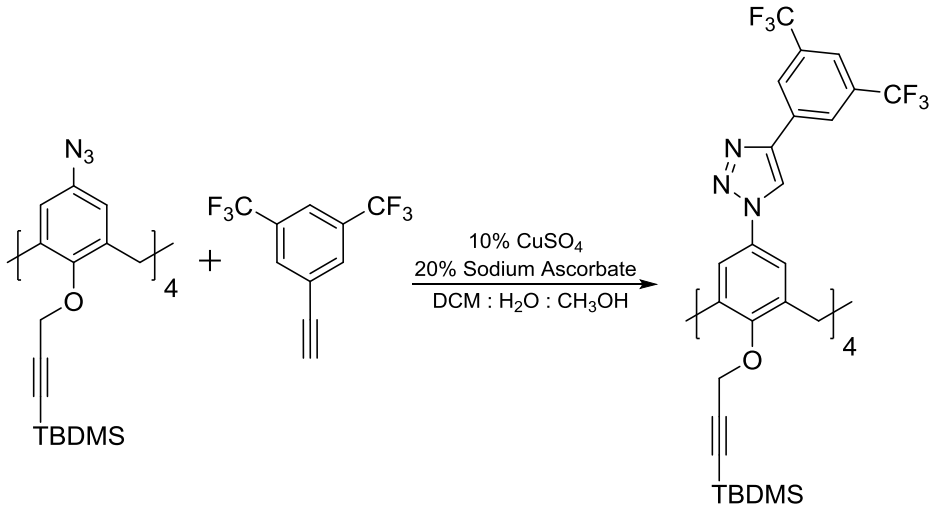

86a **91** **92**

Scheme 37: Formation of calixarene 92

The conical conformation of compound **92** was maintained during the CuAAC reaction; this was confirmed in the NMR data by the presence of the two methylene doublets and observed in the X-ray crystallographic structure shown in Figure 13.

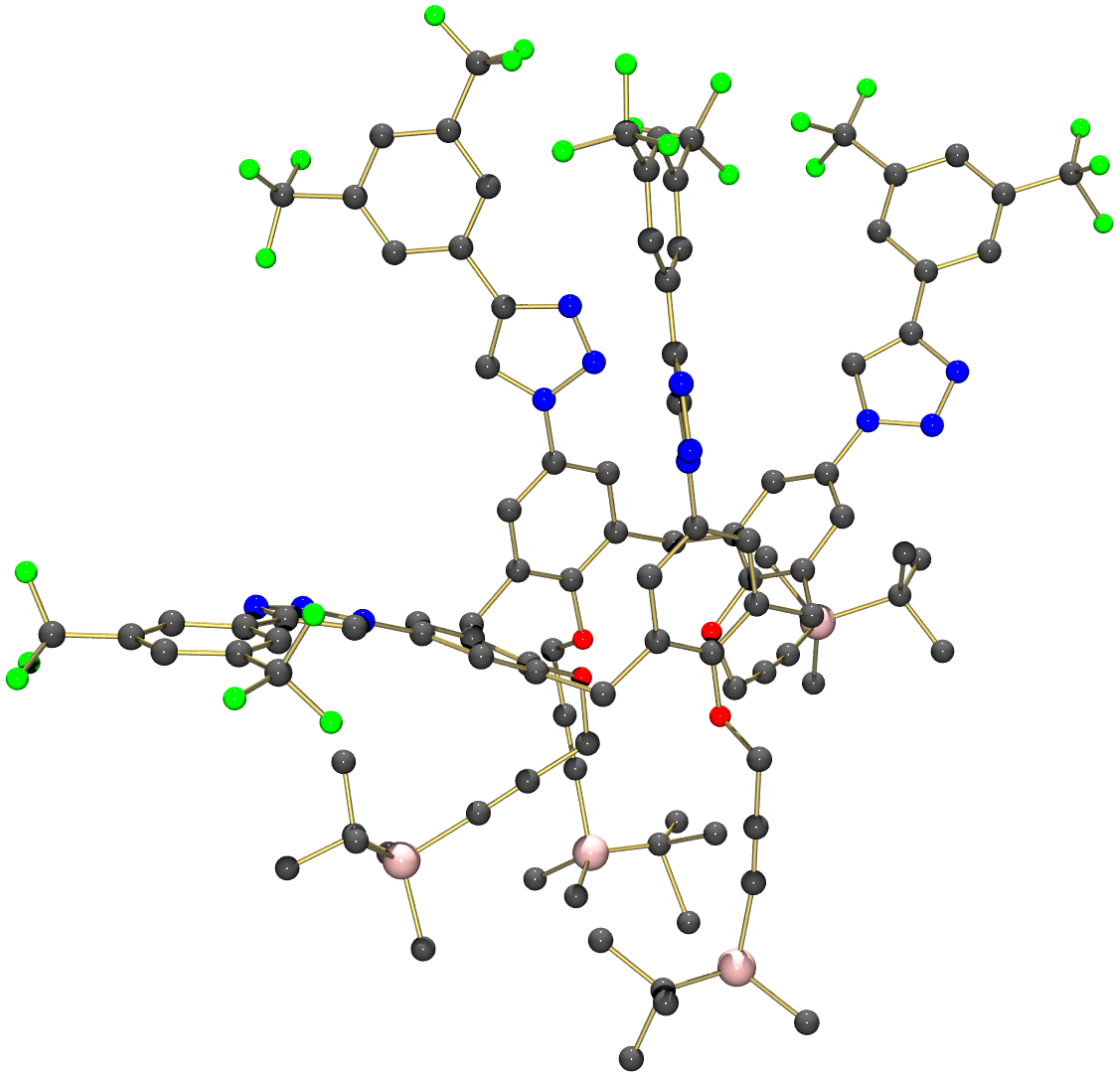

Figure 13: X-ray crystallographic structure of compound 92

2.5.1 Attachment of amino acids to the upper rim of calixarene 86a

To form the chiral cavities on the upper rim of the calixarene **86a** I attached amino acids to the calixarene using the CuAAC reaction. To do this I first needed to modify the amino acids with alkynyl groups to be able to form the triazole linkers. It was important that the propargyl groups attached onto the nitrogen atom of the amino acid and not the carboxylate functionality as the propargyl esters could be cleaved under strongly reductive conditions. Initially I speculated that the propargyl groups would attach to the nitrogen atom as opposed to the carboxylate, however I observed that the carboxylate attacked the propargyl bromide preferentially. So the carboxylate had to be first protected as the methyl ester to allow for alkylation at the nitrogen atom.

The next issue encountered was selectively forming the mono-alkylated amino acids, as opposed to the di-alkylated products that formed more favourably. I reasoned that this was caused by the secondary amine being more nucleophilic than the primary amine meaning that once one propargyl group was attached to the amine the second group attached much more readily, forming mainly the di-alkylated product. The best conditions for the formation of the monosubstituted amino acids were provided by a modified procedure based on one reported by Cho,[149] as shown in Scheme 38, although even with these optimised conditions a considerable amount of the di-alkylated product was still observed and the mono alkylated amino acid had to be isolated by flash chromatography. Obviously this was not an issue for the proline amino acid which was synthesised under slightly different conditions, as it was unlikely to be alkylated beyond the desired tertiary amine.

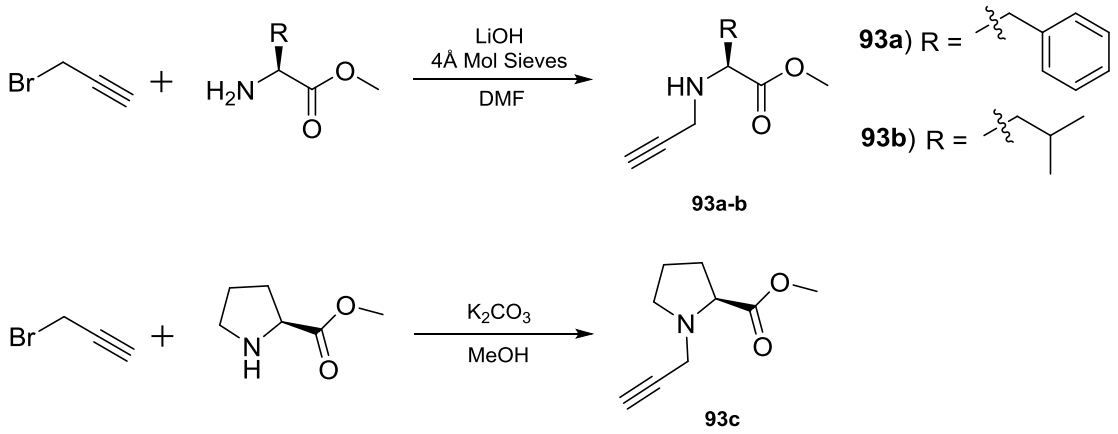

Scheme 38: Conditions used for alkylation of primary amino acids

I attempted to attach amino acids **93a**-**c** to the upper rim of calixarene **86a** using standard CuAAC reaction conditions, as described in Scheme 36. While using these conditions, however, I did not observe the formation of the desired products. Optimisation of the reaction using different sources of Cu(I), in a variety of solvents, at different temperatures, did not help the formation of the desired triazoles. The reaction was monitored using IR spectroscopy but throughout these experiments there was no decrease in the magnitude of the signal attributed to the azide vibration; it was speculated that the reaction was unable to proceed due to solubility issues, so a species of Cu(I) was synthesised that would be soluble in organic solvents, following a procedure published by Jarvis[150] wherein they synthesised tetrakis(acetonitrile)copper(I) hexafluorophate from Cu_2O in a solution of MeCN and HPF_6. The CuAAC reactions were then repeated using this new source of Cu(I) in acetonitrile and the progress of the reaction was followed by IR spectroscopy. Using the new catalyst I observed complete conversion of the azide functionalities to triazoles within 20 minutes for all three of the alkylated amino acids. An example of this is shown in Figure 14 where the reaction between **86a** and amino acid **93a** was monitored in the presence of $Cu[MeCN]_4PF_6$. At 2100 cm^{-1} the peak attributed to the azide stretch is visible at t=0 minutes but another spectrum recorded at t=20 minutes shows that the azide stretch is no longer present suggesting the reaction had gone to completion.

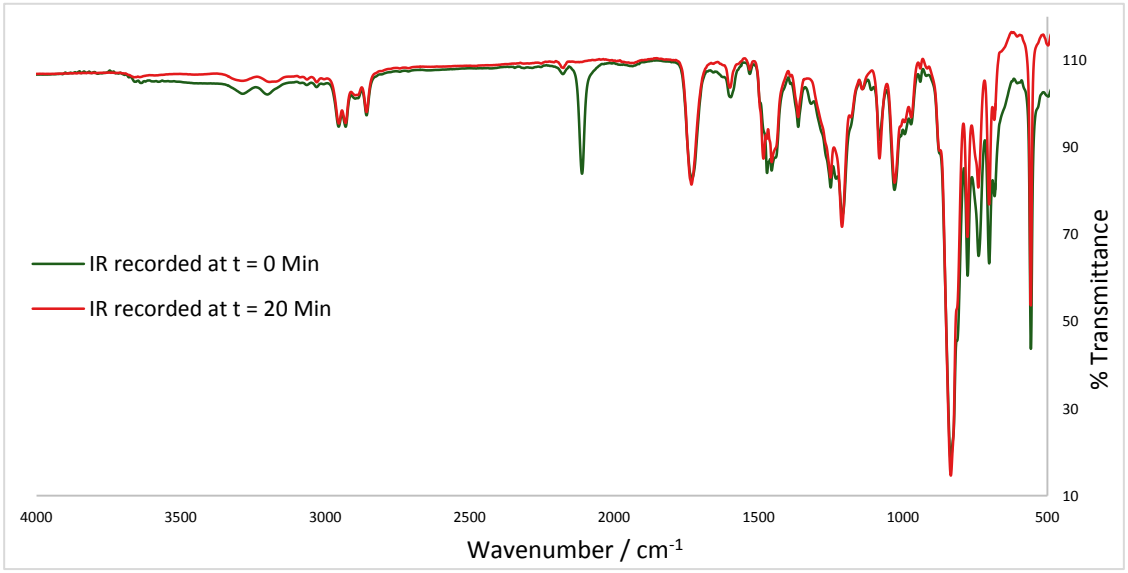

Figure 14: Overlaid IR spectra from the reaction mixture containing calixarene 86a and amino acid 93a in the presence of $Cu[MeCN_4]PF_6$

From the IR I was confident that the reaction had worked and believed a simple aqueous extraction followed by flash chromatography would afford the desired product. Unfortunately the NMR of the crude gave some peculiar results where all the signals in the NMR spectrum were broadened, suggesting the compound was complexed to the paramagnetic copper catalyst. To remove the metal an additional wash with a concentrated solution of EDTA was required and then compounds **94a**-**c** were successfully isolated using flash chromatography without any further difficulty; reaction conditions shown in Scheme 39.

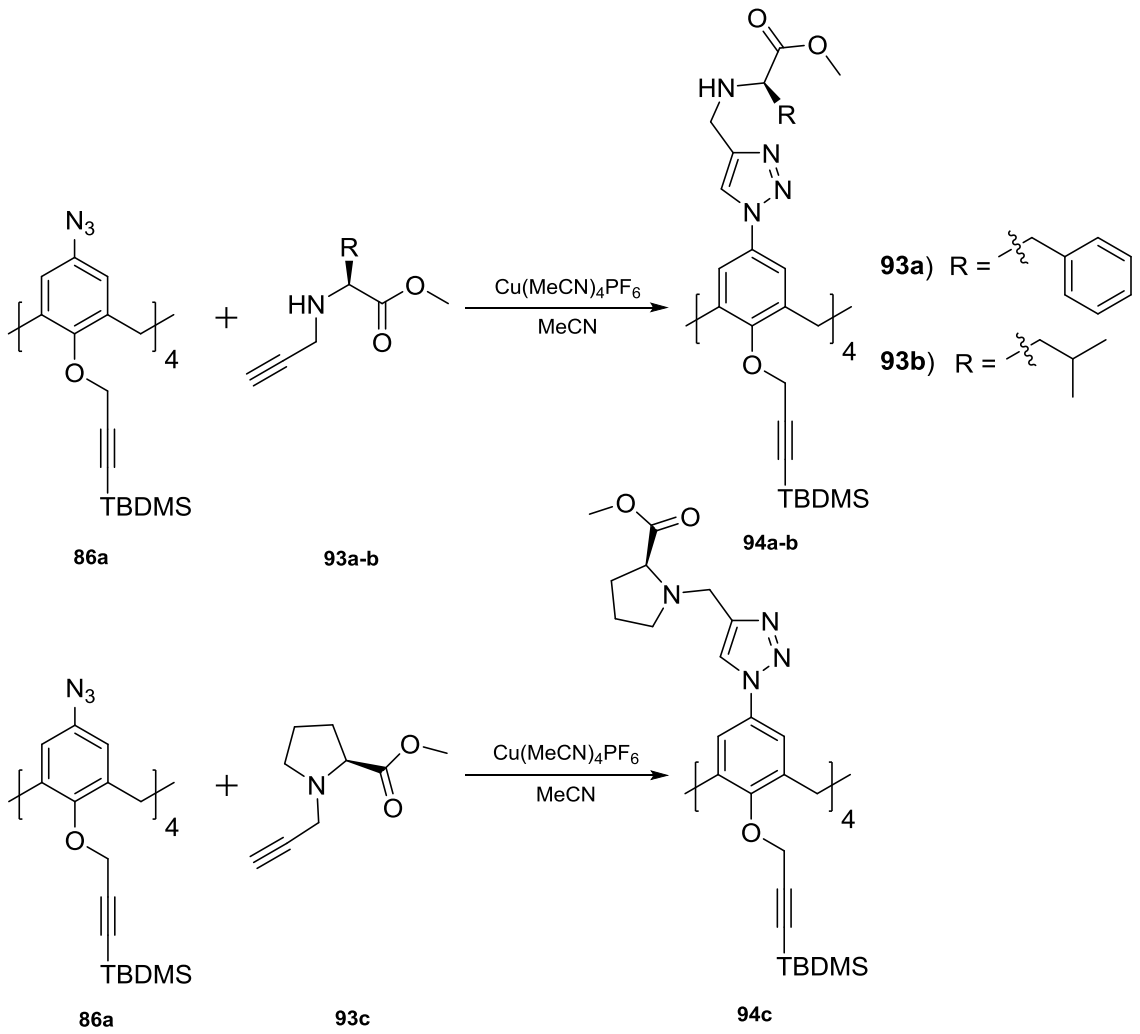

Scheme 39: Synthesis of amino acid cavities

I also investigated whether the "free" amino acids (i.e. without the methylester protecting groups present) would improve the chiral cavity by allowing for more efficient proton shuttling between the amino acid and the substrate in later research. This required the synthesis of an *N*-alkylated amino acid without a methyl ester. This was conducted by dissolving compound **93c** in a 1 M aqueous solution of LiOH, shown in Scheme 40. This amino acid was then attached to an immobilised calixarene surface using the CuAAC reaction and the modified electrode was used in the electrochemical asymmetric synthesis described in chapter 4.

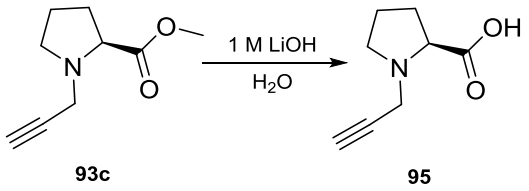

Scheme 40: Conditions used for the hydrolysis of molecule 93c

2.5.2 Attachment of ferrocenyl moieties to calixarenes 72 and 74

The synthesis of model calixarenes functionalised with large ferrocene moieties at the lower rim was conducted. It was a concern that the steric constraints at the lower rim of the macrocycle may affect the ability to react all the propargyl groups with large substrates. To test whether this would be a problem the CuAAC reaction was attempted on both calixarenes **72** and **74** with ferrocene methyl azide **96** to determine if the *t*-butyl groups would affect the reaction. Both molecules **97a** and **97b** were synthesised in good yields using the same conditions, showing that the steric constraints at the lower rim would not be detrimental to the formation of the triazole groups; conditions used described in Scheme 41.

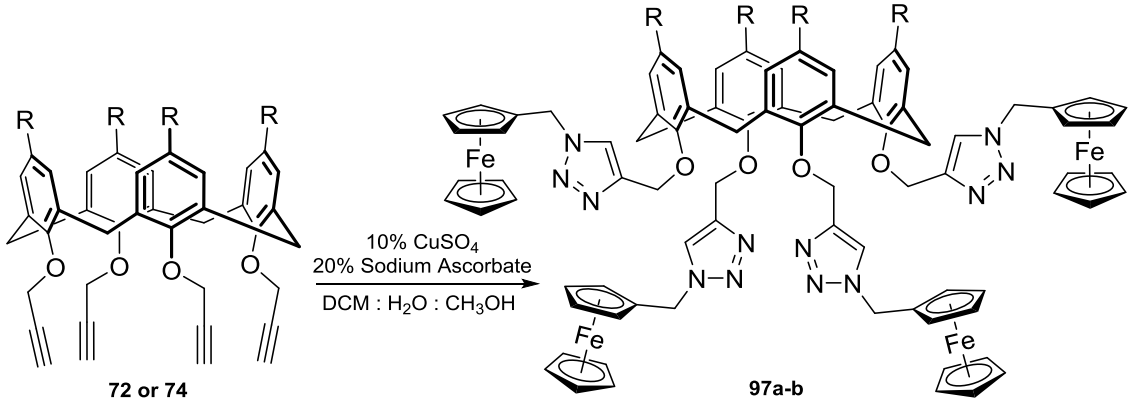

Scheme 41: CuAAC reactions at lower rim of calixarenes 72 and 74

2.6 Summary

In this chapter, I have discussed the methods used to synthesise molecules **84** and **87** which, in the next chapter, will be attached to an electrode surface. This will be achieved using the propargyl linkers of **87** or by the formation and subsequent reduction of the diazonium salt of **84**. These molecules have then been modified with substrates specifically chosen to facilitate their detection while bound to an electrode, by either XPS or electrochemical analysis. I also synthesised a small number of mono *N*-alkylated amino acids which have been attached to the upper rim of calixarene **86a** using the CuAAC reaction. We plan to recreate these macrocycles on the surface of the glassy carbon electrode to form chiral environments that will be able to promote the enantioselective electrochemical reductions described in chapter 4.

Chapter 3
Results and discussion

The chemical immobilisation and detection of calix[4]arenes on a GCE

3.1 Overview

This chapter will investigate two alternative approaches for the immobilisation of calixarenes onto an electrode surface and the subsequent functionalisation of the chemisorbed macrocycles.

The first method involved the immobilisation of calixarene **84** onto an electrode surface by the formation of a diazonium salt **85** and the electrochemical reduction of the salt to electrograft the macrocycle onto the electrode surface, by the upper rim. This modified surface was then further functionalised using the CuAAC reaction, with ferrocene motifs, to facilitate its characterisation using electrochemical techniques.

The second technique focussed on electrografting compounds **83** and **87** onto an electrode surface using pendant alkynyl groups attached to the lower rim of the macrocycle. Detection of **83** while immobilised onto the GCE was achieved by measuring the electrochemical reduction of the nitro functional groups under aqueous conditions, whereas the surfaces modified with **87** were functionalised with ferrocene or fluorine-containing probes to allow for their detection by electrochemical or XPS (X-ray photoelectron spectroscopy) analysis.

3.2 Chemical immobilisation of calixarenes onto a carbon electrode surface by the upper rim

The immobilisation of organic compounds onto carbon electrode surfaces using the reduction of aryl diazonium salts was first described by Pinson and co-workers in 1992.[151] Since then it has been shown to be a versatile method for the chemical attachment of molecules to an array of different surfaces using either electrochemical reduction[152] or chemical reducing agents, such as hypophosphorous acid,[153] to form a aryl radical that is able to bond with the carbon surface. This methodology was adapted for the immobilisation of calixarene **84** to a GCE by the formation of [*p*-tetradiazoniumcalix[4]arene]Cl_4 **85**, achieved by reaction of compound **84** with a stoichiometric amount of sodium nitrite, dissolved in a 1 M solution of hydrochloric acid at 0°C. The resulting diazonium salt **85** was then electrochemically reduced onto the surface of the electrode in an anhydrous electrochemical cell containing a 0.1 M solution of [$n$$Bu_4N$][$PF_6$] in acetonitrile to form the chemically–modified electrode surface, **S4**, as shown in Scheme 42.

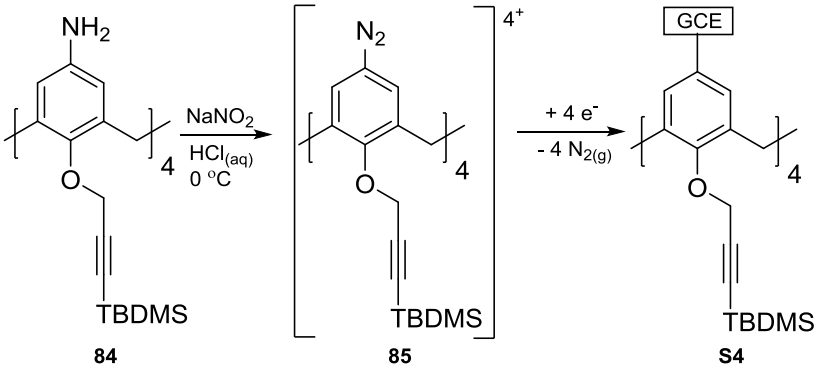

Scheme 42: The diazotisation of molecule 84 and subsequent electrochemical immobilisation onto a carbon electrode surface

The first cyclic voltammogram of diazonium salt **85**, in anhydrous conditions, revealed a large, broad, irreversible reduction at −0.35 *vs.* Ag/Ag^+ corresponding to the one–electron reduction of the diazonium salt to a phenyl radical and nitrogen gas.[154] The resulting phenyl radical may then attack the electrode surface to form a covalent C–C bond, binding the macrocycle onto the GCE surface. This was evidenced in subsequent scans by the observation of a large decrease in the magnitude of the reductive peak current and the background capacitive charging current (non-Faradaic current) of the electrode, as shown in Figure 15. This

suggested that the immobilised calixarenes, bearing the bulky silyl groups, were acting as a blocking layer on the electrode surface. This type of passivation is consistent with the electrografting of similar compounds onto a GCE as shown in previous work by Hapiot and Leroux in 2013.[155]

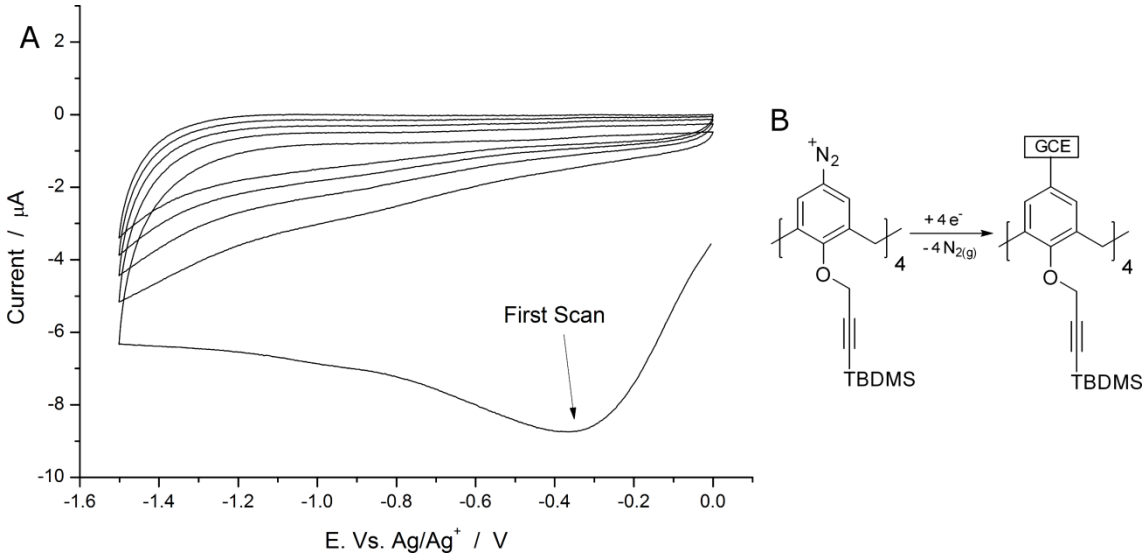

Figure 15: (A) Overlaid cyclic voltammograms of GCE modification with diazonium salt 85 recorded in CH_3CN/0.1 M [*n*Bu_4N][PF_6] at a scan rate of 100 mV s^{-1} (B) Shows the reduction of 85 onto the electrode surface forming surface S4

Having successfully electro-reduced calix[4]arene **85** onto the electrode surface further functionalisation was attempted using a protocol similar to the one described by McCreery and co-workers.[156] This involved the removal of the TBDMS groups from the immobilised calixarene surface by submerging the end of the electrode in a stirred solution of 1 M TBAF in THF, this yielded surface **S5**. The electrode surface **S5** was then thoroughly cleaned by sequential sonication in water, DCM and acetone for 5 minute intervals. This afforded a modified electrode that was functionalised with calixarenes that each possessed four free alkynyl groups attached to the exposed lower rim of the macrocycles. The pendent alkynyl groups on the surface of the modified electrode were then further reacted with ferrocenyl methyl azide **96** using the CuAAC reaction, to allow for characterisation of the immobilised macrocycles by electrochemical analysis, as shown in Scheme 43.

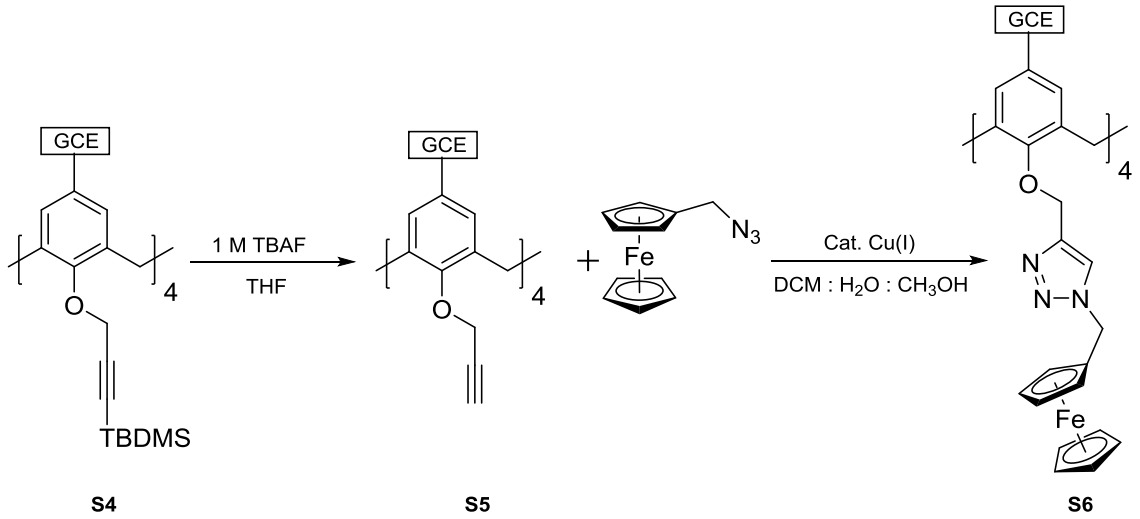

Scheme 43: Functionalisation of the immobilised calixarenes to form surface S6

After the CuAAC reaction, modified GCE **S6** was thoroughly cleaned to remove any remaining physisorbed material from the surface, before being transferred into a fresh anhydrous electrochemical cell containing a 0.1 M solution of [*n*Bu_4N][PF_6] dissolved in 10 mL of dry DCM. This surface **S6** was then used as the working electrode in the electrochemical cell and the cyclic voltammograms recorded from this system are shown in Figure 16. The CVs exhibited a well-defined reversible oxidation wave corresponding to the one–electron oxidation of the ferrocene moieties, attached to the lower rim of the immobilised calixarenes, centred at 0.16 V *vs*. $Cp_2Fe^{0/+}$.

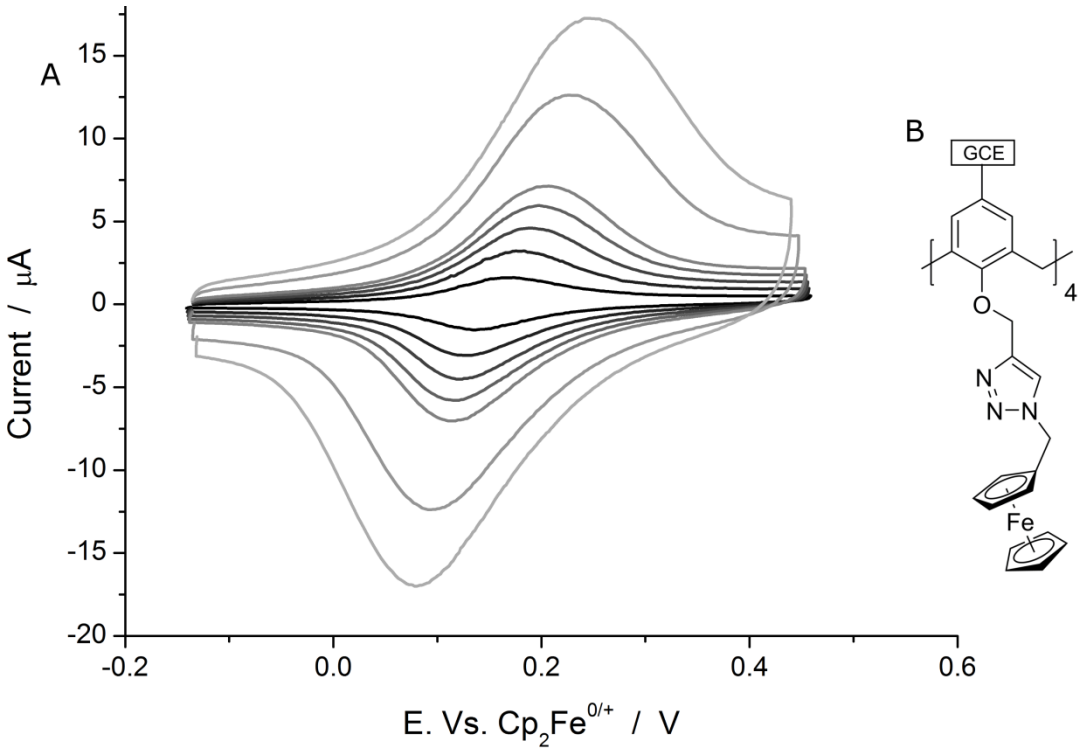

Figure 16: (A) Overlaid cyclic voltammograms recorded in CH_2Cl_2/0.1 M [nBu$_4$N][PF_6], at scan rates of 50-750 mV s^{-1} for GCE surface S6 (B) The structure of the calix[4]arene immobilized onto GCE surface S6.

To confirm that the electrochemically active species was indeed attached to the electrode surface and not simply present in the solution we needed to confirm that the redox process was not exhibiting diffusion-controlled voltammetry. This was done by plotting the oxidative and reductive peak currents, against the voltage scan rate, Figure 17, from 50 – 750 mV s^{-1}. If the analyte was in solution, and the voltammetry was therefore limited by diffusional mass transport one would expect the peak current to increase linearly with the square root of the voltage scan rate, as described by the Randels-Sevcik equation for a reversible redox process.[157,158] However, Figure 17 clearly shows that there is a linear relationship between the peak currents and voltage scan rate, diagnostic of a surface immobilised redox process, suggesting that the analyte was indeed bound onto the electrode surface.

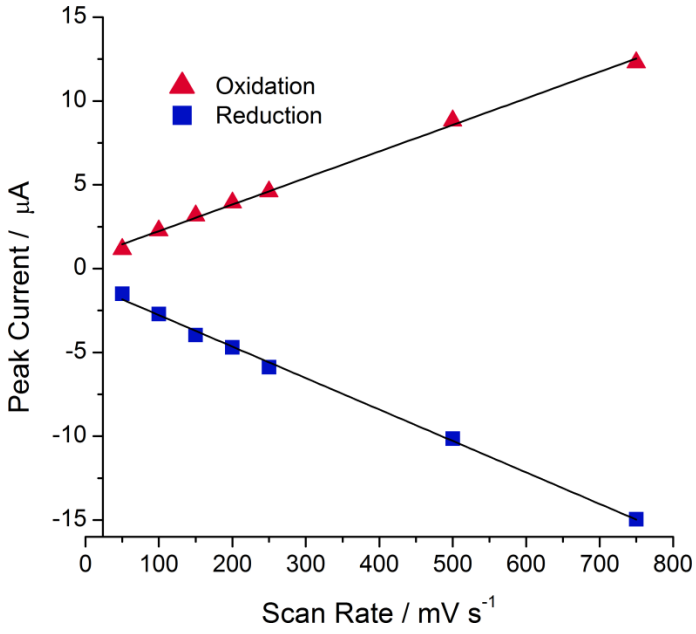

Figure 17: Plot of peak current *vs.* scan rate for both the reductive and oxidative processes of GCE surface S6.

The surface concentration of electrochemically active ferrocene centres can be derived from Faraday's Law (Equation 24).

$$\Gamma = \frac{Q}{n\mathrm{FA}}$$

Equation 24: Faraday's Law of electrolysis

Where *Q* is the charge passed (peak area divided by voltage scan rate, the value 3.41 µC was used, calculated from the average charge at scan rates between 50 – 750 mV s^{-1}), *n* is the number of electrons transferred in the redox process (for ferrocenyl groups, *n* = 1), F is Faraday's constant (96485 C mol^{-1}) and A is the geometric area of the electrode (0.071 cm^{-2}). This gave a surface concentration of ferrocene groups attached to the electrode surface of 5.0 x10^{-10} mol cm^{-2}. By assuming that all available sites on the calixarene were successfully functionalized with ferrocenyl groups (i.e. 4 ferrocene units attached per calixarene linker) I was able to calculate the surface concentration of the macrocycles on the electrode surface to be 1.3 x 10^{-10} mol cm^{-2}. It is, however, important to note that this assumption sets a lower limit on the surface concentration of the macrocycles as it is improbable that all the azido groups would have undergone the CuAAC reaction. Nevertheless, this value corresponds to a calixarene packing density of 0.75 calix nm^{-2} on the GCE.

To determine if this coverage of calixarene linkers corresponds to a monolayer on the electrode surface, a theoretical packing density of the macrocycles was calculated. This was achieved by modelling the molecules as discs on a perfectly planar surface in a hexagonal packing arrangement, meaning the theoretical value had to be adjusted by 0.907 to take into account the maximum packing density of circles (calixarenes).[159] The diameter of the calixarene was taken to be 11.6 Å (estimated from the crystallographic dimensions of structurally similar calixarenes),[160] giving an area per calixarene of 1.056 nm^2. Using these values I calculated a theoretical maximum packing density of calixarene on the electrode surface to be 0.86 calix nm^{-2}. The close agreement between the theoretical and experimental values obtained suggests the formation of a complete monolayer of calixarene linkers on the electrode surface.

3.3 Chemical immobilisation of calixarenes by the lower rim

The attachment of calixarenes onto the electrode surface by the lower rim was conducted using a similar method as that which was described by Geiger and co-workers in 2013.[133,138] They showed that both porphyrins and ferrocenyl groups could be attached to an electrode surface using pendant alkynyl groups as linkers. This was achieved via activation of the alkynes by deprotonation using a strong base and then applying an oxidative potential to the lithiated alkynyl groups to generate reactive ethynyl radicals. These intermediates are then able to attack the electrode surface to form C–C bond linkages, binding the ferrocene or porphyrins moieties securely onto the electrode surface.

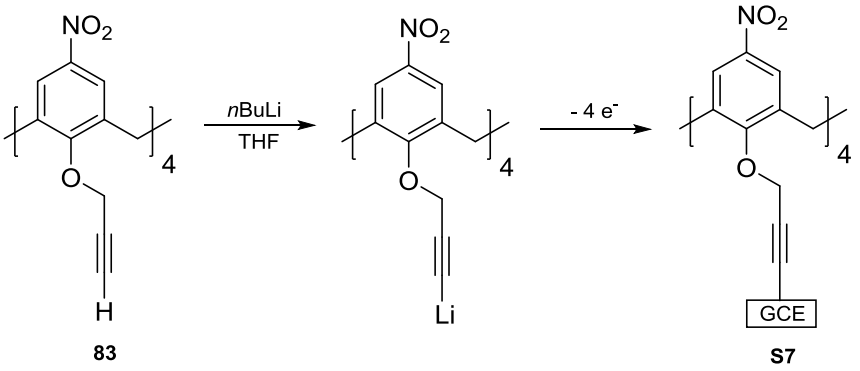

Scheme 44: Attachment of 83 to an electrode surface by the lower rim

Attachment of **83** to a GCE, Scheme 44, was performed in an anhydrous electrochemical cell containing a 0.1 M solution of [nBu$_4$N][PF$_6$] and 4 mM calixarene **83** dissolved in 10 mL dry THF cooled to −78°C. Stoichiometric *n*-BuLi (1.6 M) was then added slowly and the reaction mixture was stirred for a further 20 minutes before the electrografting was attempted. Cyclic voltammetry of the solution revealed a large irreversible oxidation wave at 0.6 V *vs.* Ag/Ag$^+$ on the first scan, corresponding to the formation of the ethynyl radical. Subsequent scans exhibited a large decrease in the peak current attributed to this oxidation and a decrease in the background capacitive charging current of the electrode, as shown in Figure 18. After the initial CV was ran, to ensure complete coverage of the working electrode a chronoamprometic (CA) experiment was conducted, using the same GCE, by holding the potential of the solution beyond that of the oxidation, at roughly 0.9 V Ag/Ag$^+$, for 300 seconds. Note that when the electrografting was attempted without the addition of *n*-BuLi no oxidation was observed, suggesting that the deprotonation of the alkynyl groups was essential for this method of attachment.

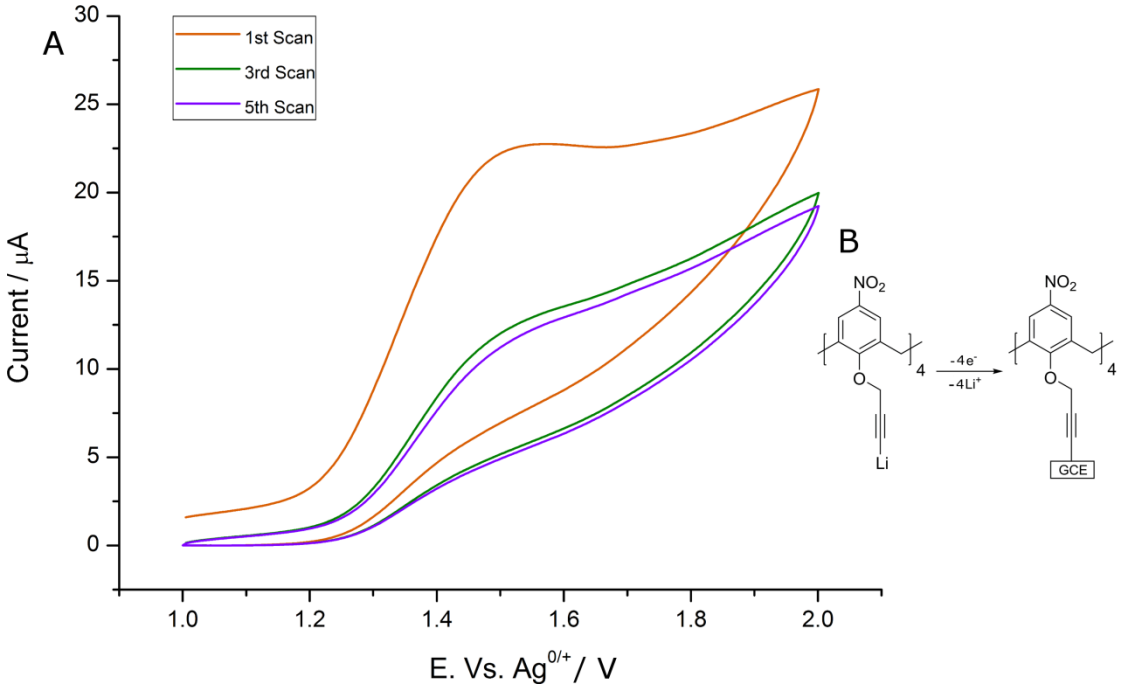

Figure 18: (A) Cyclic voltammetry obtained from the electrochemical grafting of lithiated 83 onto a GCE surface. (B) Shows the oxidative process that leads to surface S7.

3.3.1 Electrochemical analysis of carbon electrode modified with 83

GCEs modified with calixarene **83** were thoroughly cleaned by sequential sonication in water, DCM and then acetone, each for 5 minutes, to remove any physisorbed materials. The modified electrode **S7** was then placed into a fresh electrochemical cell containing a 10 mL aqueous solution of 1 M KCl and 1 M HCl. The cyclic voltammetry obtained from this system, Figure 19, shows a large irreversible reduction (peak 1) on the first scan at −0.52 V *vs.* SCE corresponding to the four-electron, four-proton irreversible reduction of the nitro functional groups to hydroxylamines.[161] After sweeping to potentials beyond the initial reduction and then reversing the scan direction the reduction, peak 1, is no longer observed, on subsequent cycles. Instead, a new reversible signal is observed, centred at 0.33 V vs. SCE (peaks 2 and 3), attributed to the two-electron, two-proton aryl hydroxylamine/aryl nitroso redox couple.[162] This voltammetric behaviour is characteristic of the redox chemistry of aryl nitro groups bound onto an carbon surface in an aqueous system, confirming the presence of *p*-tetranitrocalix[4]arene **83**.[163]

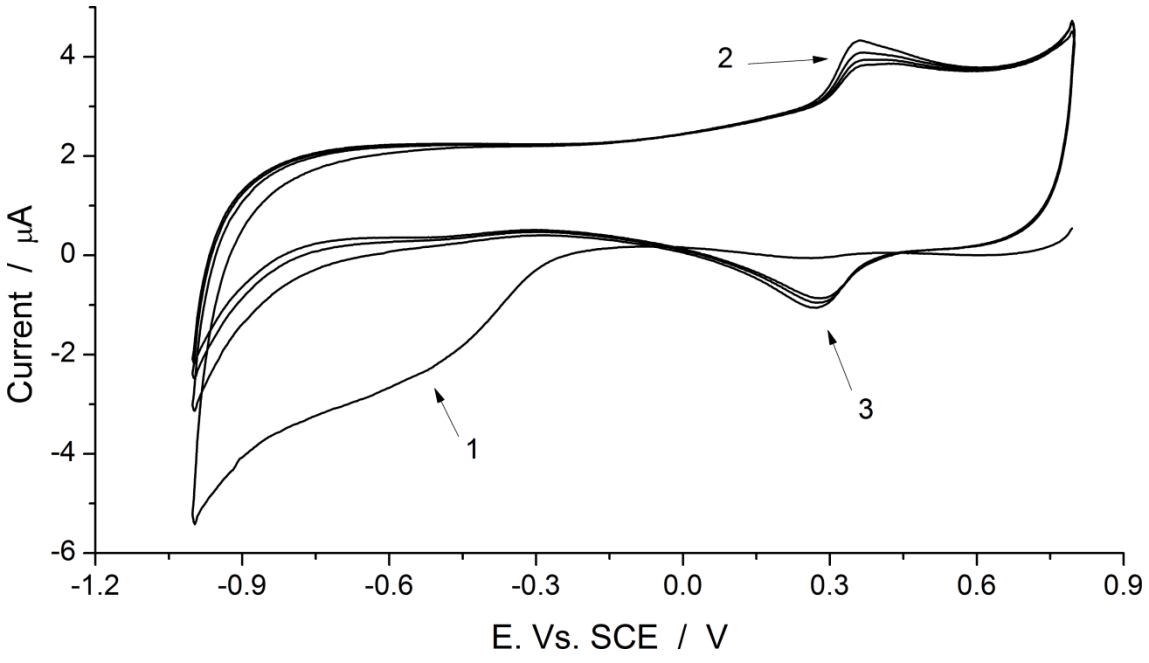

Figure 19: Overlaid cyclic voltammograms of GCE surface S7 in an aqueous solution of 1 M HCl/1 M KCl, scan rate 0.1 V s^{-1}.

Next a variable scan rate (VSR) experiment was conducted recording the cyclic voltammograms of the aryl hydroxylamine/aryl nitroso redox couple at voltage scan rates of

50-750 mV s^{-1}, as shown in Figure 20A. From this data a plot of peak current *vs.* voltage scan rate, Figure 20B, was created to show that there was a linear dependence upon the peak current and voltage scan rate. This is important because it suggests that the voltammetric response is not controlled by diffusional mass transport and is diagnostic of a surface bound redox process.

The immobilisation of calixarene **83** gave a method for the attachment of calixarenes to an electrode surface by the lower rim. The importance of this new methodology over common attachment methods utilised in the literature was the strength and versatility of the alkynyl-glassy carbon bond over the commonly used thiol-gold bonds.[164] Further development was still required to allow for modification of the immobilised macrocycles with an array of different substituents to impart their electrochemical or steric properties to the surface.

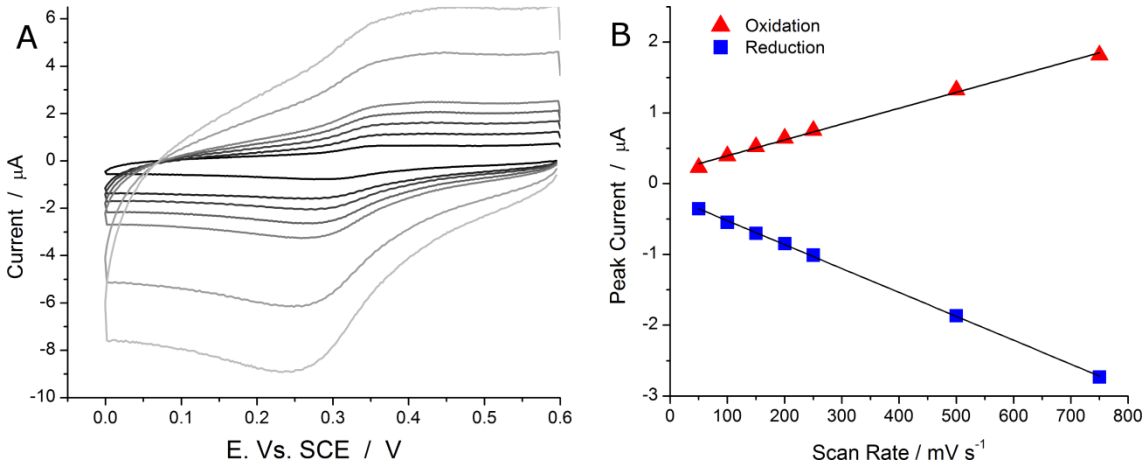

Figure 20: (A) Overlaid cyclic voltammograms recorded in an aqueous solution of 1 M HCl/1 M KCl, at scan rates 50-750 mV s^{-1} for surface S7 showing the arylhydroxylamine/arylnitroso redox couple. (B) Plot of peak current *vs.* scan rate for both the reduction and oxidation processes of the aryl hydroxylamine/aryl nitroso redox couple

3.3.2 Further modification of the immobilised calixarene surface

To facilitate further functionalisation of the electrode surface molecule **87** was synthesised as described in section **2.4**, the lower rim of which was functionalised with alkynyl groups to securely attach the macrocycle to the electrode surface while the upper rim was modified with four azido groups that have been shown to be easily modifiable using the CuAAC reaction. This allowed for further functionalization and for "tuning" of the chemical properties of the chemisorbed macrocycle after it was bound onto the electrode surface; to enable its

detection by either XPS or electrochemical analysis and to formulate chiral pockets on the surface of the GCE by further functionalisation with chiral substrates, these chiral surfaces were later used to attempt enantioselective electrochemical synthesis (described in chapter 4).

The attachment of *p*-tetraazidocalix[4]arene **87** to a GCE surface was conducted in an anhydrous electrochemical cell containing a 0.1 M solution of [nBu$_4$N][PF$_6$] and 4 mM of **87** dissolved in THF at −78°C. The alkynes were activated by the slow addition of a stoichiometric amount of *n*-BuLi (1.6 M) and stirred for 20 mins before a CV was taken to observe the oxidation of the alkynyl groups. Once the onset potential had been determined, a CA was ran and held at a potential just beyond the oxidation for 300 seconds to ensure complete coverage of the electrode surface.

Once modification of the electrode was complete the surface was thoroughly cleaned before being reacted with ethynyl ferrocene in the presence of a Cu(I) catalyst, as shown in Scheme 45. The ferrocene motifs attached to the immobilized calixarenes allowed for the surface to be easily observed by electrochemical analysis.

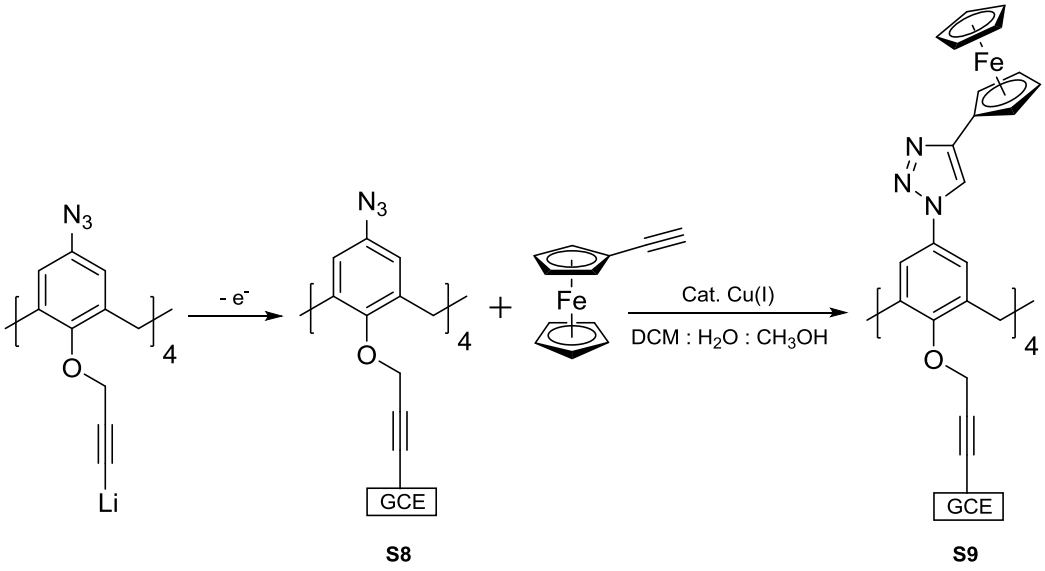

Scheme 45:Attachment of 87 to an electrode surface and post-surface modification with ethynyl ferrocene

The electrode was again thoroughly cleaned in numerous organic solvents and a 1 M solution of EDTA to ensure any physissorbed material was removed from the surface. The modified GCE **S9** was then transferred to a fresh anhydrous electrochemical cell containing a mixture of 0.1 [nBu$_4$N][PF$_6$] in dry DCM. A VSR experiment was then conducted over the range

of 50 mV s^{-1} to 750 mV s^{-1}, overlaid CVs of which are shown in Figure 21. In these scans the reversible oxidation of the ferrocene motifs was observed, centred at −0.27 *vs*. $Cp_2Fe^{0/+}$. The non-ideal wave shape exhibited in the voltammetry may have been caused by the requirement of the electrons to hop over the propargyl-ether linkers and/or lateral interaction between the charged centres located on the upper rim of the calixarenes.

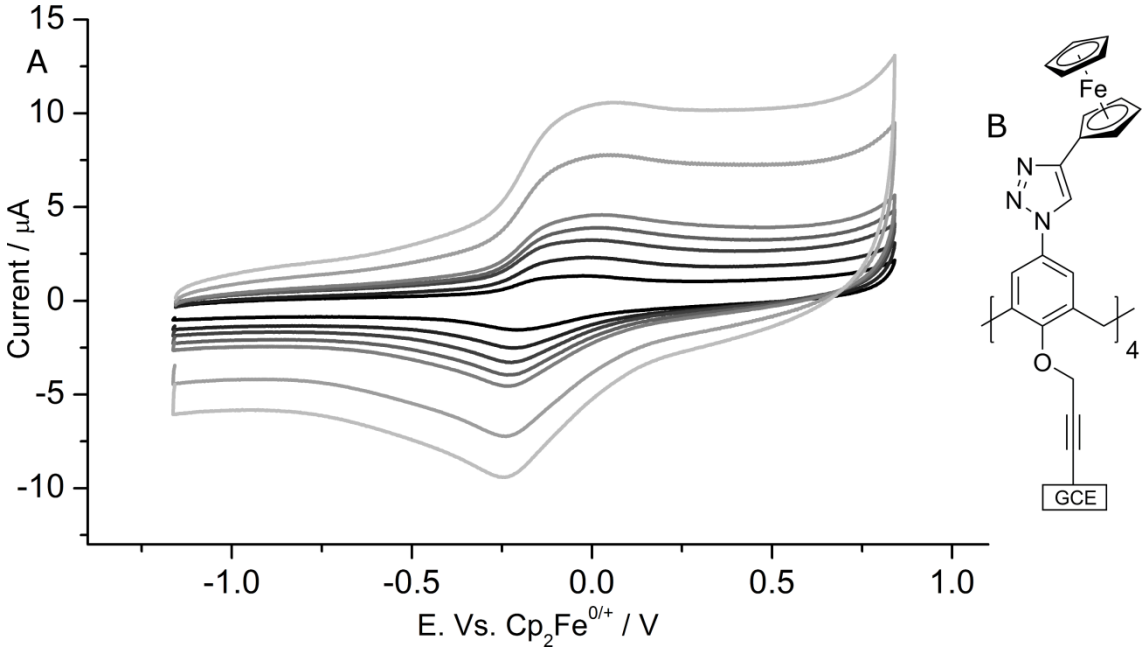

Figure 21: (A) Overlaid cyclic voltammograms recorded in CH_2Cl_2/0.1 M [nBu_4N][PF_6], at scan rates 50-750 mV s^{-1} for GCE surface S9 (B) Structure of the immobilised calixarene on surface S9

A plot of peak current *vs*. the scan rate was then created to determine if the redox active species was attached to the electrode surface or in solution. The linear relationship shown in Figure 22, between the peak current and scan rate, again suggests that the ferrocene motifs are indeed attached onto the GCE surface.

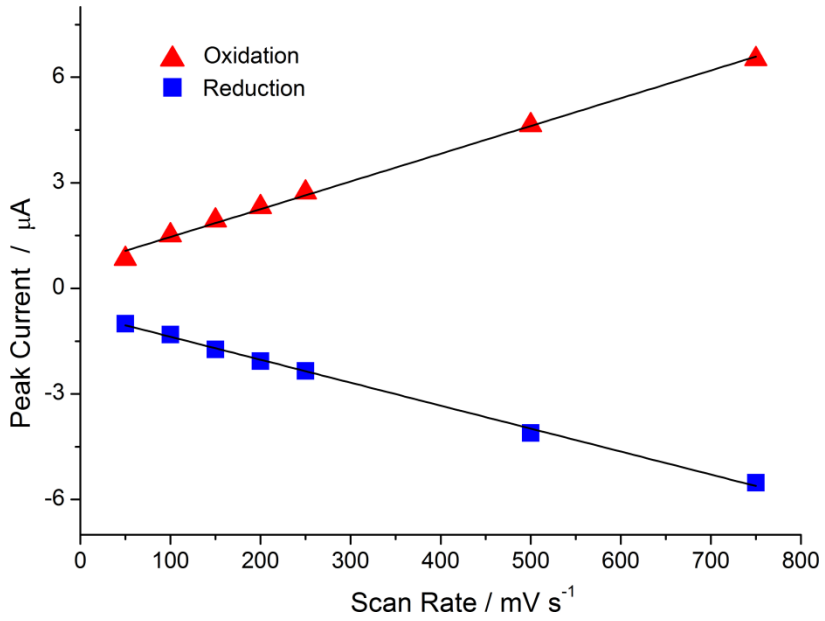

Figure 22: Plot of peak current *vs.* scan rate for both the reductive and oxidative processes of GCE surface S9 taken from the VSR experiment.

The surface concentration of ferrocene groups attached to the GCE surface was calculated using Faraday's Law, shown in Equation 24. The average charge passed during the redox process, Q, was found to be 3.7 µC, the area of the GCE, A, was 0.071 cm^{-2} and the number of electrons transferred in the redox process, *n*, was 1 per ferrocene moiety. Using these values I calculated the surface concentration of ferrocene groups to be 5.6 x 10^{-10} mol cm^{-2}. This value was then used to calculate the concentration of calixarene linkers on the electrode surface as 1.4 x 10^{-10} mol cm^{-2} corresponding to a surface coverage of 0.84 calix nm^{-2}, note that this value sets a lower limit on the number of calixarenes bound to the GCE, since it assumes that reaction of the azido groups during the CuAAC proceeded with a quantitative yield. The experimental surface coverage of the calixarenes compares favourably to the theoretical value of 0.90 calix nm^{-2}, derived from the hexagonal packing arrangement of spheres with a diameter of 11.3 Å (based upon the crystallographic data of calixarene **83**). This close agreement between the theoretical and experimental surface coverage of the calixarenes suggests the formation of a complete monolayer of macrocycles on the GCE.

XPS studies were also used to analyse the attachment and post-surface modification of calixarene **87**. This was achieved by using a GCE modified with *p*-tetraazidocalix[4]arene, fabricated using the lithiation and electrografting methodology described above, but instead of

attaching a redox active probe, the immobilised macrocycle was modified with 1-ethynyl-3,5-bis(trifluoromethyl)benzene **91** to from GCE surface **S10**, as shown in Scheme 46.

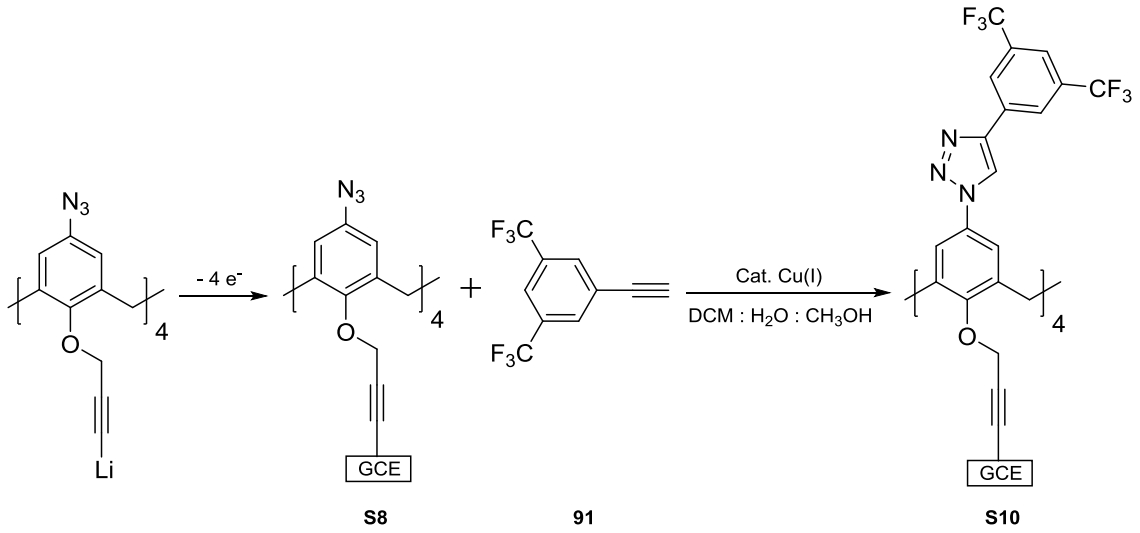

Scheme 46: Attachment of 87 to an electrode surface and post-surface modification with 1-ethynyl-3,5-bis(trifluoromethyl)benzene 91

This introduced a distinct fluorine labelled probe, which was easily observed using XPS analysis. The full survey spectrum obtained from this sample, Figure 23, shows characteristic F_{1s} and N_{1s} signals arising from the functionalised calixarenes and Cl_{2p} and Si_{2p} impurities which may have been introduced during the polishing steps or from the potting reagent used to transport the modified stubs. The large C_{1s} and O_{1s} signals arise from the structure of the modified GCE surface.

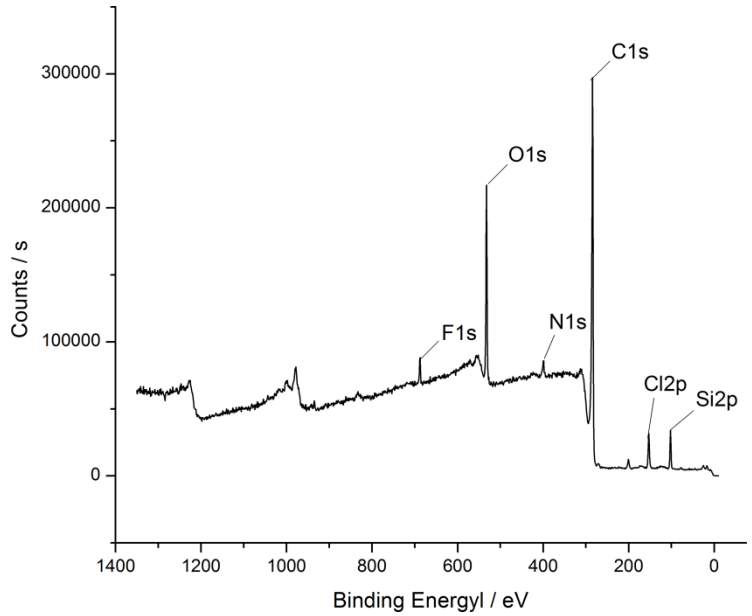

Figure 23: XPS data recorded from the modified GCE surface S10

Further evidence of the successful modification of the immobilised calixarenes using the XPS data required studying the peaks at 399.7 eV and 688.3 eV in more detail (Figure 24). The signal at a binding energy of 399.7 eV, corresponds to the N_{1s} orbital from the three nitrogen atoms in the triazole rings. It is important to note that if any of the unreacted azide groups had remained on the GCE surface one would have expected to see two characteristic nitrogen signals at 405 eV and 401 eV in a ratio of 1:2 respectively.[165] As these signals are not present, or at least are very weak, I am confident that the majority of the azido functional groups underwent conversion to the triazole linked moieties during the CuAAC reaction. Furthermore, the ratio between the $N_{1s}$and F_{1s} signals measured in the XPS spectrum, after adjusting for the relative atomic sensitivity factors,[166] revealed that the relative abundance of the two elements on the GCE surface was 1:1.9 (nitrogen : fluorine).This is close to the 1:2 nitrogen : fluorine ratio that would be expected if the CuAAC reaction had gone to completion, suggesting almost quantitative conversion of the azido groups to the triazole linked moieties . This reaction was also tested under similar conditions in solution to show that molecule **92** could be readily synthesized and maintained the conical confirmation, as shown in Figure 13 in chapter 2.

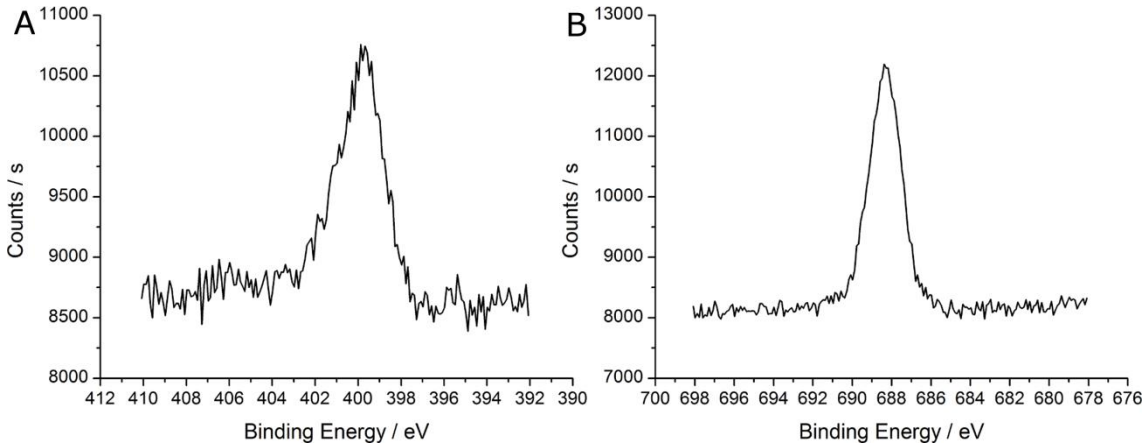

Figure 24: XPS spectra recorded over: (A) the N1s region; (B) the F1s region of GCE modified surface S10

3.4 Summary

In summary, I have described two methods for the formulation of a monolayer of immobilised calix[4]arenes upon a GCE surface, attached by either the upper or lower rim of the macrocycle. These immobilised compounds have then been chemically modified in a near quantitative fashion, *after* their attachment to the carbon electrode surface, using the CuAAC reaction. This allowed for the introduction of various functional "probe moieties" onto the surface-immobilized calixarene structures to facilitate their detection and characterisation by either electrochemical or XPS analytical methods, to confirm their presence on the electrode surface and to calculate the surface concentration of the chemisorbed species.

Chapter 4

Results and discussion

Electrochemical reductions of pro-chiral substrates

4.1 Overview

In previous chapters I have discussed the fabrication of a monolayer of calixarenes onto a GCE surface and the post-surface functionalisation of these surfaces using the CuAAC reaction. In this chapter the modified macrocyclic surface **S8** was to be reacted with amino acids **93a-c** to form chiral functionalities upon the electrode surface. These chiral surfaces were to be utilised in enantioselective electrochemical reductions of pro-chiral substrates.

To test the chiral electrodes the development of electrosynthetic reductions that could be carried out reliably using a GCE were investigated. Initially, the reduction of pro-chiral ketones, 1-indanone **98** and 1-acetylpyridine **99** (structures shown in Figure 25**)**, to the corresponding alcohols was attempted in both aqueous and non-aqueous systems but these reactions proved to be too unreliable due to the rapid passivation of the electrode surface, during the electrolysis, and the formation of pinacol by-products.

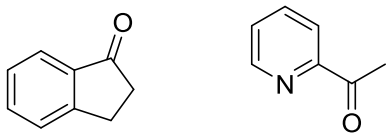

98 **99**

Figure 25: Molecular structures of 1-inadanone 98 and acetyl pyridine 99

Since the reductions involving **98** and **99** were unsuccessful, the focus of the research was shifted to the electrocarboxylation of pro-chiral ketones to the corresponding α-hydroxylcarboxylic acids following on from the research conducted by Chan and co-workers.[167] These reactions proved to be more reliable and were repeated using the chiral GCEs. The products created from the chiral systems were then tested for an enantiomeric excess using HPLC analysis.

4.2 Preliminary electrochemical reductions of ketones to alcohols

4.2.1 Electrochemical reduction of 1-indanone 98

The electrochemical reduction of 1-indanone **98** was attempted in both aqueous and non-aqueous conditions, to determine whether the compound would be a suitable substrate for use in asymmetric bulk electrolysis reactions, using the chiral electrode surfaces. 1-indanone was chosen because It was hoped that the steric hindrance afforded by the bicyclic system would help promote the formation of 1-indanol **100** over the pinacol side product, **101**, the formation of which is a common issue encountered in these types of systems.[55]

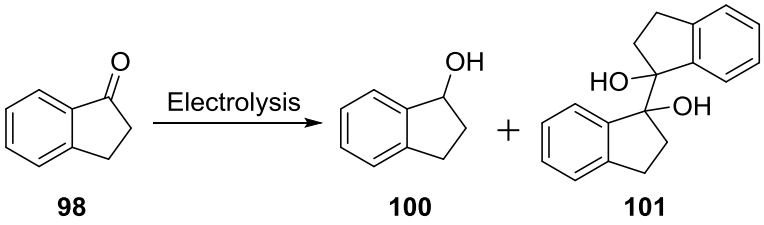

Scheme 47: Generalised electrochemical reduction of 98 to alcohol 100 and formation of the possible pinacol side product 101

4.2.1.1 Electrochemical reduction of 1-indanone in aqueous media

The electrochemical reduction of **98** was tested in an aqueous system using 10 mM of the substrate dissolved in 10 mL of an aqueous solution containing 0.1 M KCl as the electrolyte. A CV recorded from this system showed that there was only one irreversible reduction at −1.68 V *vs.* SCE, and an irreversible oxidation at 1.80 V *vs.* SCE. The presence of only one reductive signal was a concern because it suggested the substrate was being electrolysed to pinacol **101**, which is a one–electron process. Whereas, the formation of the desired alcohol **100** would require a two–electron process, which would be likely to appear as two irreversible reductive signals each corresponding to the transfer of one electron to the substrate. The only way that the one reduction signal could result in the formation of **100** was if the second reductive process was occurring at a more positive potential than the first reduction which would result in the peak at −1.68 V *vs.* SCE corresponding to a two–electron process. To confirm whether the reductive signal was a one– or two–electron process a VSR

experiment was conducted, shown in Figure 26A, and using the peak currents at different scan rates I was able to quantify the number of electrons transferred in the redox event.

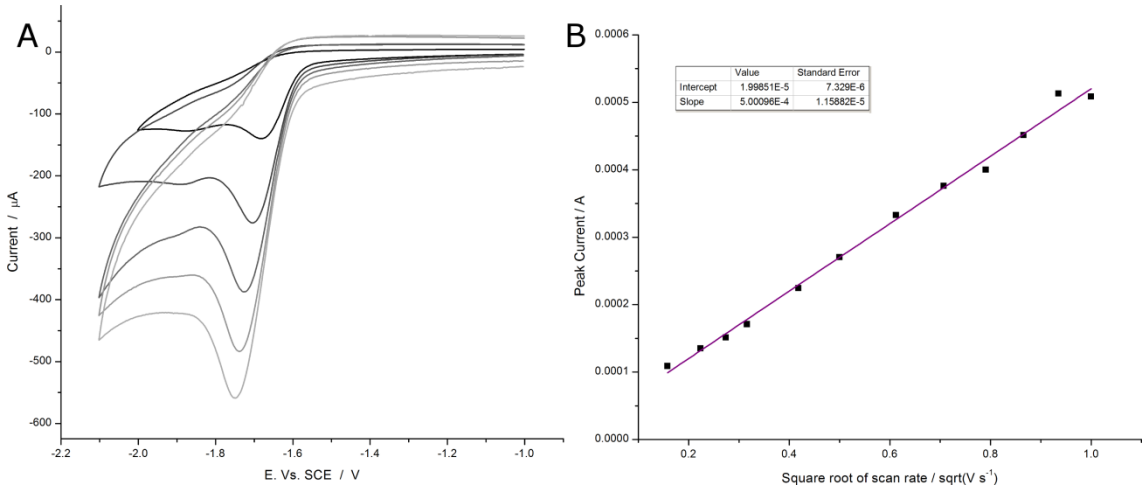

Figure 26: (A) VSR experiment of a 10 mM solution of 1-indanone dissolved in an aqueous solution of 0.1 M KCl at scan rates of 50 – 1000 mV s^{-1} (B) Plot of peak current *vs*. square root of scan rate.

Once the VSR experiment was complete a plot of the peak current *vs.* the square root of the voltage scan rate was created, Figure 26B, and used to determine the number of electrons passed during the reductive process, using the Randles–Sevcik equation as shown in Equation 25.

$$i_p = 268600 n^{\frac{3}{2}} A D^{\frac{1}{2}} C v^{\frac{1}{2}}$$

Equation 25: The Randles–Sevcik equation at 25 °C for a reversible system. i_p is the peak current in V. *n* is the number of electrons transferred in the redox event. *A* is the area of the electrode (0.071 cm^2). *D* is the diffusion co-efficient in cm^2 s^{-1}. *C* is the concentration in mol cm^{-3} (0.00001 mol cm^{-3}). *v* is the scan rate in V s^{-1}

The gradient of the graph shown in Figure 26B, 0.0005 A $s^{1/2}$ $V^{-1/2}$ was to used to calculate the number of electrons passed during the reductive process. This was achieved by rearrangement of Equation 25 to Equation 26 as shown below.

$$n = \left(\frac{m}{268600AD^{\frac{1}{2}}C}\right)^{\frac{2}{3}}$$

Equation 26: Rearranged Randles-Sevcik equation. m is the gradient in A $s^{1/2}$ $V^{-1/2}$ obtained from Figure 26B.

The diffusion co-efficient of 1-indanone in an aqueous system was calculated to be 7.11 x 10^{-6} cm^2 s^{-1}, determined experimentally using DOSY NMR. These values were used to calculate the number of electron passed during the electrochemical reduction to be 0.99. This suggested that the reduction at −1.68 V corresponded to a one–electron process and that this would result in the formation of pinacol side product **101** or that the second reduction was beyond the limits of the aqueous system and so was not observed. Because of this the reduction of 1-indanone in an aqueous media was determined to be unusable for the enantioselective reductions using the chiral electrodes.

4.2.1.2 Electrochemical reduction of 1-indanone in organic media

The electrochemical reduction of 1-indanone was also investigated under anhydrous conditions. This was conducted in an anhydrous electrochemical cell containing a 10 mM solution of 1-indanone dissolved in 10 mL of dry acetonitrile using 0.1 M [*n*Bu_4N][PF_6] as the electrolyte. A VSR experiment was obtained from this setup, the results of which are displayed in Figure 27A, showing one large irreversible reduction at -1.85 *vs.* $Ag^{0/+}$.

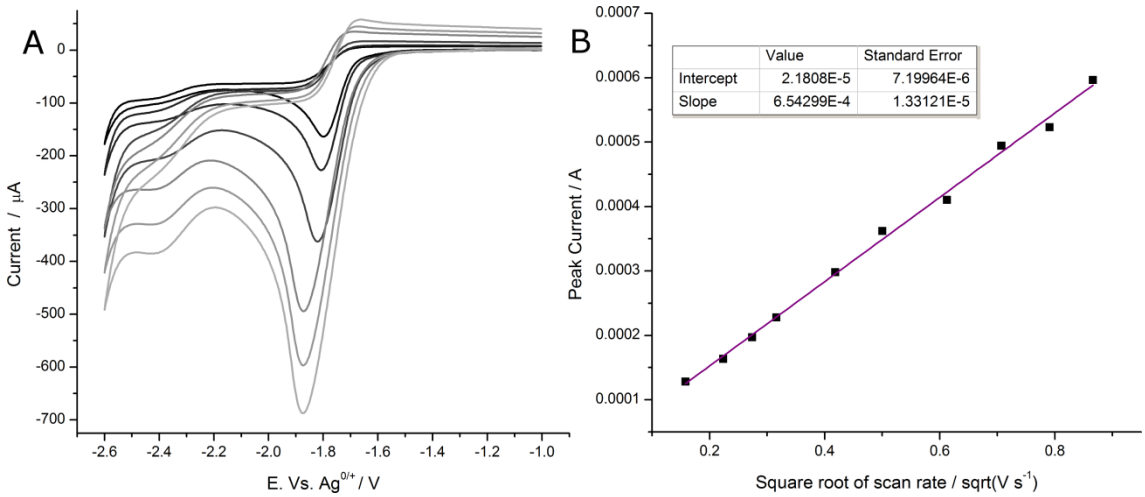

Figure 27: (A) VSR experiment conducted using a 10 mM solution of 1-indanone dissolved in 10 mL of acetonitrile using 0.1 M of [*n*Bu$_4$N][PF$_6$] as the electrolyte at scan rates of 50 – 1000 mV s^{-1} (B) Plot of peak current vs square root of scan rate.

Using Equation 26 the number electrons transferred during this redox event was calculated from the following variables; *m* was obtained from the gradient of the graph (0.00065x10^{-4} A s$^{1/2}$ V$^{-1/2}$) shown in Figure 27B, *A* is the area of the electrode calculated from geometric measurements (0.071 cm^2), *C* is the concentration of the 1-indanone (1 x 10^{-5} mol cm^{-3}) and *D* is the diffusion co-efficient of 1-indanone in acetonitrile which was determined by DOSY NMR spectroscopy to be 2.75 x 10^{-5} cm^2 s^{-1}. From these values and using Equation 26 the number of electrons passed during the redox event was calculated to be 0.76, indicating that the reductive process corresponded to the transfer of one electron. This suggested that the electrochemical reduction of 1-indanone in anhydrous conditions was forming the pinacol product or that the second reductive process, required for the formation of the alcohol, occurs at a potential lower than the breakdown of the solvent system. To test this the reduction of 2-acetylpyridine was investigated because it has been shown to be more readily reducible.[69]

4.2.2 Electrochemical reduction of 2-acetylpyridine 99

The electrochemical reduction of 2-acetylpyridine was conducted under aqueous conditions following a modified literature procedure described by Kariv and co-workers.[70] Modification of the literature method was required because in their research they used a mercury pool working electrode and I needed to develop a system that could be used to test the modified GCEs. The reduction was conducted using 10 mM of 2-acetylpyridine dissolved in 5 mL of 4.5 pH acetate buffer and 5 mL of ethanol. From this solution a VSR experiment was

conducted, shown in Figure 28. The CVs obtained from the VSR showed two reductive signals at −1.19 V and −1.79 V *vs.* SCE.

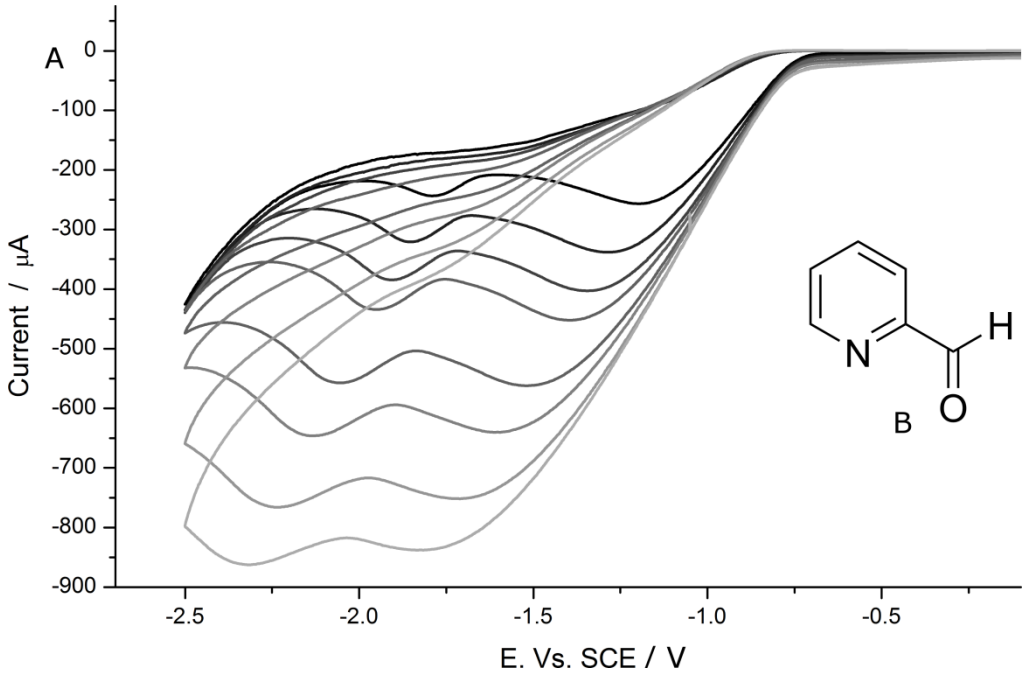

Figure 28: (A) VSR experiment of a 10 mM solution of 2-acetylpyrdene dissolved in a mixture of 4.5 pH sodium acetate buffer solution and ethanol (1 : 1) at scan rates 50 – 750 mV s^{-1}. (B) Structure of 2-acetylpyridine 99

Bulk electrolysis of compound **99** was attempted in both a compartmentalised and de-compartmentalised electrochemical cell by holding the potential of the solution at –2.6 V *vs* SCE over a 24 hour period. Formation of product was monitored during this process by IR spectroscopy and TLC but no conversion of the starting material was observed, to either the alcohol or pinacol. Purification and isolation of materials in the electrochemical cell was attempted but only starting materials and electrolyte was recovered. As there was no observable formation of the desired products I progressed to another electrosynthetic reduction involving the use of carbon dioxide in an electrocarboxylation reaction.

4.3 Preliminary electrocarboxylation of pro-chiral ketones

The electrocarboxylation reactions described in this section involve the two–electron reduction of prochiral ketones such as, 4-methylbenzophenone **102a**, to the corresponding α-hydroxycarboxylic acids **103**, in the presence of carbon dioxide gas (shown in Scheme 48). These types of reaction have increased in popularity in recent research as they facilitate a

pathway to make important drug precursors such as hydroxyl-naproxen **106** and hydroxyl-ibuprofen in good yields without the need of toxic reagents.[168] Asymmetric electrocarboxylation of these compounds is present in the literature by using alkaloid additives to induce chirality onto the substrates, achieving enantiomeric excesses of up to 32.8%.[58]

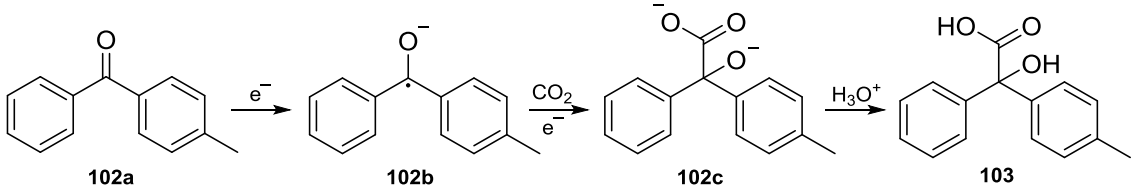

Scheme 48: Mechanism of the electrochemical carboxylation of 4-methylbenzophenone 102a in the presence of carbon dioxide

4.3.1 Analytical electrocarboxylation of 4-methylbenzophenone 102a

The electrocarboxylation of 4-methylbenzophenone **102a** was attempted using a modified literature procedure that was described by Wang and co-workers in 2012.[169] They reported the synthesis of several α-hydroxycarboxylic acids by bulk electrolysis in the presence of carbon dioxide gas. The electrocarboxylation of **102a** was the first that I attempted because it is a pro-chiral substrate that reduces at a relatively low potential when compared to other compounds, such as **105** and **108.** Due to this it was believed that the reaction would be less likely to passivate the electrode surface as the electrochemical cell could be held at a potential further from the breakdown of the solvent system. It is important to note that the use of the magnesium counter electrode in these systems was not a trivial choice. It has been shown, in previous research, to play an important role in the efficiency of the electrocarboxylations by acting as a sacrificial electrode and the presence of the magnesium ions in solution is believed to stabilise the carboxylate intermediates.[55]

Before the electrolysis reaction was conducted an electrochemical cell was setup containing 0.1 M of **102a** dissolved in 10 mL of DMF using 0.1 M of [nBu$_4$N][I] as the electrolyte. The solution was saturated with argon gas and a CV of the system was recorded between 0 V and −2.5 V *vs*. $Ag^{0/+}$, Figure 29A. In the CV obtained from this system two reductive signals were observed at −1.72 V and at −2.19 V *vs.* $Ag^{0/+}$. Presumably, these were caused by the two consecutive one–electron reductions of **102a** to the alcohol. For future work it would be

interesting to go back and attempt to form the corresponding alcohol but at this stage of research focus was put onto the formation of **103**. The system then saturated with CO_2 gas and another CV was recorded between 0 V and −2.25 V *vs.* $Ag^{0/+}$, Figure 29B. Interestingly, in the presence of an excess of carbon dioxide only one reductive process was observed at -1.84 V *vs*. $Ag^{0/+}$, the onset of this new peak appeared to be similar to the first reduction that was observed in Figure 29A. The increase in charge passed in the CO_2 saturated system suggests that the process now corresponds to a multi-electron transfer, presumably two electrons. Which occurs because the radical anion formed from the single electron reduction of 4-methylbenzophenone reacts spontaneously with CO_2 and the resulting intermediate is rapidly reduced to form the di-anion **102c**, after protonation during the workup this forms the desired product product **103**.[170] In the literature some researchers believe that the alcoholic anion **102c** is stabilised by a second molecule of CO_2 but either way the general reaction scheme remains the same.[171]

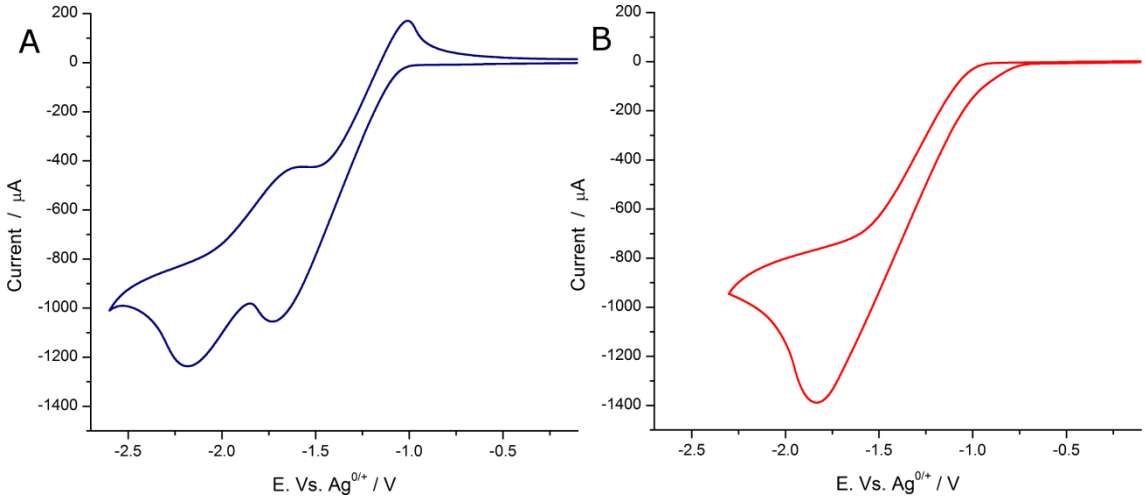

Figure 29: CVs obtained from a 0.1 M solution of 4-methylbenzophenone dissolved in DMF containing 0.1 M of [*n*Bu_4N][I] as the electrolyte at a scan rate of 100 mV s^{-1}. (A) While the system was saturated with argon. (B) While the system was saturated with carbon dioxide.

When attempting the bulk electrolysis of **102a** in the presence of an excess of carbon dioxide I encounter that the GCE surfaces were being rapidly passivated during the CV. This was an issue because the reaction needed to be reliable and form an isolatable amount of the product without passivation of the electrode, otherwise when using the modified GCEs the passivation would drastically affect the electrode surface. Figure 30 shows a LSV (Linear sweep voltammetry) experiment that was conducted in an electrochemical cell containing a 0.1 M

solution of **102a** dissolved in bench degassed DMF that was dried over 4 Å molecular sieves containing [*n*Bu$_4$N][I] as the electrolyte. After each scan the electrochemical cell was stirred and the potential window of the next scan was increased by 100 mV starting at −0.9 V and ending at −2.6 V *vs*. Ag$^{0/+}$.

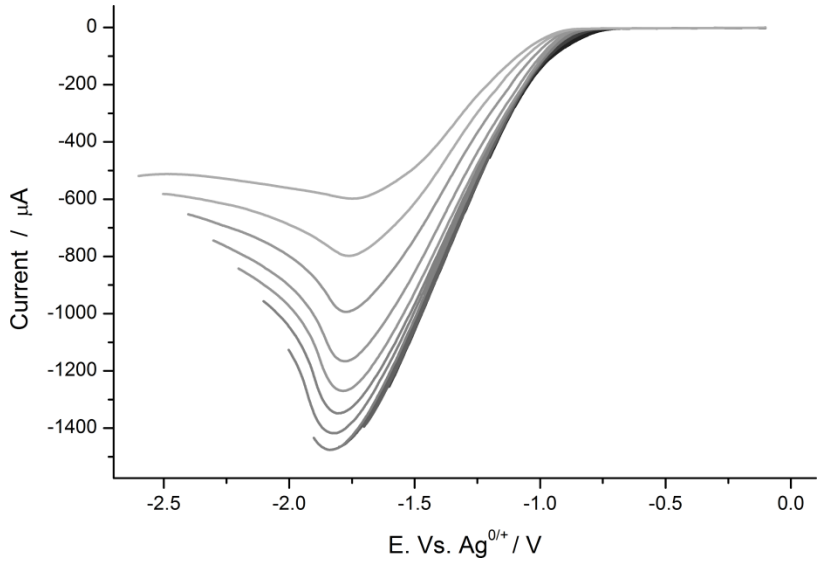

Figure 30: LSV experiments obtained from a electrochemical cell containing a 0.1 M solution of 4-methylbenzophenone dissolved in DMF with 0.1 M [*n*Bu$_4$N][I] as the electrolyte at a scan rate of 100 mV s^{-1}

These LSV experiments were conducted to demonstrate how fast these organic systems passivated the surface of the GCEs after the cell reached the reductive potential of the substrates. It is interesting that passivation was not observed in the aqueous systems while reducing 1-indanone, section **4.2.1.1,** or 2-acetylpyridine, section **4.2.2,** however in the organic solvent systems the reductions, especially when using DMF, would fully passivate the electrode surface after a single CV, if any water was present in the electrochemical cell. This would be a problem when using the modified GCEs in these test systems because renewal of the electrode surface, by polishing the GCE, would remove the immobilised calixarenes from the surface. Fortunately, it appeared that under scrupulously dry conditions the reduction of **102a** was more reliable and did not passivate the electrode surfaces as rapidly.

4.3.2 Bulk electrocarboxylation of 4-methylbenzophenone 102a

The bulk electrolysis of **102a** was conducted in a three necked anhydrous de-compartmentalised electrochemical cell that contained a 10 mL solution of dry DMF in which was dissolved 0.1 M 4-methylbenzophenone and 0.1 M [*n*Bu$_4$N][I] following a modified

procedure that was reported by Wang and co-workers.[169] The solution was saturated and held under an atmosphere of CO_2 before a CV was recorded at 100 mV s^{-1}, to determine the position of the reductive signal. A CA experiment was then conducted, to electrolyse the substrate, and the potential of the cell was held at the potential of the peak current for 72 hours. Throughout the bulk electrolysis reaction the solution was rapidly stirred and bubbled with CO_2 to ensure that the saturation of the solution was maintained and limit any diffusional effects, the result of the CA is shown in Figure 31.

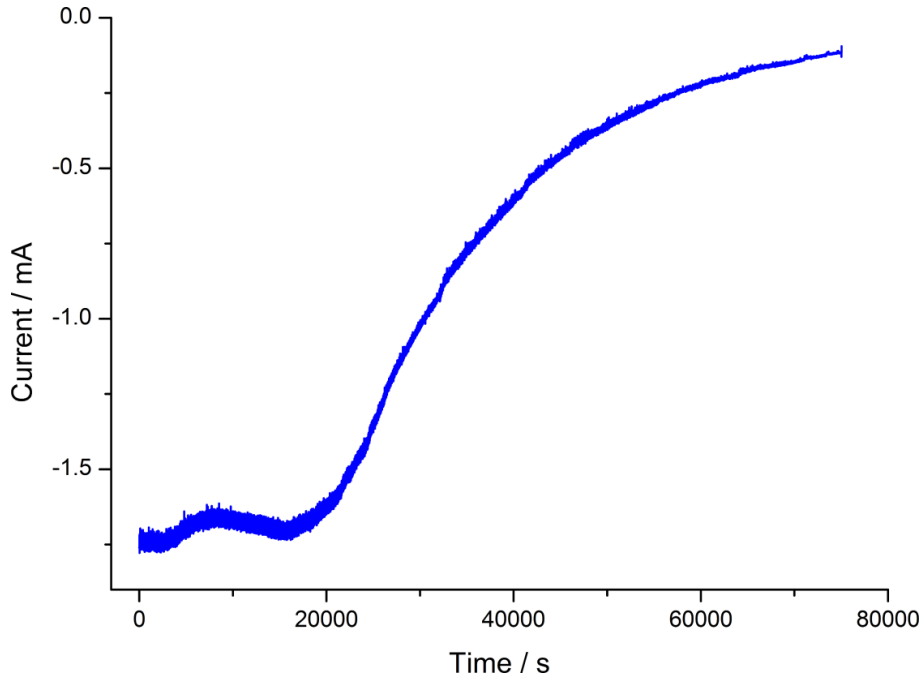

Figure 31: CA obtained from the bulk electrolysis of a 0.1 M solution of 4-methylbenzophenone in DMF containing 0.1 M [*n*Bu_4N][I] while saturated with CO_2.

The product **103** was isolated as the methyl ester **104** following the procedure described in the experimental section. The esterification of the carboxylic acid **103** was conducted because it simplified the purification procedure and allowed for analysis by reverse phase chiral HPLC to determine whether there was an enantiomeric excess in the products. The reaction yield of the two-step process, from compound **102a** through the bulk electrolysis and after the esterification, was 50 mg, 0.2 mmol (20%). The charge passed during the bulk electrolysis was determined by integration of the CA, shown in Figure 31, to be 65.2 C. By dividing the charge passed by Faraday's constant (96485 C mol^{-1}) the number of moles of electrons passed during the electrochemical reaction was calculated to be 0.67 mmol. As the

reduction of 4-methylbenzophenone to compound **103** is a two–electron process a quantitative Faradaic yield would have resulted in 0.34 mmol of product being formed. By comparing this value with the moles of product that were isolated, I calculated the Faradaic efficiency of the bulk electrolysis to be 58%, note this sets a lower limit on the Faradaic yield because it assumes the esterification reaction ran to completion.

These yields were determined to be reasonable and would facilitate a method in which to test the chiral calixarene electrodes. The conditions described at the beginning of this section (and in more details in the experimental section) were utilised for all the bulk electrolysis reactions described throughout this chapter.

4.3.3 Bulk electrocarboxylation of 6′-Methoxy-2′-acetonaphthone 105

The bulk electrocarboxylation of **105** and subsequent esterification was conducted using the procedure described in Scheme 49. Compound **105** was of particular interest because the α-hydroxycarboxylic acid **106** is a drug precursor and can be used for the synthesis of naproxen.

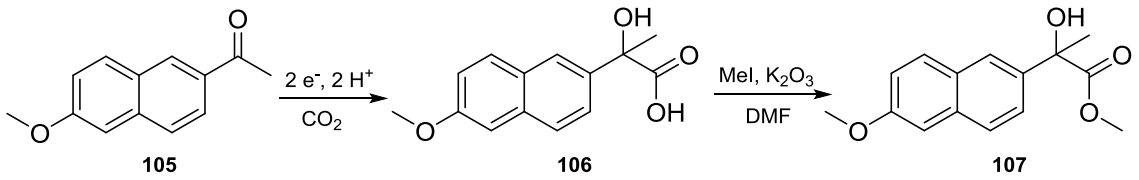

Scheme 49: Scheme showing the electrocarboxylation of compound 105 and subsequent alkylation to form the isolatable product 107

Before the electrolysis was attempted CVs were conducted on a solution containing 0.1 M of **105** dissolved in 10 mL DMF using 0.1 M of [nBu$_4$N][I] as the electrolyte. The system was saturated with argon and a CV was recorded, Figure 32A. Initially I had expected to observe two separate reduction signals each corresponding to a one–electron reduction of **105** to the alcoholic product. Instead only one irreversible reduction was observed at −1.83 V *vs*. $Ag^{0/+}$. This suggested that either **105** was being reduced by a one–electron process and forming the pinacol by-product or that the second reduction required to form the alcoholic product was occurring at a more positive potential than what was required for the second electron reduction of 4-methylbenzophenone **102a**, possibly beyond the breakdown of the solvent

system. It was a concern that in the carbon dioxide saturated system the radical anion would react preferentially with another radical anion to form the pinacol before it would be able to react with the CO_2. This was tested by bubbling the solution contained in the electrochemical cell with CO_2 for 30 minutes and obtaining another CV from this system, Figure 32B. In the CO_2 saturated solution the irreversible reduction signal increased drastically in size suggesting that in the presence of the CO_2 gas the reduction corresponded to a two–electron transfer process opposed to the one–electron reduction observed in the argon saturated system.

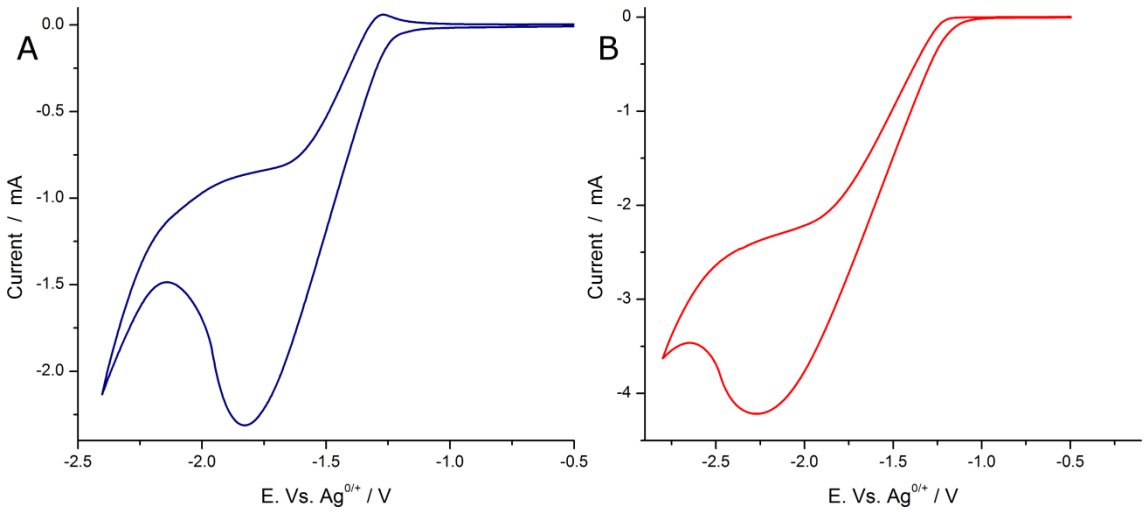

Figure 32: CVs obtained from a 0.1 M solution of 105 dissolved in DMF containing 0.1 M of [*n*Bu$_4$N][I] as the electrolyte at a scan rate of 100 mV s^{-1}. (A) While the system was saturated with argon. (B) While the system was saturated with carbon dioxide.

Once the potential of the reduction in the CO_2 saturated system was determined, from the CV shown in Figure 32B, a CA experiment was conducted by holding the potential of the electrochemical cell at −1.7 V *vs*. $Ag^{0/+}$ for 72 hours, as shown in Figure 33. During the bulk electrolysis the cell was continuously stirred and bubbled with CO_2 gas to ensure that the reaction mixture remained saturated.

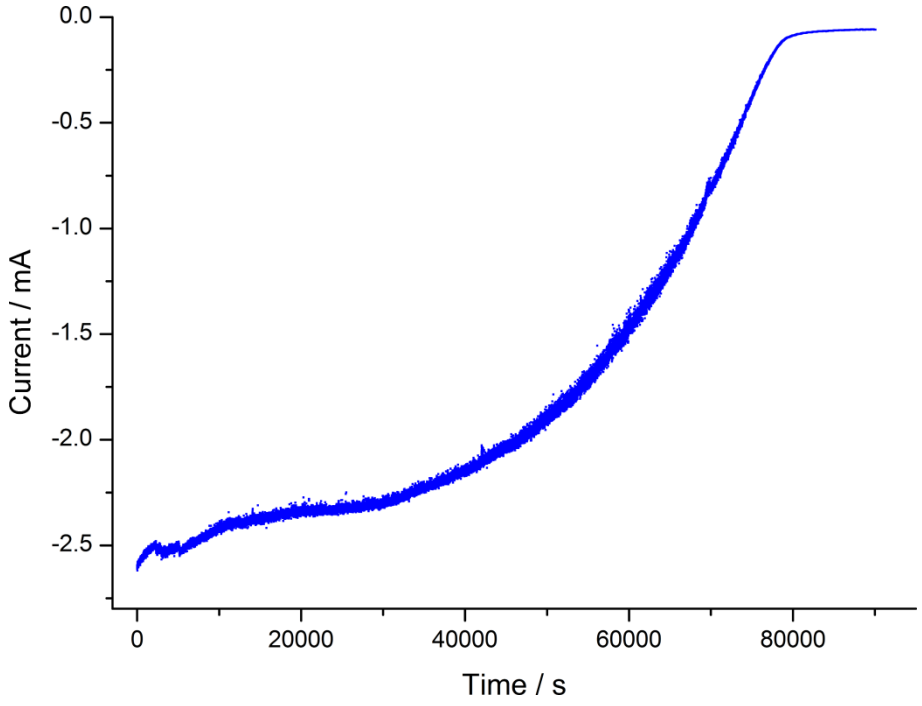

Figure 33: CA obtained from the bulk electrolysis of a 0.1 M solution of 105 in DMF containing 0.1 M of [*n*Bu_4N][I] while saturated with CO_2

After the electrolysis experiment, compound **106** was isolated pure as the methyl ester **107** with a reaction yield of 45 mg (0.18 mmol, 18%) from compound **105**, over the two steps. To calculate the Faradaic yield the charge, 147.5 C, was determined from integration of Figure 33 this corresponded to the transfer of 1.5 mmol of electrons during the CA experiment. This indicated that the total Faradaic yield of the two–electron electrochemical carboxylation of compound **105** was 23%. It is important to note that this yield is lower than the yield that was achieved for the electrolysis of compound **102a**. This was a trend that was observed throughout the reductions of this series of ketones that as the molecule became harder to reduce, reduced at a lower potential, the Faradaic and reaction yields decreased. I believe this is due to the cell having to be held at a potential closer to the solvent breakdown making these reactions less reliable and more readily passivating the electrode surface. Even with the lower yield obtained from compound **105** due to its importance as a drug precursor this molecule was still used as one of the test molecules in the asymmetric electrosynthetic reductions.

4.3.4 Bulk electrocarboxylation of acetophenone 108

The electrocarboxylation of acetophenone **108** was intended to be another test substrate for the asymmetric reductions but as will be described in a later section another

substrate was required due to some unexpected results that were obtained when attempting the electroreduction of substrate **108**, using the calixarene modified electrodes. The bulk electrolysis and esterification of **108**, in the presence of CO_2, using a blank electrode followed the reaction pathway shown in Scheme 50.

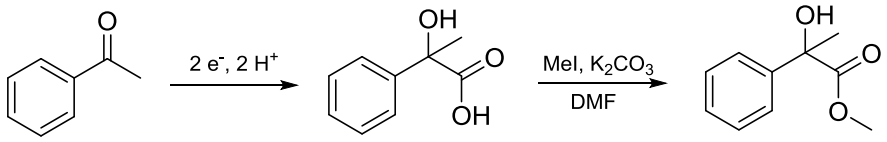

108 **109** **110**

Scheme 50: Scheme showing the expected product from the electrocarboxylation of compound 108 and subsequent alkylation.

Before the electrocarboxylation of **108** was attempted, CVs were obtained from an anhydrous electrochemical cell containing 0.1 M of the substrate dissolved in 10 mL DMF using 0.1 M [nBu$_4$N][I] as the electrolyte to analyse the reductions, in both argon and CO_2 saturated environments, Figure 34. The results from these CVs were consistent with the reductions of the more difficult to reduce ketones (such as compound **105**), exhibiting a single reduction in the argon system at −2.15 V *vs.* $Ag^{0/+}$, with the second reduction not being observed. Presumably the substrates with only one aryl group attached to the ketone were not as effective at stabilising the radical anion intermediate compared to the di-aryl system, 4-methylbenzophenone **102a**. There was also a comparatively small oxidative signal at −0.26 V *vs.* $Ag^{0/+}$ which had not been observed in any of the other systems, this may be caused by the oxidation of the radical anion. The system was then saturated with CO_2 and another CV was recorded, Figure 34B, whereupon the reductive peak shifted slightly to −2.80 V *vs.* $Ag^{0/+}$ but the onset potential remained very similar to the onset of the reduction observed in the argon system. Furthermore, compared to the argon saturated CV the size of the peak increased dramatically which suggested that the reductive process was now attributed to a multi-electron transfer which was characteristic of electrocarboxylation of these types of systems.

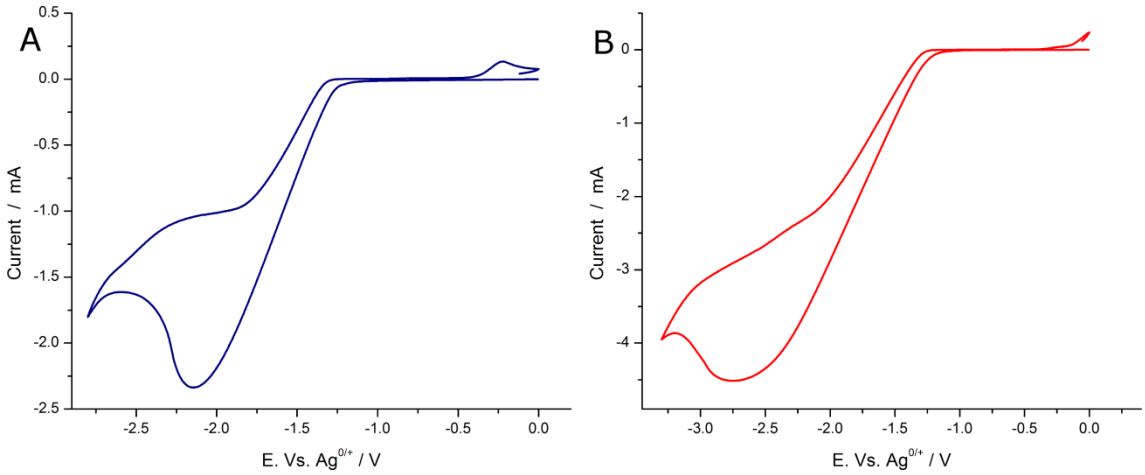

Figure 34: CVs obtained from a 0.1 M solution of 108 dissolved in DMF containing 0.1 M of [*n*Bu$_4$N][I] as the electrolyte at a scan rate of 100 mV s^{-1}. (A) While the system was saturated with argon. (B) While the system was saturated with carbon dioxide.

This molecule reduced at a lower potential then either of the previous substrates and as such it was expected to be the lowest yielding out of all the substrates tested so far. Following the standard procedure the solution, containing the substrate, was exposed to a reductive potential of −2.70 V *vs.*Ag$^{0/+}$ while being bubbled with CO_2 to maintain saturation of the solution with the gas and rapidly stirred for 72 hours. The results of bulk electrolysis reaction are shown in Figure 35.

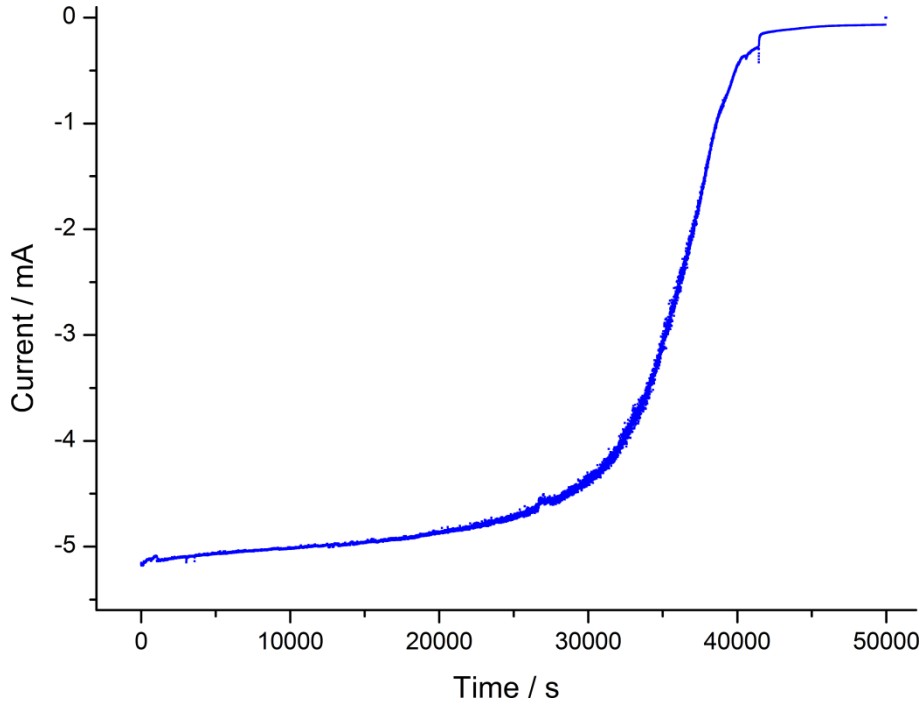

Figure 35: CA obtained from the bulk electrolysis of a 0.1 M solution of 108 in DMF containing 0.1 M [*n*Bu$_4$N][I] and saturated with CO$_2$

The reaction yield of the bulk electrolysis, shown in Figure 35, of compound **108** on the unmodified GCE electrode was only 10 mg (0.06 mmol, 5.6%). The Faradaic yield was calculated using the charge passed during the bulk electrolysis by integration of the CA, 176.4 C, this corresponded to a Faradaic efficiency of 6.1%. Both of these yields are much lower than those obtained for molecules **102a** and **105** which is consistent with the trend that as the molecules reduced at lower potentials the yields of the electrosynthetic reactions decreased. Although the reaction yield was low, at this point, it was determined that substrate **108** could still be used in the enantioselective reductions for the chiral calixarene electrodes. It is important to note that during the isolation procedure of the methyl ester **110** a small amount of methyl 4-acetylbenzoate **114** was detected by NMR.

4.3.5 Bulk electrocarboxylation of 4-methoxyacetophenone 111

The electrocarboxylation of **111** was investigated because of the methyl 4-acetylbenzoate by-product that was formed during the electrolysis of **108**. It was believed that substitution of the *para* position would stop the formation of the unwanted side product

which became more of an issue when reducing the substrate using the chiral electrodes. The electrosynthetic reaction and subsequent esterification of **111** is shown in Scheme 51.

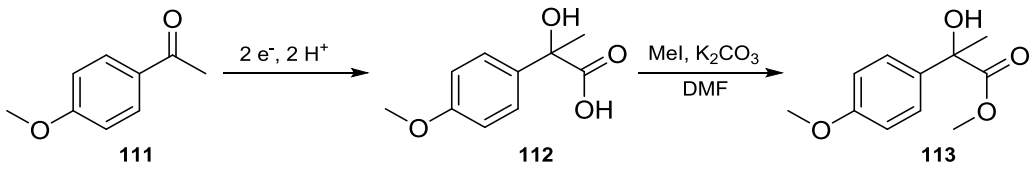

Scheme 51: Scheme showing the electrocarboxylation of compound 111 and subsequent alkylation to form the isolatable product 113

This system was tested in argon and CO_2 saturated environments using an anhydrous electrochemical cell containing 0.1 M of **111** using 0.1 M of [*n*Bu_4N][I] as the electrolyte. The CV obtained from the argon system, Figure 36A, showed a single irreversible reduction at −2.1 *vs.* $Ag^{0/+}$, again, presumably the second reductive single is beyond the breakdown of the solvent system and therefore is not observed. The solution was then saturated with CO_2 gas and another CV was obtained the results of which are shown in Figure 36B. The reductive signal increased dramatically in size while in the presence of CO_2 suggesting that the reductive processes had changed from a one–electron reduction to a multi-electron reduction, which was common for these types of systems. Furthermore although the position of the peak current shifted, the onset potential of the reduction remained very similar to the signal observed in the argon saturated system.

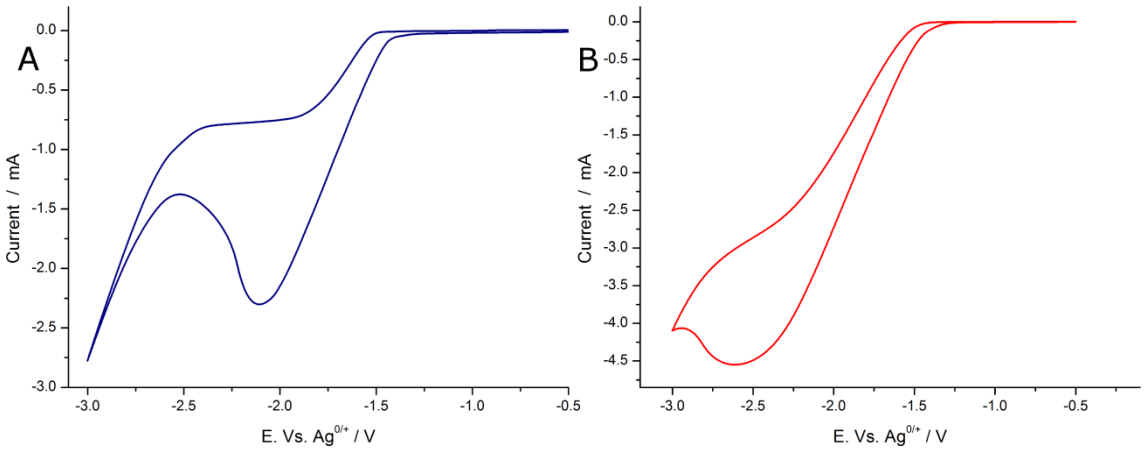

Figure 36: CVs obtained from a 0.1 M solution of 111 dissolved in DMF containing 0.1 M of [*n*Bu$_4$N][I] as the electrolyte at a scan rate of 100 mV s^{-1}. (A) While the system was saturated with Argon. (B) While the system was saturated with carbon dioxide.

Electrocarboxylation of **111** was conducted by holding the potential of the electrochemical cell at −2.7 V *vs.* Ag$^{0/+}$ for 72 hours, as shown in Figure 37. Unfortunately, due to a shift in the *pseudo*-reference electrode (silver electrode) during the bulk electrolysis reaction the experiment had to be stopped and the potential had to be increased to −2.9 V. This was a reoccurring problem that was encountered during the electrosynthetic reductions of **111** presumably caused by the low potential required to drive the reaction promoting unwanted side reactions that caused passivation the silver electrode.

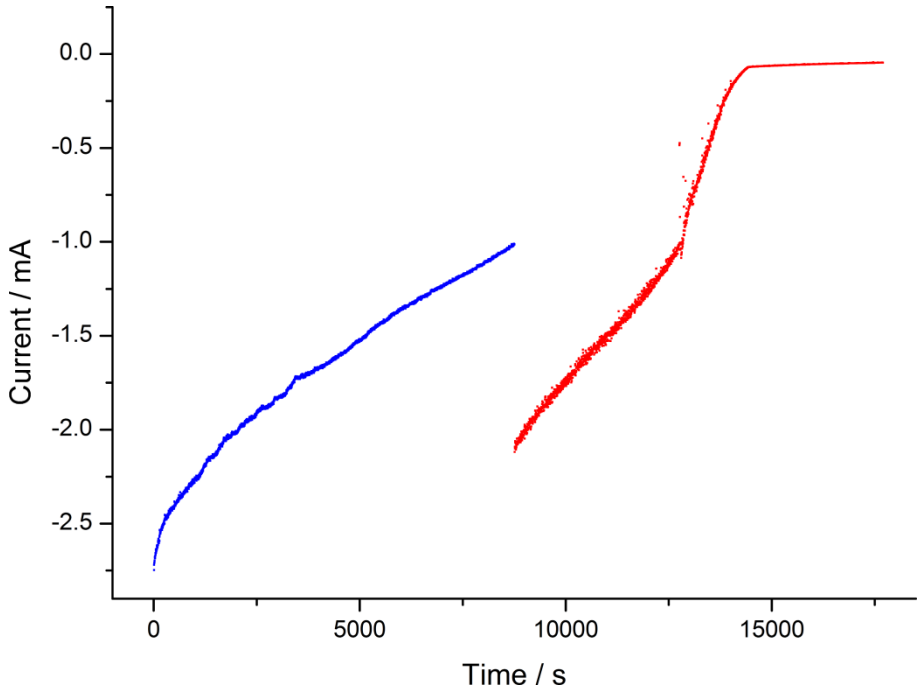

Figure 37: CA obtained from the bulk electrolysis of a 0.1 M solution of 111 in DMF containing 0.1 M [*n*Bu$_4$N][I] and saturated with CO$_2$

Once the bulk electrolysis was complete the combined yield from the reduction and subsequent esterification was calculated to be 5 mg (0.24 mmol, 2.4 %). The Faradaic efficiency was also calculated using the charge, 21.5 C, passed during the CA experiment, which corresponded to a transfer of 0.22 mmol of electrons during the reduction. By comparing the number of elections transferred with the number of mols of **113** isolated the Faradaic efficiency was determined to be 21%. The yield and efficiency of this reduction was relatively low when compared to the electrolysis of compounds **102a**, **105** and **108**, possibly due to the potential required to drive this reaction being relatively low and therefore closer to the solvent breakdown. This would facilitate more possible side reactions and cause faster passivation of the electrode surface bringing an abrupt end to the reaction. Despite the reduction of **111** being low yielding it was preferable to the reduction of **108** due to there being no formation of the *p*-carboxylated by-product that was very difficult to separate from the desired product.

4.4 Formation of the chiral electrode surfaces

Having developed several electrocarboxylation reactions using different substrates I was now ready to test the chiral calixarene surfaces for enantiomeric selectivity. The chiral

electrode surfaces were created by oxidation of the "lithio-activated" calixarene **87** forming modified surface **S8** and the subsequent reaction of these surfaces with amino acids **93a-93c** and **95** in the presence of a Cu(I) catalyst to form the chemisorbed chiral calixarenes electrodes, as shown in Scheme 52.

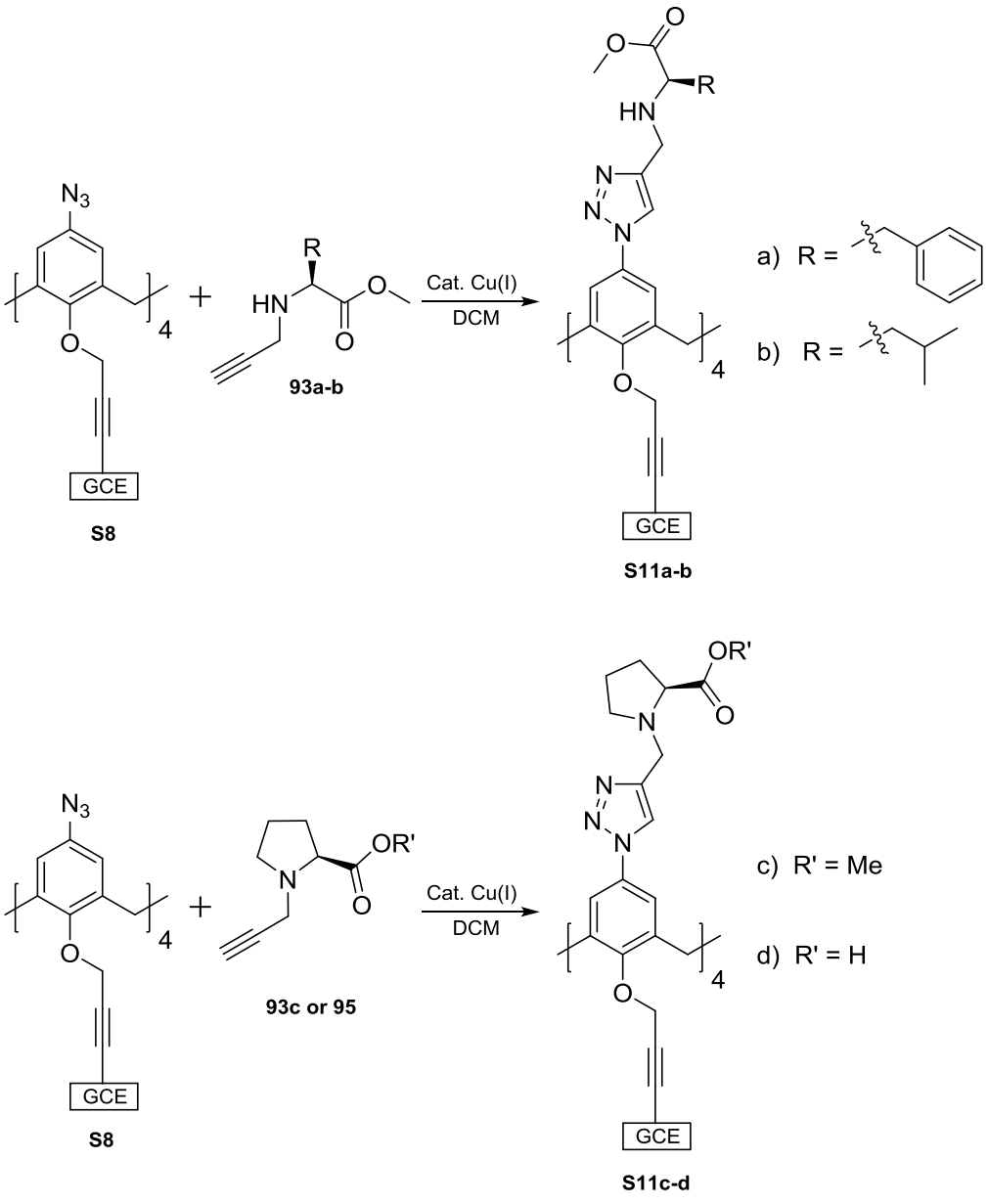

Scheme 52: Post surface functionalisation of S8 with chiral amino acids

4.5 Electrocarboxylation reactions using chiral calixarene carbon electrodes

The electrocarboxylation reactions were conducted in an electrochemical cell containing 0.1 M of the substrate dissolved in 10 mL DMF using 0.1 M of [nBu$_4$N][PF$_6$] as the electrolyte. Before the electrolysis was conducted the solution was saturated with CO_2 and a CV, was recorded at 100 mV s^{-1}, to determine the potential of the peak current. The solution was then held at the potential of the peak current for 72 hours while the mixture was continuously stirred and bubbled with CO_2 gas. Once complete the reaction mixture was purified using the procedure described in the experimental section and the ratio of enantiomers was determined by HPLC analysis.

4.5.1 Electrocarboxylation of 102a using modified calixarene surfaces

The electrocarboxylation of molecule **102a** was conducted using chiral carlixarene surfaces **S11a-d** forming compound **103**. The results of these reduction reactions are shown in Table 1.

Table 1: Results from the bulk electrolysis of compound 102a using the chiral electrode surfaces S11a-d

GCE surface used in electrolysis	Potential of electrolysis vs $Ag^{0/+}$ / V	Charge passed / C	Reaction yield	Faradaic yield	Enantiomeric Excess
Blank	−1.4	65.2	20%	62%	0%
S11a	−1.4	123.9	40%	63%	0%
S11b	−1.4	*	24%	*	0%
S11c	−1.4	39.8	16%	80%	0%
S11d	−1.6	135.2	48%	69%	0%

*** During this run the charge passed was not recorded due to a computer fault.**

From the reductions of **102a** with the chiral electrodes **S11a-d** showed no selectivity towards either of the enantiomers and as such only the formation of racemic product **103** was detected. However, usage of the calixarenes surfaces appeared to aid the formation of racemic product **103** as shown by the increase in reaction yield and Faradaic efficiency while using the

modified surfaces. Presumably this was caused by the calixarenes making the electrode surface more resilient to passivation when compared to the blank glassy carbon electrodes.

HPLC analysis of compound **104** was conducted after each electrolysis reaction using an AD-H chiral column and a mobile phase of 95 : 5 hexane : isopropanol. Figure 38 shows an example HPLC trace that was obtained from the electrochemical reduction of **102a** using chiral surface **S11c**.

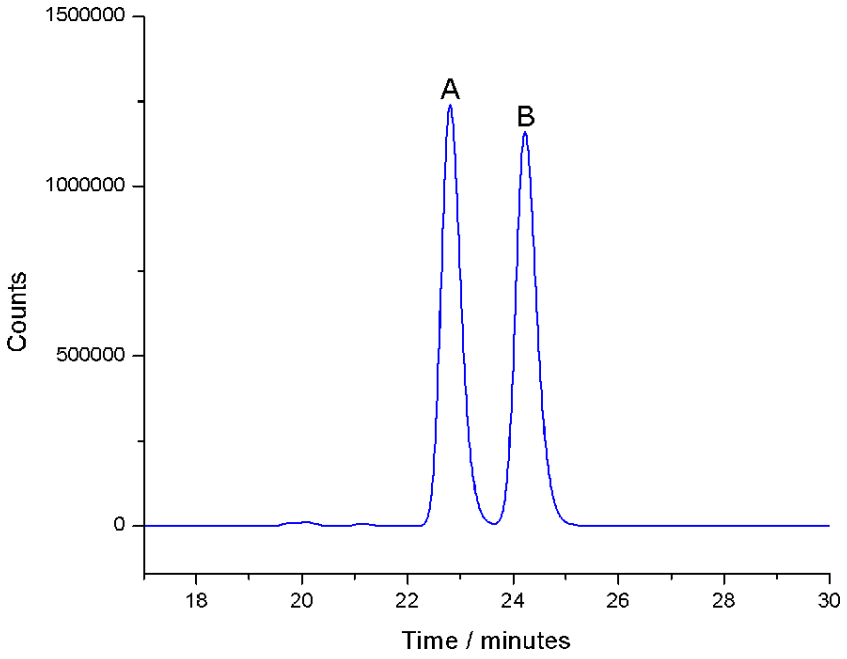

Figure 38: HPLC of racemic product 104 formed using modified GCE surface S11c. (A) Retention time: 28.8 minutes, Area: 3320000 (50.2%). (B) Retention time: 24.2 minutes, Area: 33000000 (49.8%).

4.5.2 Electrocarboxylation of 105 using modified calixarene surfaces

The electrocarboxylations and subsequent esterification of **105** to compound **107** was attempted using calixarene modified electrode surfaces **S11a-d** and the resulting product was monitored by chiral HPLC to determine the enantiomeric excess of the resulting α-hydroxyester. The results of these electrochemical reductions are displayed in Table 2.

Table 2: Results from the bulk electrolysis of compound 105 using the chiral electrode surfaces S11a-d

GCE surface used in electrolysis	Potential of electrolysis vs $Ag^{0/+}$ / V	Charge passed / C	Reaction yield	Faradaic yield	Enantiomeric Excess
Blank	−1.7	147.5	18%	23%	0%
S11a	−1.7	152.7	30%	38%	0%
S11b	−1.7	131.1	45%	67%	0%
S11c	−1.7	*	2.3%	*	0%
S11d	−1.7	167.4	47%	54%	0%

*** During this run the charge passed was not recorded due to a computer fault.**

The reduction of **105** using the modified GCE surfaces did not form a product with an enantiomeric excess, instead the HPLC traces obtained from these systems determined the product **107** to have been formed as a racemic mixture of enantiomers. Although, in the calixarene modified systems it was observed that the reaction yield and Faradaic efficiency had increased significantly when compared to the same reduction using the unmodified GCEs, especially when using surface **S11b** where the reaction and Faradic yields increased by over 100% compared to the unmodified GCE! The only exception to this was when using GCE surface **S11c** where the electrode appeared to become passivated at an unusually fast rate, possibly due to contamination by a small amount of water, which brought about an abrupt end to the electrolysis resulting in the low yield.

An example HPLC trace obtained from **107** formed using modified electrode surface **S11d**, is shown in Figure 39. The trace was obtained using an AD-H chiral column with a mobile of 95 : 5 (hexane : isopropanol).

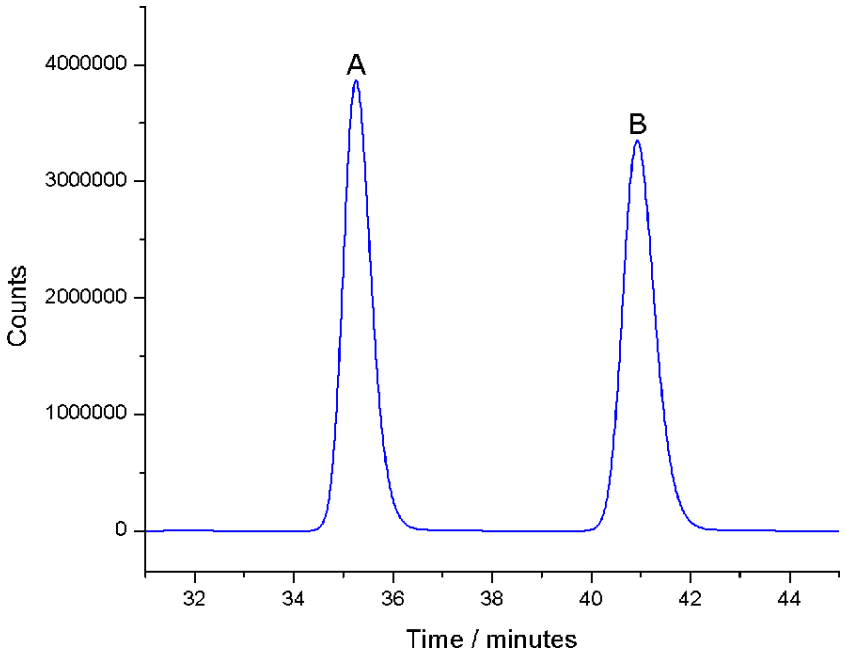

Figure 39: HPLC trace of the product formed from the bulk electrolysis of 105 using GCE surface S11d after esterification. (A) Retention time: 35.3 minutes, Area: 158000000 (49.9%). (B) Retention time: 40.9 minutes, Area: 159000000 (50.1%).

4.5.3 Electrocarboxylation of 111 using modified electrode surfaces S11a-d

The final substrate that was tested using all of the chiral GCE surfaces was compound **111**. This molecule as stated in section **4.3.4** was the most difficult to reduce due to the potential required to drive the reaction being relatively close to the breakdown of the DMF/[*n*Bu_4N][I] system, I believe that being so close to the solvent breakdown promoted the passivation of both the GCE and silver electrode surfaces causing the potential of the cell to drift. This meant that during these experiments the potential of the cell had to be adjusted to account for the change in the position of the peak current. This is shown in the "potential of electrolysis" of Table 3 by the inclusion of two different potentials, as in all cases the voltage of the electrochemical cell had to be increased during the electrolysis to aid the formation of the desired product. The exception was the reduction of **S11d** which required a much stronger reductive potential before the formation of any product was observed and could not be increased due to already being at the limit of the electrochemical solution.

Table 3: Results from the bulk electrolysis of compound 111 using the chiral electrode surfaces S11a-d

GCE surface used in electrolysis	Potential of electrolysis vs $Ag^{0/+}$ / V	Charge passed / C	Reaction yield	Faradaic yield	Enantiomeric Excess
Blank	−2.7, −2.9	21.5 C	2.4%	21%	0%
S11a	−2.1, −2.9	23.2 C	2.4%	20%	0%
S11b	−2, −2.7	56.1 C	33%	73%	0%
S11c	−2, −2.7	112.6 C	24%	32%	0%
S11d	−3	131.7 C	2.4%	3.5%	0%

The reaction of compound **111** proved to be the most unreliable of all the electrocarboxylation reactions attempted with several of the electrolysis reactions resulting in the formation of only 5 mg of product after spending 72 hours held at the potentials described. The modification of the electrode surfaces with the calixarenes appeared to make very little difference to the rate at which the system passivated the electrode surfaces, which resulted in the modified electrodes making very little difference to the reaction and faradaic yields of the reductions.

From the electrosynthetic reductions of compound **111** using the chiral electrode surfaces **S11a-d** there was no observable enantiomeric selectivity in the formation of compound **113**. This was determined by analysis of the products using an AD-H column with a mobile phase of 95 : 5 (hexane : isopropanol) an example of which is shown in Figure 40.

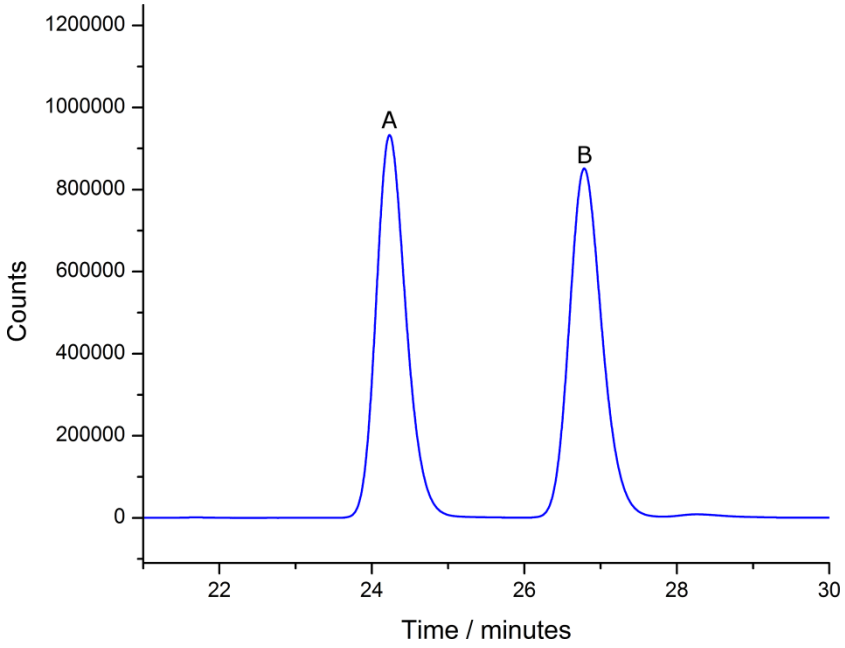

Figure 40: HPLC trace of compound 113 formed from the electrolysis and subsequent esterification of 111 using electrode surface S11a. (A) Retention time: 24.2 minutes, Area: 25600000 (50.2%). (B) Retention time: 26.8 minutes, Area: 25400000 (49.8%).

4.5.4 The unusual reduction of 108 using electrode surface S11c

When the asymmetric electrocarboxylation of substrate **108** was attempted using electrode surface **S11c** some peculiar results were obtained. Instead of forming the expected carboxylic acid **110**, as the main product, the modified GCE produced mainly compound **114** with only a small amount of **110** and **115** present (after esterification), as shown in Scheme 53.

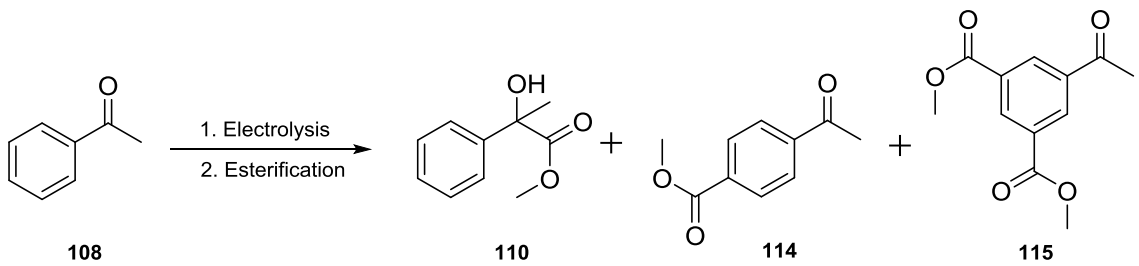

Scheme 53: Electrocarboxylation of compound 108 using calixarene surface S11c

There is very little mention of aryl ring carboxylation in the literature using electrochemical techniques apart from by Filardo and co workers[172] wherein they observed the formation of a small amount of **114**, using a blank carbon working electrode. Their results are similar to what was observed in my research when using a blank GCE. However, when using the modified carbon electrode 12 mg of compound **114** was isolated, contaminated by only a small amount of **115**, and only 4 mg of **110** was isolated, again contaminated by a small amount of **115**. Note the formation of **114** and **115** was determined by NMR and mass spectrometry and was shown to match literature values.[173,174] These results seemed very promising for the development of a system that could selectively electrochemically carboxylate an aryl ring using the modified surfaces. Unfortunately, due to time constraints, the regioselective properties of surface **S11c** were not fully investigated. The reason for this was at the time the focus of the research was on developing systems that could be used to test the modified electrodes for selectivity between the chiral forms of the α-hydroxycarboxylic acids and as this system formed only trace amounts of the desired product the reduction of **108** was not investigated further.

4.6 Conclusion

In this chapter the electrochemical properties of compounds **98** and **99** in both anhydrous and aqueous systems were investigated and the electrosynthetic reductions of these substrates were attempted. Unfortunately, during the bulk electrolysis of these compounds, the formation of the alcoholic products was not observed. So the focus of the research moved to the electrocarboxylation of compounds **102a**, **105**, **108** and **111** to the corresponding α-hydroxycarboxylic acids.

From the CVs of the pro-chiral ketones **102a**, **105**, **108** and **111** in the argon saturated environments I observed two separate one–electron reductions. However once the electrochemical solution was saturated with CO_2 the initial reduction increased dramatically in size suggesting the reduction now corresponded to a multi-electron process and the second reduction was no longer present. This suggests that once the first reduction occurred the radical anion rapidly reacted with a molecule of CO_2 and the intermediate that formed was able to spontaneously reduce at the reduction potential of the initial reduction to form the α-hydroxycarboxylic acid product.

Preliminary bulk electrolysis reactions of these substrates, on a blank GCE, showed the reduction to be reliable and all four substrates produced enough isolatable products to allow full analysis by NMR and chiral HPLC. These reductions were repeated using calixarene

surfaces **S11a-d** but unfortunately no enantiomeric selectivity was observed using the chiral electrodes. However when using the modified surfaces both the Faradaic efficiency and reaction yields obtained in the bulk electrolysis improved suggesting that new surfaces slowed down the rate at which the GCE were being passivated.

Chapter 5

Conclusions and future work

5.1 Conclusions

This thesis has demonstrated two methods that result in the formation of a monolayer of calix[4]arenes and allows for their detection/characterisation while attached onto the electrode surface. This involved the synthesis and full characterisation of molecules **84** and **87** which were covalently bound onto the electrode using either the propargyl ether linkers at lower rim, in the case of **87**, or the formation and subsequent reduction of the diazonium salts at upper rim, in the case of **84**. Once immobilised upon the electrode surface, the macrocycles were shown to be easily modifiable with an array of different substrates using the CuAAC reaction. This allowed for the attachment of electrochemical labels onto the chemisorbed calixarenes facilitating their detection by electrochemical techniques, leading to the determination of a complete monolayer coverage of the macrocyclic scaffolds. The formation of these bi-functional two-faced or Janus calixarenes offers a simple and yet highly versatile methodology that facilitates the immobilisation of a wide range of substrates onto a carbon-based electrode surface.

The next stage of my research described the use of these chiral calixarene surfaces in the asymmetric electrochemical reductions of prochiral ketones. To facilitate this research, a lengthy investigation into the electrosynthetic reduction of compounds **98** and **99** to the corresponding alcohols was conducted and the problems associated with these systems were discussed. These difficulties redirected the focus of my research to the electrocarboxylation of compounds **102a**, **105**, **108** and **111** to the corresponding α-hydroxylcarboxylic acids, while in the presence of CO_2 gas. Bulk electrolysis of these compounds using a blank GCE showed this reaction to be reliable with all four substrates producing enough isolatable products to allow for full characterisation by NMR and HPLC analysis. Regrettably, when using the chiral calixarene surfaces **S11a-d**, racemic mixtures of the products were isolated, although there was an increase in the Faradaic efficiency and isolated yields of the products obtained when using these modified surfaces.

5.2 Future work

A part of this research that urgently requires revisiting is the unexpected electrocarboxylation of **108** while using modified electrode surface **S11c**, as discussed in section **4.5.4**. On a blank electrode the main product formed from this electrolysis (after esterification) was compound **110**, but when the reaction was repeated with a calixarene-modified surface the major product became the *p*-carboxylated compound **114**. This is an unusual result and has only been reported once before in the literature (to the best of my

knowledge) as a minor side product.[172] This opens up the possibility for the development of a new electrosynthetic methodology that could be used to regioselectively electrocarboxylate aryl rings but requires further testing with other calixarene-modified surfaces and different substrates.

Another aspect of this work that requires more attention is the size of the chiral peptide chains attached to the upper rim of the immobilised calixarenes. It was a concern that the size of the chiral pockets may not be sufficient enough to accommodate the prochiral substrates efficiently for the enantioselective electrolysis reactions. To address this problem the next step in my research would be to lengthen the amino acid chains to increase the size of the chiral cavity to promote the insertion of the substrates into the calixarenes, hopefully facilitating the formation of enantiopure products.

I also wanted to modify the electrode surfaces with calixarenes that possess inherent chirality, as it would have been interesting to investigate the effect that this has on the formation of optically active compounds. A calixarene becomes inherently chiral when two different substituents are added onto adjacent aryl rings making the two rings inequivalent; note that the substituents themselves could also be chiral. Calixarenes functionalised in this manner have already been shown to be effective in asymmetric reactions in solutions. [114,115,175]

Moving away from calixarenes, another class of molecules that may show promise in asymmetric electrosynthetic reductions are cyclodextrins. The synthesis and modification of electrodes with these compounds is already extremely well documented and further modification of the surfaces may not be required due to the cyclodextrins themselves already being chiral.[176–179] These modified surfaces have found use in the literature as electrochemical sensors[180–182] and are commonly employed as a chiral stationary phase in the enantioseparation of chiral molecules by HPLC.[183] This shows that these surfaces are both electrochemically active, allowing the transfer of electrons to their guest substrates, as well as being able to differentiate between enantiomers of chiral molecules. Furthermore, these compounds have also shown promise as asymmetric catalysts when bond to a metallic centre in the solution phase.[184–186] It is for these reasons that I suggest the application of these compounds for heterogeneous electrochemical asymmetric reduction is investigated.

Chapter 6

Experimental

6.1 General considerations

Anhydrous reactions were performed under a dry atmosphere of nitrogen or argon (BOC Gasses) using either Schlenk line techniques (a dual manifold inert gas/vacuum lines) or conducted in a MBraun glovebox. All glassware used in anhydrous reactions was dried in a 160 °C oven over night and then flame dried under vacuum prior use.

6.2 Materials

6.2.1 Gases

Nitrogen gas (O_2 free) and argon gas (O_2 free) were both purchased from BOC gases and dried prior to use by being passed through a drying column containing P_4O_{10} and 4 Å molecular sieves. CO_2 gas (99.8%) was purchased from BOC Gasses and was dried before use by being passed through a drying column containing P_4O_{10}. NO_2 gas was generated *in situ* by the reaction of nitric acid and copper powder and was used directly.

6.2.2 Solvents

Anhydrous solvents were dried by refluxing over either sodium/benzophenone (tetrahydrofuran and diethyl ether) or calcium hydride (dichloromethane and acetonitrile) under an inert atmosphere of nitrogen and were collected by distillation. Before use the distilled solvents were sparged with nitrogen gas to remove trace amounts of dissolved oxygen and stored over activated 4 Å molecular sieves. Water, when used in aqueous electrochemical reactions, was thoroughly sparged with nitrogen to remove dissolved oxygen prior to use. Anhydrous DMF (99.8%) was purchased from Sigma−Aldrich, stored over 4 Å molecular sieves and sparged with nitrogen gas to remove dissolved oxygen.

Deuterated NMR solvents, $CDCl_3$ (99.8%), DMSO-d_6 (99.9%), CD_3CN (99.8%) and CD_3OD (99.8%), were purchased from Cambridge Isotope Laboratories Inc. and used without further purification.

6.2.3 Reagents and literature compounds

Commercially available reagents were purchased from either Sigma Aldrich (Gillingham, UK) or Fluorochem (Hadfield, UK) and used without further purification unless stated otherwise. Flash chromatography was performed on silica gel (SiO_2, 70-200 micron mesh 60 Å) purchased from Alfa Aesar. Thin layer chromatography was performed using silica gel 60 Å F254 pre coated plates.

Literature compounds **76**,[187] **77**,[140] **78a**,[140] **78b**[140] and **79**[141] were synthesised using the procedures described in the literature, in the references given.

6.3 Instruments

NMR spectra were recorded using a Bruker Avance DPX-500 MHz spectrometer. Chemical shifts were reported in ppm and referenced to an appropriate standard, for ^{1}H (residue solvent peak), ^{13}C (residue solvent peak) and ^{19}F ($CFCl_3$). The ^{1}H NMR data is reported as: singlet (s), doublet (d), triplet (t), quartet (q), multiplet (m), broad (br) and the *J* coupling constants are given in Hz.

IR spectra were recorded using a PerkinElmer μ-ATR spectrum II spectrometer. X-ray photoelectron spectroscopy (XPS) was performed using a Thermo Scientific K-alpha instrument using monochromatic Al X-rays. All XPS spectra were then corrected relative to the graphitic C_{1s} peak position at 284.97 eV.[166] X-ray crystallographic details are given section **6.8.**

6.4 Electrochemical methods

6.4.1 General methods

All electrochemical experiments were performed under an inert atmosphere of nitrogen or argon gas, apart from the electro-synthetic reactions that were conducted under an atmosphere of dry CO_2. Electrochemical measurements were performed using a computer-controlled potentiostat (Model PGSTAT 302N, Autolab, Utrecht) at ambient temperatures using dry solvents unless stated otherwise.

Electrochemical experiments were conducted using a standard three–electrode configuration consisting of a glassy carbon working electrode, either 3.0 mm (BasiTechnicol, USA) or 6.0 mm in diameter (see section **6.4.2**), a bright platinum wire (99.99%, GoodFellow, UK) or a magnesium ribbon (used only for electrosynthetic reduction) (>99.5%, Sigma Aldrich, UK) counter electrode, and a reference electrode of either silver wire (*pseudo*-reference) (99.99%, GoodFellow, UK) for non-aqueous measurements or a saturated calomel electrode (SCE) (Radiometer, Denmark) for aqueous measurements.

The electrodes were thoroughly cleaned between experiments. The GC surfaces were renewed by successive polishing with diamond paste slurries of decreasing particle size ranging from 3.0 µm to 0.1 µm (Kemmet, U.K.), the electrode was sonicated in deionised water between each polishing step to remove any adhered materials before being rinsed with ethanol and allowed to dry. The Pt electrodes were flame-cleaned. The silver and magnesium electrodes were

cleaned by polishing on a chamois leather cloth using 0.25 µm alumina slurry; they were then rinsed with deionised water to remove any particulates. The saturated calomel electrode was cleaned with deionised water, stored in a saturated solution of KCl and rinsed prior to use.

6.4.2 In house design of 6.0 mm GCE

A 6.0 mm diameter GC rod (Type 2, Alfa Aesar, UK) was wet cut into 3-4 mm thick cross-sections using a diamond blade. A separate 10 mm PEEK rod (Direct Plastics Ltd) was cut into a 700 mm section and a 3 mm wide column was drilled through the centre and widened to 5.5 mm at one end to a depth of 5 mm. The PEEK rode was then warmed using a heat gun set to 300 °C and the GC section was pressed into the widened recess. The opposite face of the shaft was then tapped using a 4 mm tap dye to a depth of 10 mm to form a screw thread within the bore. Silver ink (Sigma Aldrich, UK) was pipetted down the shaft to ensure good connection to the GC and a steel spring was placed at the bottom of the tube in contact with the GC. Once the ink had dried the surface was finished by sanding sequentially with 120, 400, 800, 1000, 1500, 2000 and 2500 grade wet and dry paper.

A 5.0 mm diameter 30 mm length section of PEEK was then cut and a 10 mm screw thread was created using a dye so that it matched the thread inside the other PEEK section. A 3 mm central hole was drilled through the smaller PEEK section and a 3 mm copper rod (RS Components, UK) was pressed through the hole. The copper rode was then placed through the central shaft of the larger section of PEEK and carefully tightened until a contact was formed, which was confirmed by use of a continuity tester (multimeter). Before use, the GCE was polished using the normal procedure.

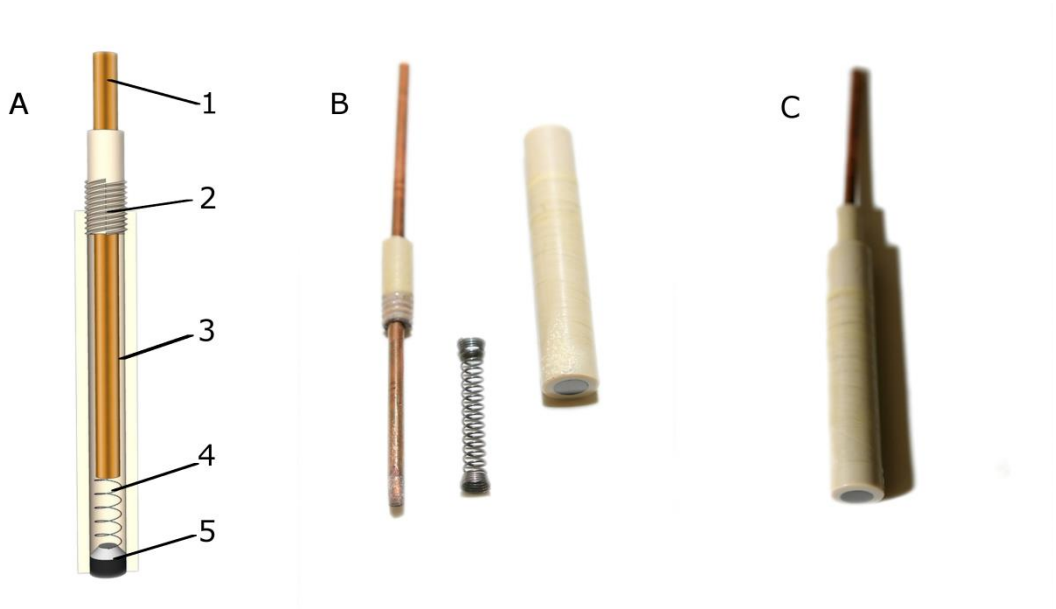

Figure 41: (A) Schematic showing the insides of the assembled 6 mm GCE (1) Copper rod (2) Screw to maintain contact with GC stub (3) PEEK shaft (4) Spring (5) GC stub (B) Photo of unassembled 6 mm GCE (C) Photo of assembled 6 mm GCE.

6.5 Synthetic procedures

6.5.1 Synthesis of 60

The preparation of **60** was achieved using a scaled up version of the procedures reported independently by Gutsche, and later of Simaan and Biali.[135,188] *p*-Tert-butylphenol (200 g, 1.33 mol) and NaOH (1.20 g, 0.03 mol) were added to a three-necked 3L round bottom flask fitted with an overhead stirrer. The flask was purged with nitrogen, followed by the addition of 37% formaldehyde solution (128 mL, 1.66 mol) and left to stir at 120 °C whilst removing water via a right-angled condenser. To the resulting deep-yellow viscous mass that forms, warm diphenyl ether (600 mL, 3.79 mol) is added to dissolve the contents of the flask, and then heated at 110-120 °C to remove water via a condenser (a continuous stream of nitrogen gas is required to aid water removal). After all the water has been removed (4-5 hours), the brown solution in the flask was heated to 260 °C for 4 hours. The reaction was then allowed to cool (overnight), to which ethyl acetate (1.5 L, 15.3 mol) was added and the reaction was left to stir for 1 hour at room temperature. The resulting beige-solid was filtered off affording **60** as a beige powder (95.0 g, 44%). ^{1}H NMR (500 MHz, $CDCl_3$): 1.21 (36H, s), 3.49 (4H, d, *J* = 13.0 Hz), 4.26 (4H, d, *J* = 13.0 Hz), 7.05 (8H, s), 10.34 (4H, s). ^{13}C NMR (125 MHz,

$CDCl_3$): 31.5, 32.8, 34.2, 126.1, 127.8, 144.5, 146.8; IR (neat, ν / cm^{-1}) 3167 (phenol), 2951, 1738, 1481, 1360, 1239, 1200, 1039.[94]

6.5.2 Synthesis of 71

Dry calixarene **60** (10.0 g, 15.1 mmol) was dissolved in dry toluene (200 mL) and heated for 1 hour at 50 °C. Aluminium trichloride (10.0, 75.0 mmol) was added and the reaction was then stirred for 3 hours, at which point the mixture was cooled to 0 °C and quenched by the addition of 1 M hydrochloric acid (240 mL). The organic layer was separated, washed with water (3 x 100 mL), dried over $MgSO_4$ and filtered. The filtrate was concentrated *in vacuo* to form a yellow oil followed by trituration with diethyl ether to yield **71** as a light yellow powder (5.0 g, 78%). ^{1}H NMR (500 MHz, $CDCl_3$): 3.59 (4H, s, br), 4.32 (4H, s, br), 6.78 (4H, t, *J* = 7.6 Hz), 7.10 (8H, d, *J* = 7.6 Hz), 10.25 (4H, s). ^{13}C NMR (125 MHz, $CDCl_3$): 31.05, 31.85, 77.16, 122.39, 129.13, 148.92; IR (neat, ν / cm^{-1}): 3135, 2934, 1594, 1463, 1448, 749, 733.

6.5.3 Synthesis of 72

Dry calixarene **71** (2 g, 4.7 mmol) and sodium hydride (0.5 g, 20.7 mmol) were dissolved in acetonitrile (40 mL) at 0 °C while stirring. The mixture was allowed to stir for 1 hour before the addition of propargyl bromide (80 wt% solution in toluene, 3.0 g, 20.2 mmol), the solution was then warmed to room temperature and the reaction was continued for 48 hours. The reaction was quenched by the addition of cold water (100 mL), and the product was extracted with dichloromethane (3× 50 mL) and dried over $MgSO_4$. The filtrate was concentrated *in vacuo* followed by trituration with methanol to yield **72** as a beige powder (1.2 g, 45%). ^{1}H NMR (500 MHz, $CDCl_3$): 2.47 (4H, t, *J* = 2.4 Hz), 3.22 (4H, d, *J* = 13.5 Hz), 4.63 (4H, d, *J* = 13.5 Hz), 4.78 (8H, d, *J* = 2.4 Hz), 6.66 (4H, m), 6.72 (8H, d, *J* = 7.1 Hz). ^{13}C NMR (125 MHz, $CDCl_3$): 32.03, 61.31, 74.84, 80.66, 123.41, 128.40, 135.56, 155.16; IR (neat, ν / cm^{-1}): 3279, 2912, 2123, 1585, 1456, 1429, 1199, 1184, 998.

6.5.4 Synthesis of 74

Following a modified procedure reported by Chetcuti,[189] calixarene **60** (30 g, 46.3 mmol), potassium carbonate (27.2 g, 260 mmol) and propargyl bromide (80 wt% solution in toluene, 33.7 g, 286 mmol) were refluxed in acetonitrile (500 mL) for 48 h. The reaction mixture was filtered, and the filtrate evaporated to dryness. Re-dissolving the resulting residue in dichloromethane, followed by trituration with methanol yielded **74** as a cream powder (19.0 g, 51%). ^{1}H NMR (500 MHz, $CDCl_3$): 1.08 (36H, s), 2.48 (4H, t, *J* = 2.3 Hz), 3.16 (4H, d, *J* = 13.0 Hz), 4.60 (4H, d, *J* = 13.0 Hz), 4.80 (8H, d, *J* = 2.3 Hz), 6.79 (8H, s). ^{13}C NMR (125 MHz, $CDCl_3$):

31.5, 32.5, 34.0, 61.2, 74.5, 81.3, 125.1, 134.4, 145.7, 152.5; IR (neat, ν / cm^{-1}): 3295, 2954, 2120 (alkyne), 1745, 1593, 1476, 1362, 1190, 1120, 1017, 1003.

6.5.5 Synthesis of 80

Calixarene **79** (200 mg, 0.3 mmol) and sodium hydride (88 mg, 3.7 mmol) were dissolved in dry acetonitrile (50 mL) at 0 °C. The reaction mixture was stirred for 30 minutes before propargyl bromide (80 wt% solution in toluene, 2 mL, 4.88 mmol) was added, the reaction was then allowed to warm up to room temperature and stirred for 24 hours. The reaction was quenched by the addition of cold water (100 mL), extracted with dichloromethane (3× 50 mL), and concentrated under vacuum before being purified by flash chromatography to yield **80** as a yellow solid (110 mg, 37%). ^{1}H NMR (500 MHz, $CDCl_3$): 2.46 (4H, t, *J* = 2.4 Hz), 2.48 (4H, t, *J* = 2.4 Hz), 3.16 (4H, d, *J* = 13.5 Hz), 3.36 (8H, s), 4.57 (4H, d, *J* = 13.5 Hz), 4.65 (8H, d, *J* = 2.4 Hz), 4.72 (8H, d, *J* = 2.4 Hz), 6.60 (8H, s). ^{13}C NMR (125 MHz, $CDCl_3$): 31.9, 40.3, 52.3, 61.4, 75.0, 75.2, 77.8, 80.5, 128.1, 129.2, 135.5, 154.5, 171.0. IR (neat, ν / cm^{-1}): 2948, 2128, 1738, 1471, 1433, 1282, 1147, 1011. HRMS: m/z: $[M + NH_4]^+$ Calcd for $C_{60}H_{48}O_{12}$, 978.3484, found 978.3479.

6.5.6 Synthesis of 81

To a 3 necked 100 mL round bottom flask, *tert*-butyldimethylsilyl chloride (14.7 g, 97.5 mmol) was dissolved in anhydrous THF (50 mL). In a separate flask **74** (12 g, 16.2 mmol) was added and dissolved in anhydrous THF (100 mL), this was then cooled to -78 °C, and over a period of 15 minutes whereupon lithium bis(trimethylsilyl)amide solution (1.0 M in THF, 100 mL, 97.5 mmol) was added, resulting in a dark brown reaction mixture. After 30 mins the solution containing *tert*-butyldimethylsilyl chloride in THF was added dropwise, *via* cannula to the deprotonated calixarene, **74**. After complete addition, the flask was allowed to warm to room temperature overnight. The reaction was then quenched by the addition of a saturated solution of ammonium chloride (100 mL). The organic layer was separated, and the aqueous layer washed with dichloromethane (100 mL). The organic extracts were combined, dried over $MgSO_4$, and remaining solvents were removed *in vacuo*. The product **81** was isolated as a light brown solid (12.0 g, 64%). ^{1}H NMR (500 MHz, $CDCl_3$): 0.09 (24H, s), 0.90 (36H, s), 1.06 (36 H, s), 3.12 (4H, d, *J* = 13.0 Hz), 4.52 (4H, d, *J* = 13.0 Hz), 4.83 (8H, s), 6.75 (8H, s). ^{13}C NMR (125 MHz, $CDCl_3$): -4.5, 16.6, 26.3, 31.5, 32.7, 34.0, 61.4, 89.5, 103.6, 124.9, 134.8, 145.3, 152.1; IR (neat, ν / cm^{-1}): 2952, 2929, 2855, 2167 (alkyne), 1739, 1480, 1361, 1248, 1196, 1120, 1040; HRMS: *m/z*: $[M + NH_4]^+$ Calcd for $C_{80}H_{120}O_4Si_4$, 1274.8607, found 1274.8581

6.5.7 Synthesis of 82

To a round bottom flask, cooled to 0 °C, was added **81** (13 g, 10.4 mmol) dissolved in dichloromethane (130 mL) and glacial acetic acid (130 mL). Using a dropping funnel, 90% fuming red nitric acid (54 mL, 1.29 mol) was added dropwise at 0 °C. After complete addition, the flask was allowed to warm to room temperature overnight. The reaction was then poured into iced water (200 mL), and the organic layer was separated by extraction. The aqueous layer was washed with dichloromethane (50 mL x3), and the remaining organic phases were combined, dried over $MgSO_4$, and any remaining solvent was evaporated *in vacuo*. Re-dissolving the resulting residue in dichloromethane, followed by trituration with methanol yielded **82** as a cream powder (4.6 g, 37%). ^{1}H NMR (500 MHz, $CDCl_3$): 0.08 (24H, s), 0.86 (36H, s), 3.44 (4H, d, *J* = 14.0 Hz), 4.66 (4H, d, *J* = 14.0 Hz), 4.91 (8H, s), 7.71 (8H, s). ^{13}C NMR (125 MHz, $CDCl_3$):-4.7, 16.5, 26.0, 32.3, 62.6, 93.4, 99.9, 124.2, 136.3, 144.0, 159.7; IR (neat, ν / cm^{-1}): 2952, 2885, 2857, 2929, 2179 (alkyne), 1738, 1714, 1587, 1524 (nitro asymmetric), 1462, 1345 (nitro symmetric), 1251, 1205, 1096; HRMS: *m/z*: $[M + NH_4]^+$ Calcd for $C_{80}H_{120}O_4S_{i4}$, 1230.5501, found 1230.5497.

6.5.8 Synthesis of 83

Calixarene **82** (1 g, 0.82 mmol) was dissolved in a 1M solution of tetra-*n*-butylammonium fluoride (TBAF) in THF (16.5 mL, 16.5 mmol) at room temperature, the reaction was monitored by TLC. Once complete the reaction was quenched by the addition of cold water (100 mL), and the product was extracted with dichloromethane (3x 50 mL) washings of the aqueous layer. The combined organic layers were then washed with water (2x 100 mL) and dried over $MgSO_4$. The filtrate was concentrated *in vacuo*, and the residue was purified using flash chromatography (acetone/petroleum ether 1:4) to afford **83** as a pale yellow-orange solid (0.34 g, 55%). ^{1}H NMR (500 MHz, CDCl3): 2.60 (4H, t, *J* = 2.0 Hz), 3.49 (4H, d, *J* = 14.0 Hz), 4.72 (4H, d, *J* = 14.0 Hz), 4.86 (8H, d, *J* = 2.0 Hz), 7.71 (8H, s). ^{13}C NMR (125 MHz, CDCl3): 26.0, 62.6, 93.4, 99.9, 124.2, 136.3, 144.0, 159.7; IR (neat, ν / cm^{-1}): 3287, 3079, 2931, 2120 (alkyne), 1704, 1585, 1519 (nitro asymmetric), 1459, 1342 (nitro symmetric), 1202, 1093; HRMS: m/z: $[M + NH_4]^+$ Calcd for $C_{40}H_{32}N_5O_{12}$, 774.2042, found 774.2044.

6.5.9 Synthesis of 84

Calix[4]arene **82** (4 g, 3.3 mmol) was dissolved in ethanol (200 mL), to which $SnCl_2.(H_2O)_2$ (40 g, 177 mmol) was added and stirred at room temperature for 15 minutes. The reaction mixture was then submitted to reflux for 48 h. After allowing the reaction to cool to room temperature, 10% NaOH solution (200 mL) was added to basify the reaction mixture and

the solution was stirred for 30 minutes. Extraction of the aqueous layer with dichloromethane (3x 200 mL), followed by drying of the organic extracts over $MgSO_4$ and solvent evaporation under reduced pressure afforded compound **84** as a light brown solid (2.05 g, 58%). ^{1}H NMR (500 MHz, $CDCl_3$): 0.08 (24H, s), 0.90 (36H, s), 2.93 (4H, d, *J* = 13.0 Hz), 4.45 (4H, d, *J* = 13.0 Hz), 4.69 (8H, s), 6.11 (8H, s). ^{13}C NMR (125 MHz, $CDCl_3$): -4.5, 16.6, 26.2, 31.1, 61.7, 89.4, 103.7, 115.6, 136.2, 141.2, 148.2; IR (neat, ν / cm^{-1}): 3325 (amine), 2954, 2928, 2855, 2173 (alkyne), 1606 (amine), 1471, 1361, 1249, 1207, 1097; HRMS: m/z: $[M + H]^+$ Calcd for $C_{64}H_{93}N_4O_4Si_4$, 1093.6267, found 1093.6269.

6.5.10 Synthesis of 85

Calixarene **84** (27.3 mg, 0.025 mmol) was dissolved in 0.5 M HCl (5 mL) at 0 °C to which was added $NaNO_2$ (7 mg, 0.10), the reaction was then stirred for 3 hours. The product was extracted with dichloromethane (3x 20 mL) and concentrated under reduced pressure to afford compound **85** as a crude solid, which was then used to form compound **86b** or electrografted onto a GCE surface without further purification. ^{1}H NMR (500 MHz, $CDCl_3$): 0.11 (24H, s), 0.90 (36H, s), 4.15 (4H, d, *J* = 13.4 Hz), 4.55 (4H, d, *J* = 13.4Hz), 4.99 (8H, s), 8.84 (8H, s). IR (neat, ν / cm^{-1}): 2954, 2929, 2857, 2268 (N_2^+ stretch), 1568, 1461, 1258, 1031.

6.5.11 Synthesis of 86a

To a stirred solution of **84** (1.5 g, 1.37 mmol) in trifluoroacetic acid (TFA) (10 mL) at 0 °C was added $NaNO_2$ (900 mg, 13 mmol) dissolved in cold water (2 mL), the mixture was then stirred for 10 minutes. After this time a solution of NaN_3 (1.8 g, 26 mmol) in cold water (2 mL) was slowly added and the reaction was stirred for 45 minutes. Dichloromethane (10 mL) was then added and the reaction was allowed to warm up to room temperature overnight. The reaction was diluted with water and extracted with dichloromethane (3x 25 mL). The combined organic layers were dried over $MgSO_4$, filtered and concentrated *in vacuo*. The residue was then purified by flash chromatography (ethyl acetate/petroleum ether 1:10) to afford **86a** as pale yellow powder (1.0 g, 67 %). ^{1}H NMR (500 MHz, $CDCl_3$): 0.08 (24H, s), 0.88 (36H, s), 3.13 (4H, d, *J* = 13.6 Hz), 4.53 (4H, d, *J* = 13.6 Hz), 4.73 (8H, s), 6.37 (8H, s). ^{13}C NMR (125 MHz, $CDCl_3$): -4.6 16.6, 26.1, 62.0, 91.0, 102.0, 118.7, 134.8, 137.0, 152.1, IR (neat, ν / cm^{-1}): 2953, 2927, 2856, 2177 (alkyne), 2107 (azide), 1656, 1587, 1468, 1361, 1317, 1249, 1233, 1201, 1024; HRMS: m/z: $[M + NH_4]^+$ Calcd for $C_{64}H_{88}N_{13}O_4Si_4$, 1214.6154, found 1214.6153.

6.5.12 Synthesis of 86b

Calixarene **85** was dissolved in dichloromethane (5 mL) and sodium cyanide (5 mg, 0.1 mmol) was carefully added to the reaction, which was then stirred for 24 hours. Once

complete the reaction was quenched by the addition of a 1 M solution of NaOCl before extraction into dichloromethane (3x 20 mL) and concentration under reduced pressure. The resulting residue was purified by flash chromatography (acetone/petroleum ether 2:6) which afforded **86b** as a light brown solid (6 mg, 20% from **84** over two steps). ^{1}H NMR (500 MHz, $CDCl_3$): 0.08 (24H, s), 0.86 (36H, s), 3.48 (4H, d, *J* = 13.8 Hz), 4.67 (4H, d, *J* = 13.8 Hz), 4.97 (8H, s), 7.43 (8H, s) IR (neat, ν / cm^{-1}): 2954, 2928, 2856, 2266 (Cyano), 2184, 1723, 1462, 1393, 1260.

6.5.13 Synthesis of 87

Calixarene **86a** (750 mg, 0.63 mmol) was dissolved in a 1M solution of TBAF in THF (13 mL, 13 mmol), the reaction was monitored by TLC. Once complete the reaction was quenched by the addition of cold water (100 mL), and the product was extracted with dichloromethane (3x 50 mL). The combined organic layers were then washed with water (2x 100 mL), dried over $MgSO_4$. The filtrate was concentrated *in vacuo*, and the residue was purified using flash chromatography (acetone/petroleum 1:4) to afford **87** as a yellow solid (0.25 g, 54%). ^{1}H NMR (500 MHz, $CDCl_3$): 2.48 (4H, t, *J* = 2.1 Hz), 3.17 (4H, d, *J* = 13.8 Hz), 4.59 (4H, d, *J* = 13.8 Hz), 4.70 (8H, d, *J* = 2.1 Hz), 6.39 (8H, s). ^{13}C NMR (125 MHz, $CDCl_3$): 32.1, 61.6, 75.5, 79.9, 118.9, 135.1, 136.9, 152.4; IR (neat, ν / cm^{-1}): 3295, 2921, 2195 (alkyne), 2104 (azide), 1587, 1529, 1467, 1366, 1314, 1232, 1201, 1001; HRMS: *m/z*: $[M + NH_4]^+$ Calcd for $C_{40}H_{32}N_{13}O_4$, 758.2695, found 758.2689.

6.5.14 Synthesis of 89

$CuSO_4$ (15 mg, 0.06 mmol) and sodium ascorbate (24 mg, 0.12 mmol) were dissolved in 5 mL ethanol:water (1:1). To which was added **86a** (180 mg, 0.15 mmol) and **88** (69 mg ,0.68 mmol) dissolved in 5 mL dichloromethane, the reaction mixture was rapidly stirred for 24 hours. Once complete 50 mL of water was added and the product was extracted with dichloromethane (3x 20 mL), dried over $MgSO_4$ and concentrated *in vacuo.* The residue was then purified using column chromatography (acetone/petroleum 2:8) to yield **89** as a beige solid (95 mg, 41%). ^{1}H NMR (500 MHz, $CDCl_3$): 0.12 (24H, s), 0.91 (36H, s), 3.45 (4H, d, *J* = 13.5 Hz), 4.79 (4H, d, *J* = 13.5 Hz), 4.97 (8H, s), 7.27 (12H, m) 7.32 (8H, t, *J* = 7.4 Hz), 7.74 (8H, d, *J* = 7.4 Hz), 7.96 (4H, s). ^{13}C NMR (125 MHz, $CDCl_3$): -4.5, 16.6, 26.1, 32.6, 62.4, 92.0, 101.3, 118.1, 120.9, 126.0, 128.3, 128.8, 130.1, 133.0, 136.9, 148.3, 155.0. IR (neat, ν / cm^{-1}): 2954, 2928, 2856, 2175, 1595, 1478, 1457, 1221, 1250. HRMS: *m/z*: $[M + H]^+$ Calcd for $C_{96}H_{108}N_{12}O_4Si_4$, 1606.7792, found 1606.7763.

6.5.15 Synthesis of 90

Calixarene **89** (140 mg, 0.09 mmol) was dissolved in a 1 M solution of TBAF in THF (570 mg, 1.8 mmol) at room temperature, the reaction was then stirred for 24 hours. Once the reaction as complete (determined by TLC), water (50 mL) was added and the product was extracted into dichloromethane (3x 50 mL) and concentrated *in vacuo* before being purified by flash chromatography (acetone/petroleum ether 2:3) to yield **90** as a light yellow powder (90 mg, 87%). ^{1}H NMR (500 MHz, $CDCl_3$): 2.60 (4H, t, *J* = 2.4 Hz), 3.45 (4H, d, *J* = 13.7 Hz), 4.80 (4H, d, *J* = 13.7 Hz), 4.89 (8H, d, *J* = 2.4 Hz), 7.22 (4H, t, *J* = 7.3 Hz), 7.26-7.31 (16H, m), 7.72 (8H, d, *J* = 7.3 Hz), 8.03 (4H, s). ^{13}C (125 MHz, $CDCl_3$): 32.4, 61.9, 76.3, 79.4, 118.2, 120.9, 126.0, 128.2, 128.8, 130.1, 133.0, 136.6, 148.1, 155.2. IR (neat, ν / cm^{-1}): 2963, 2930, 2863, 2118, 1699, 1595, 1477, 1220. HRMS: *m/z*: $[M + NH_4]^+$ Calcd for $C_{72}H_{52}N_{12}O_4$, 1166.4573 found 1166.4568.

6.5.16 Synthesis of 92

$Cu(SO_4)$ (82.5 mg, 0.33 mmol) dissolved in 5 mL ethanol:water (1:1) was slowly added to a solution of sodium ascorbate (32.7 mg, 0.17 mmol) in 5 mL ethanol:water (1:1). A separate vessel was charged with calixarene **86a** (50 mg, 0.041 mmol) and 1-ethynyl-3,5-bis(trifluoromethyl)benzene **91** (45.3 mg, 0.19 mmol) to which the copper solution was slowly added and the reaction mixture was allowed to stir for 1 hour. Dichloromethane (10 mL) was then added and the reaction mixture was rapidly stirred overnight. Once complete, confirmed by TLC, the reaction was quenched by the addition of cold water (50 mL), and the product was extracted with dichloromethane (3× 25 mL) washings of the aqueous layer, dried over $MgSO_4$. The filtrate was concentrated *in vacuo*, and the residue was purified using flash chromatography (acetone/petroleum ether 2:7) to afford **92** as a yellow solid (56 mg, 64%). ^{1}H NMR (500 MHz, $CDCl_3$): 0.12 (24H, s), 0.91 (36H, s), 3.47 (4H, d, *J* = 13.9 Hz), 4.82 (4H, d, *J* = 13.9 Hz), 4.96 (8H, s), 7.79 (4H, s), 8.09 (4H, s), 8.18 (8H, s). ^{19}F NMR (471 MHz, CDCl3): 63.1. ^{13}C NMR (125 MHz, CDCl3): -4.55, 1.17, 16.57, 26.11, 30.96, 32.50, 62.50, 92.31, 100.94, 118.95, 120.73, 121.99, 123,23 (q, *J* = 33.6 Hz), 125.80, 132.22 (q, *J* = 33.6 Hz), 137.24, 145.67, 155.44; IR (neat, ν / cm^{-1}): 2954, 2930, 2869, 2179 (alkyne), 1596, 1486, 1373, 1277, 1130; HRMS: m/z: $[M + NH4]^+$ Calcd for $C_{104}H_{104}F_{24}N_{13}O_4S_{i4}$, 2166.7023, found 2166.7010.

6.5.17 Synthesis of 93a

Activated 4Å molecular sieves (2.7 g) were milled and added to a round bottomed flask containing DMF (20 mL) and LiOH (240 mg, 10 mmol), this mixture was stirred for 20 minutes. L-phenylalanine methyl ester hydrochloride (1 g, 4.65 mmol) was then added and the solution was stirred for another 45 minutes before the addition of propargyl bromide (80 wt% solution

in toluene, 0.94 mL, 8.4 mmol) the reaction was then continued for 24 hours. At which point the solids were removed by filtration, concentrated *in vacuo* and purified by flash chromatography (EtOAc/petroleum ether 1:8) to yield **93a** as an oil (550 mg, 56%). ^{1}H NMR (500 MHz, $CDCl_3$): 1.98 (1H, br, s), 2.20 – 2.18 (1H, m), 3.44 – 3.32 (1H, m), 3.66 – 3.64 (1H, m), 3.77 – 3.72 (1H, m), 7.32 – 7.12 (1H, m). ^{13}C NMR (125 MHz, $CDCl_3$): 36.7, 39.3, 51.7, 61.1, 71.9, 81.1, 126.8, 128.4, 129.1, 136.8, 174.2. IR (neat, ν / cm^{-1}): 3290, 3028, 2950, 1732 (ester), 1454, 1434, 1201, 1772, 1129.

6.5.18 Synthesis of 93b

Activated 4Å molecular sieves (3.2 g) were milled and added to a round bottomed flask containing DMF (20 mL) and LiOH (286 mg, 11.9 mmol), this mixture was stirred for 20 minutes. L-leucine methyl ester hydrochloride (1 g, 5.5 mmol) was then added and the solution was stirred for another 45 minutes before the addition of propargyl bromide (80 wt% solution in toluene, 1.1 mL, 9.9 mmol) the reaction was then continued for 24 hours. At which point the solids were removed by filtration, concentrated *in vacuo* and purified by flash chromatography (EtOAc/petroleum ether 1:8) to yield **93b** as an brown oil (459 mg, 46%). ^{1}H NMR (500 MHz, $CDCl_3$): 0.85 (6H, m, *J* = 6.6 Hz), 1.46 – 1.36 (m, 2H), 1.67 (1H, m, *J* = 6.6 Hz), 2.15 (1H, t, *J* = 2.4 Hz), 3.28 (1H, m, *J* = 2.4,) 3.41 – 3.35 (2H, m), 3.65 (3H, d, *J* = 1.0 Hz). ^{13}C NMR (125 MHz, $CDCl_3$): 22.1, 22.7, 24.8, 36.9, 42.5, 51.7, 58.5, 71.6, 175.8. IR (neat, ν / cm^{-1}): 3293, 2955, 2870, 1732 (ester), 1468, 1434, 1197, 1149. 991

6.5.19 Synthesis of 93c

L-proline methyl ester hydrochloride (1.6 g, 9.7 mmol), K_2CO_3 (4.0 g, 30 mmol) and propargyl bromide (80% wt% solution in toluene, 2.15 mL) were all added to a reaction vessel containing 40 mL methanol and stirred for 24 hours. EtOAc (100 mL) was added to the reaction and the solids were removed by filtration. The filtrate was then concentrated *in vacuo* and purified by flash chromatography (EtOAC/petroleum ether 1:5) to yield **93c** as an brown oil (600 mg, 40%). ^{1}H NMR (500 MHz, $CDCl_3$): 1.78 – 1.70 (1H, m), 1.87 – 1.80 (1H, m), 1.91 (1H, m, *J* = 9.2 Hz), 2.08 (1H, m, *J* = 9.0), 2.15 (1H, t, *J* = 2.4 Hz), 2.65 (1H, m, *J* = 9.0 Hz), 3.01 – 2.95 (1H, m), 3.36 (1H, m, *J* = 9.2 Hz), 3.58 – 3.47 (2H, m, *J* = 2.4 Hz), 3.65 (3H ,s). ^{13}C NMR (125 MHz, $CDCl_3$): 23.2, 29.5, 41.1, 51.9, 52.2, 62.5, 73.2, 78.3, 174.0. IR (neat, ν / cm^{-1}): 2951, 2881, 2830, 1754 (ester), 1421.

6.5.20 Synthesis of 94a

Calixarene **86a** (50 mg, 0.042 mmol), amino acid **93a** (55 mg, 0.25 mmol), and $[(MeCN)_4Cu]PF_6$ (63 mg, 0.17 mmol) were charged into a round bottomed flask and dissolved in

dry dichloromethane (20 mL). The reaction was monitored by IR until the azide stretch at 2100 cm^{-1} was no longer observed. Once the reaction had progressed to completion, water (50 mL) was added and the product was extracted into dichloromethane (3 x 20 mL). The organic layer was washed with a 1 M aqueous solution of EDTA (30 mL) and concentrated *in vacuo* before being purified by flash chromatography (acetone/petroleum ether 4:5) to yield **94a** as a light brown solid (45 mg, 52%). ^{1}H NMR (500 MHz, $CDCl_3$): 0.11 (24H, s), 0.90 (36H, s), 2.04 (4H, s), 2.92 (8H, m), 3.39 (4H, d, *J* = 13.4 Hz), 3.63 (12H, s), 3.76 (4H, d, *J* = 13.9 Hz), 3.90 (4H, d, *J* = 13.9 Hz,), 4.75 (4H, d, *J* = 13.4 Hz), 4.95 (8H, s), 7.18 – 7.02 (28H, m), 7.30 (4H, s). ^{13}C NMR (125 MHz, $CDCl_3$): -4.6, 16.5, 26.1, 32.5, 39.7, 51.9, 62.3, 62.5, 91.9, 101.3, 120.2, 120.7, 126.8, 128.4, 129.4, 133.0, 136.7, 137.5, 147.1, 154.8, 174.8. IR (neat, ν / cm-1): 2951, 2928, 2855, 1732 (ester), 1595, 1484, 1205. HRMS: m/z: $[M + 2H]^{2+}$ Calcd for $C_{116}H_{144}N_{16}O_{12}Si_4$, 1034.0200, found 1034.0196.

6.5.21 Synthesis of 94b

Calixarene **86a** (100 mg, 0.084 mmol), amino acid **93b** (92 mg, 0.50 mmol), and $[(MeCN)_4Cu]PF_6$ (126 mg, 0.34 mmol) were charged into a round bottomed flask and dissolved in dry dichloromethane (20 mL). The reaction was monitored by IR until the azide stretch at 2100 cm^{-1} was no longer observable. Water (50 mL) was then added and the product was extracted into dichloromethane (3 x 20 mL). The organic layer was washed with a 1 M aqueous solution of EDTA (30 mL) and concentrated *in vacuo* before being purified by flash chromatography (Acetone/petroleum ether 4:7) to yield **94b** as a beige solid (116 mg, 60%). ^{1}H NMR (500 MHz, $CDCl_3$): 0.08 (24H, s) 0.87 (36H, s), 0.92 – 0.78 (24H, m), 1.55 – 1.44 (8H, m), 1.70 (4H, m), 2.02 (4H, br, s), 3.35 (4H, d, *J* = 13.6 Hz), 3.37 (4H, m), 3.69 (12H, s), 3.75 (4H, d, *J* = 14.0 Hz), 3.89 (4H, d, *J* = 14.0 Hz), 4.71 (4H, d, *J* = 13.6 Hz), 4.89 (8H, s), 7.10 (8H, d, *J* = 14.0 Hz), 7.64 (4H, s). ^{13}C NMR (125 MHz, $CDCl_3$): -4.6, 16.5, 22.5, 22.8, 25.0, 26.1, 32.4, 42.7, 43.3, 51.8, 59.8, 62.2, 91.9, 101.3, 120.4, 120.7, 120.8, 133.0, 154.8, 176.0. IR (neat, ν / cm-1): 2954, 2929, 2857, 2176, 1733 (ester), 1597, 1485, 1205, 1035. HRMS: m/z: $[M + 2H]^{2+}$ Calcd for $C_{104}H_{152}N_{16}O_{12}Si_4$, 966.0512, found 966.0507.

6.5.22 Synthesis of 94c

Calixarene **86a** (100 mg, 0.084 mmol), amino acid **93c** (84 mg, 0.50 mmol), and $[(MeCN)_4Cu]PF_6$ (126 mg, 0.34 mmol) were charged into a round bottomed flask and dissolved in dry dichloromethane (20 mL). The reaction was monitored by IR until the azide stretch at 2100 cm^{-1} was no longer observable. Water (50 mL) was then added and the product was extracted into dichloromethane (3 x 20 mL). The organic layer was washed with a 1 M aqueous

solution of EDTA (30 mL) and concentrated *in vacuo* before being purified by flash chromatography (dichloromethane/acetone/methanol 7:6:0.1) which yielded **94c** as a yellow solid (80 mg, 51%). ^{1}H NMR (500 MHz, $CDCl_3$): 0.08 (24H, s), 0.87 (36H, s), 1.80 – 1.69 (4H, m), 1.98 – 1.82 (8H, m), 2.13 – 2.06 (4H, m), 2.50-2.44 (4H, m), 3.16-3.10 (4H, m), 3.46 – 3.34 (4H, m), 3.35 (4H, d, *J* = 13.5 Hz), 3.63 (12H, s), 3.80 (4H, d, *J* = 13.8 Hz), 3.98 (4H, d, *J* = 13.8 Hz), 4.71 (4H, d, *J* = 13.5 Hz), 4.90 (8H, s), 7.15 (8H dd, *J* = 10.4, 2.5 Hz), 7.71 (4H, s). ^{13}C NMR (125 MHz, $CDCl_3$): -4.6, 16.5, 23.1, 26.1, 29.5, 48.5, 52.0, 53.4, 62.2, 64.9, 91.9, 101.3, 120.6, 120.7, 121.3, 132.9, 136.7, 144.8, 154.8, 174.4. IR (neat, ν / cm-1): 2951, 2938, 2855, 2178, 1735 (ester), 1596, 1484, 1203, 1174. HRMS: m/z: $[M + H]^+$ Calcd for $C_{100}H_{136}N_{16}O_{12}Si_4$, 1866.9699, found 1866.9667.

6.5.23 Synthesis of 95

Amino acid **93c** (340 mg, 2.03 mmol) was dissolved in 5 mL methanol and a 1 M solution of LiOH (5 mL) was slowly added to the reaction, the mixture was then stirred for 1 hour. Once complete the reaction was neutralised using a 1 M solution of HCl and dichloromethane (20 mL) was added. The product was then extracted into water (3 x 10 mL) and concentrated under reduced pressure. The residue was then dissolved in methanol, filtered and concentrated *in vacuo* to yield **95** as a brown oil (220 mg, 59%). ^{1}H NMR (500 MHz, CD_3CN) 0.74 – 0.63 (1H, m), 0.90 – 0.79 (2H, m), 1.26 – 1.14 (1H, m), 1.92 (1H, t, *J* = 2.6 Hz), 2.07 – 2.01 (1H, m), 2.50-2.41 (1H, m), 2.95-2.78 (2H, m, *J* = 2.6 Hz), 3.11-2.98 (1H, m). HRMS: m/z: $[M + H]^-$ Calcd for $C_8H_{11}NO_2$, 152.0717, found 152.0718.

6.5.24 Synthesis of 97a

$Cu(SO_4)$ (175 mg, 0.7 mmol) dissolved in 5 mL ethanol:water (1:1) was slowly added to a solution of sodium ascorbate (70 mg, 0.35 mmol) in 5 mL ethanol:water (1:1). A separate vessel was charged with calixarene **74** (69.6 mg, 0.087 mmol) and ferrocenyl methyl azide **96** (45.3 mg, 0.19 mmol) to which was added the copper solution and the reaction mixture was allowed to stir for 1 hour. Dichloromethane (10 mL) was added and the reaction mixture was rapidly stirred overnight. Once complete, as monitored by TLC, the reaction was quenched by the addition of cold water (50 mL), and the product was extracted with dichloromethane (3× 25 mL) and dried over $MgSO_4$. The filtrate was concentrated under reduced pressure, and the residue was purified by flash chromatography (acetone/petroleum ether 1:3) to afford **97a** as a yellow solid (60 mg, 39%) ^{1}H NMR (500 MHz, $CDCl_3$): 1.03 (36H, s), 2.72 (4H, d, *J* = 11.2 Hz), 3.99 (4H, d, *J* = 11.2 Hz), 4.36 – 4.16 (36H, m), 4.90 (8H, s), 5.22 (8H, s), 6.61 (8H, s), 7.61 (4H, s). ^{13}C NMR (125 MHz, $CDCl_3$): 31.45, 31.60, 33.83, 49.89, 66.55, 68.80 - 69.0, 81.94, 123.98,

124.89, 134.07, 144.54, 144.75, 151.95; IR (neat, ν / cm^{-1}): 3094, 2960, 2865, 2243, 1601, 1478, 1462, 1194; HRMS: m/z: $[M + H]^+$ Calcd for $C_{100}H_{109}N_{12}O_4Fe_4$, 1766.6123, found 1766.6096.

6.5.25 Synthesis of 97b

$Cu(SO_4)$ (175 mg, 0.7 mmol) dissolved in 5 mL ethanol:water (1:1) was slowly added to a solution of sodium ascorbate (70 mg, 0.35 mmol) in 5 mL ethanol:water (1:1). A separate vessel was charged with **72** (50 mg, 0.087 mmol) and ferrocenyl methyl azide **96** (45.3 mg, 0.19 mmol) to which the copper solution was slowly added and the reaction mixture was allowed to stir for 1 hour. Dichloromethane (10 mL) was added and the reaction mixture was rapidly stirred overnight. Once complete, as monitored via TLC, the reaction was quenched by the addition of cold water (50 mL), and the product was extracted with dichloromethane (3× 25 mL), and dried over $MgSO_4$. The filtrate was concentrated *in vacuo*, and the residue was purified by flash chromatography (acetone/petroleum ether 1:3) to afford **97b** as a yellow solid (85 mg, 64%). ^{1}H NMR (500 MHz, $CDCl_3$): 2.86 (4H, d, *J* = 13.0 Hz), 4.09 (4H, d, *J* = 13.0 Hz), 4.28 – 4.14 (36H, m), 4.96 (8H, s), 5.19 (8H, s), 6.51 (12H, s), 7.66 (4H, s). ^{13}C NMR (125 MHz, $CDCl_3$): 31.27, 49.90, 66.50, 68.78, 68.87, 68.93, 81.86, 122.56, 123.90, 128.11, 135.30, 144.19, 154.63; IR (neat, ν / cm^{-1}): 3085, 2919, 2243, 1709, 1584, 1457, 1432, 1195; HRMS: m/z: $[M + 2H]^{2+}$ Calcd for $C_{84}H_{78}N_{12}O_4Fe_4$, 771.1834, found 771.1831.

6.6 Electrografting and post surface modification

6.6.1 Formation of GCE surface S4

Calixarene (24 mg, 0.2 mmol) **85** was added to a fresh anhydrous electrochemical cell containing a 10 mL solution of 0.1 M $[n\text{Bu}_4\text{N}][PF_6]$ in acetonitrile. The surface was then modified by potential cycling of the cell five times between 0 V and -1.5 V vs Ag/Ag^+. The electrode surface was thoroughly cleaned by sonication in acetone, dichloromethane and then water, each for five minutes intervals. This yielded surface **S4**.

6.6.2 Post surface modification of modified surface S4

Removal of the TBDMS protecting groups from surface **S4** was conducted by sub-merging the GCE stub in a stirring solution of 1 M TBAF (10 mL) in THF for 14 hours. The electrode was then removed from the solution and cleaned by sonication in acetone, dichloromethane and then water. This yielded modified surface **S5**.

The CuAAC reaction, with the now, unprotected alkynyl groups and ethynyl ferrocene, was conducted by submersion of the stub **S5** in a stirring solution of copper(II) sulfate (50 mg, 0.2 mmol) and sodium ascorbate (20 mg, 0.1 mmol) in 10 mL of 1:1 ethanol:water, to which was

added a solution of **96** (10 mg, 0.05 mmol) in 2 mL dichloromethane. The reaction was performed for 12 hours after which the GCE was then removed from the solution and cleaned by sonication in acetone, dichloromethane, 1 M EDTA and then water to yield modified surface **S6**.

6.6.3 Electrografting of compound 83 onto a GCE to form surface S7

Calixarene **83** (30 mg, 0.04 mmol) was dissolved in an anhydrous electrochemical cell containing 10 mL of a 0.1 M solution of [nBu$_4$][NPF$_6$] in THF. The mixture was cooled to −78 °C and nBuLi (1.6 M in hexanes, 0.2 mL, 0.016 mmol) was added drop wise, the reaction mixture was then stirred for 5 minutes. The surface of the GCE was modified by potential cycling of the cell between 0 V and 2 V before being held at a potential positive of the peak potential for 5 minutes. The electrode was then removed from the electrochemical solution and cleaned by sonication in acetone, dichloromethane and then water to produce modified surface **S7**.

6.6.4 Formation of GCE surface S8

Calixarene **87** (30 mg, 0.04 mmol) was dissolved in an anhydrous electrochemical cell containing 10 mL of a 0.1 M solution of [nBu$_4$][NPF$_6$] in THF. The mixture was cooled to −78 °C. nBuLi (1.6 M in petroleum ether, 0.2 mL, 0.016 mmol) was added drop wise, the reaction mixture was then stirred for 5 minutes. The surface of the GCE was then modified by potential cycling of the cell between 0 V and 2 V before being held at a potential positive of the peak potential for 5 minutes. The electrode was then removed from the electrochemical and cleaned by sonication in acetone, dichloromethane and then water to produce modified surface **S8**.

6.6.5 CuAAC reaction of S8 with ethynyl ferrocene

Ferrocene moieties were added to the exposed azides on the surface of **S8** by using the CuAAC reaction. This was conducted by submerging the modified GCE stub **S8** in a stirring solution of copper(II) sulfate (50 mg, 0.2 mmol) and sodium ascorbate (20 mg, 0.1 mmol) in 10 mL of 1:1 ethanol:water to which was added ethynyl ferrocene (10 mg, 0.05 mmol) dissolved in 2 mL dichloromethane, the reaction was continued for 24 hours. The electrode was then removed from the solution and cleaned by sonication in acetone, dichloromethane, 1 M EDTA and then water to produce modified surface **S9**.

6.6.6 CuAAC reaction of S8 with 91

The fluorine probes, 1-ethynyl-3,5-bis(trifluoromethyl)benzene, were added to the exposed azides on surface of **S8** using the CuAAC reaction. This was conducted by submerging

the modified GCE stub **S8** in a stirring solution of copper(II) sulfate (50 mg, 0.2 mmol) and sodium ascorbate (20 mg, 0.1 mmol) in 10 mL of 1:1 ethanol:water to which was added 1-ethynyl-3,5-bis(trifluoromethyl)benzene **91** (12 mg, 0.05 mmol) dissolved in 2 mL dichloromethane, the reaction was continued for 24 hours. The electrode was then removed from the solution and cleaned by sonication in acetone, dichloromethane, 1 M EDTA and then water to produce modified surface **S10**.

6.6.7 General method for the modification of electrode surface S8 with *N*-alkylated amino acids (93a-c or 95)

Modified GCE **S8** was submerged in a stirring solution of $[(MeCN)_4Cu]PF_6$ (18 mg, 0.05 mmol) and *N*-alkylated amino acid (**93a-c** or **95**) (0.05 mmol) in 5 mL dry acetonitrile, the reaction was continued for 24 hours. The electrode was then removed from the solution and thoroughly cleaned by sonication in acetone, dichloromethane, 1 M EDTA and then water to produce modified surfaces **S11a-d**.

6.7 Electro-synthetic reductions

6.7.1 General procedure

The pro-chiral ketone (0.001 mol) was dissolved in a 10 mL solution of dry DMF containing $[n\text{Bu}_4\text{N}][\text{I}]$ (0.37 g, 0.001 mol). The solution was then saturated with CO_2 and a CV was recorded between -0.4 V and -3 V to determine the potential of the peak current at 100 mV s^{-1}. The solution was then held at this potential for 48 hours while being bubbled with CO_2 and rapidly stirred. The electrode setup used in these systems was comprised of a magnesium ribbon counter electrode, silver reference electrode and either an unmodified GCE or **S11a-d** as the working electrode.

6.7.2 Formation and purification of 104

Once the electrolysis of compound **102a**, using the procedure described in **5.5.2.1**, was complete potassium carbonate (138 mg, 1.0 mmol) and MeI (0.19 ml, 0.4 mmol) were added to the solution which was heated to 60 ^{o}C for 3 hours. The mixture was then concentrated under reduced pressure, dissolved in diethyl ether (25 mL) and washed with water (3x25 mL), before being purified by flash chromatograph (acetone/petroleum ether 1:8) to yield **104** as a pure white solid. ^{1}H NMR (500 MHz, $CDCl_3$): 2.36 (3H, s), 3.86 (3H, s), 4.16 (1H, s), 7.18 – 7.14 (2H, m), 7.37 – 7.28 (5H, m), 7.46 – 7.41 (2H, m). ^{13}C NMR (125 MHz, $CDCl_3$): 21.2, 53.7, 81.1, 127.4, 127.5, 128.1, 128.2, 129.0, 138.0, 139.2, 142.1, 175.2. IR (neat, ν / cm^{-1}): 3513, 3028, 2959, 1716 (ester), 1431, 1255, 1155.

6.7.3 Formation and purification of 107

Once the electrolysis of compound **105**, using the procedure described in **5.5.1**, was complete the solution was concentrated under reduced pressure and the residue was stirred in 50 mL of 1 M HCl for 20 minutes. The product was then extracted into diethyl ether (3x 25 mL) before an alkaline solution of 1 M NaOH (50 mL) was added and the mixture was stirred for 10 minutes. The aqueous layer was then washed with diethyl ether (3x 25 mL) before being acidifed and the product extracted into diethyl ether (3x 25 mL). The solution was then concentrated under reduced pressure and the resulting residue was take up into chloroform (20 mL). The white precipitate that formed was isolated by filtration and then dissolved in DMF (10 mL), to which was added potassium carbonate (138 mg, 1.0 mmol) and MeI (0.19 mL, 0.4 mmol), the mixture was then stirred at 60 °C for 3 hours before being concentrated under reduced pressured and then purified by flash chromatography (acetone/petroleum ether 1:6) to yield **107** as a pure white solid. ^{1}H NMR (500 MHz, $CDCl_3$): 1.89 (3H, s) 3.78 (3H, s), 3.92 (3H, s), 7.12 (1H, d, *J* = 2.5 Hz), 7.16 (1H, dd, *J* = 9.0, 2.5 Hz), 7.61 (1H, dd, *J* = 9.0, 1.8 Hz), 7.74 (2H, t, *J* = 9.0 Hz), 7.95 (1H, d, *J* = 1.8 Hz). ^{13}C NMR (125 MHz, $CDCl_3$): 26.7, 53.4, 55.4, 75.9, 105.5, 119.2, 124.0, 127.1, 128.6, 129.9, 134.1, 137.9, 158.1, 176.3. IR (neat, ν / cm^{-1}): 3455, 2993, 2961, 1736 (ester), 1630, 1604, 1439.

6.7.4 Formation and purification of 113

Once the electrolysis of compound **111**, using the procedure described in **5.5.2.1**, was complete potassium carbonate (138 mg, 1.0 mmol) and MeI (0.19 ml, 0.4 mmol) were added to the solution which was heated to 60 ^{o}C for 3 hours. The mixture was then concentrated under reduced pressure, dissolved in diethyl ether (25 mL) and washed with water (3x25 mL), before being purified by flash chromatograph (acetone/petroleum ether 1:8) to yield **111** as a pure white solid. ^{1}H NMR (500 MHz, $CDCl_3$): 1.77 (3H, s), 3.71 (1H, s), 3.77 (3H, s), 3.80 (3H, s), 6.90 – 6.86 (2H, m), 7.55 – 7.39 (2H, m). ^{13}C NMR (125 MHz, $CDCl_3$): 26.80, 53.34, 55.41, 75.54, 113.80, 126.61, 134.98, 159.34, 176.51. IR (neat, ν / cm^{-1}): 3515, 3011, 2994, 2959, 2835, 1714 (ester), 1507, 1247.

6.7.5 Formation and purification of compounds 110, 114 and 115

Once the electrolysis of compound **108**, using the procedure described in **5.5.2.1**, was complete potassium carbonate (138 mg, 1.0 mmol) and MeI (0.19 ml, 0.4 mmol) were added to the solution which was heated to 60 ^{o}C for 3 hours. The mixture was then concentrated under reduced pressure, dissolved in diethyl ether (25 mL) and washed with water (3x25 mL), before being purified by flash chromatograph (acetone/petroleum ether 1:5).

While using an unmodified GCE compound **110** was isolated as the major product. ^{1}H NMR (500 MHz, $CDCl_3$): 1.79 (3H, s), 3.73 (1H, s), 3.78 (3H, s), 7.32 – 7.28 (1H, m), 7.38 – 7.33 (2H, m), 7.56 – 7.53 (2H, m).

While using modified GCE surface S8c compound **114** was isolated as the major product. ^{1}H NMR (500 MHz, $CDCl_3$): 2.65 (3H, s) 3.95 (3H, s), 3.99 (1H, s), 8.01 (2H, d, *J* = 8.4 Hz), 8.13 (2H, d, *J* = 8.4 Hz); HRMS: m/z: $[M + H]^+$ Calcd for $C_{10}H_{10}O_3$, 178.0630, found 179.0708.

And a small amount of **115** was also detected. ^{1}H NMR (500 MHz, $CDCl_3$): 2.70 (3H, s), 3.99 (6H, s), 8.78 (2H, d, *J* = 1.5 Hz), 8.87 (1H, t, *J* = 1.5 Hz); HRMS: m/z: $[M + H]^+$ Calcd for $C_{12}H_{12}O_5$, 236.0685, found 237.0756.

6.8 X-ray crystallographic data and data collection

Single crystals of **83** were grown by slow evaporation of solvents (petroleum ether and acetone (5:1)); a suitable crystal was selected, encapsulated in a viscous perfluoropolyether and mounted on an Oxford Diffraction Xcaliber-3 single crystal *X*-ray diffractometer using Mo Kα radiation (λ = 0.71073 Å) where the crystal was cooled to 140 K during data collection. The data was reduced and an absorption correction performed using Oxford Diffraction CrysAlisPro.[190] Using WinGX,[191] the structure was solved by Dr David Hughes using ShelXS-97, and then refined with ShelXL version 2014/7.[192,193]

Of the four *O*-alkynyl fragments, one is modeled with a two-component disorder, with 76.5% corresponding to the target *O*-alkynyl fragment; while the remainder is replaced by a simple hydroxyl group and an acetone molecule which occupies the space of the ethyne group. This $–OCH_2CCH$ / $–OH{\cdot}CH_3C(O)CH_3$ alternative grouping is the only site of disorder in the calixarene molecule. An additional molecule of solvent of crystallization (acetone) was also present in the asymmetric unit, although highly disordered.

Single crystals of **92** were grown from a saturated toluene solution at −25 °C; data collection and processing was performed at the UK National Crystallographic Service at the University of Southampton.[194] Using Olex2,[195,196] the structure was solved by Dr Robin J Blagg using ShelXS version 2014/7, and then refined with ShelXL version 2014/7.[193]

Of the eight CF_3 fragments, three were modelled with a two-component rotational disorder about the $F_3C–C$ bond, and for four of them it was necessary to model a two-component disorder for the entire 3,5-$(CF_3)_2C_6H_3$ fragments related by a *pseudo*-rotation about the phenyl−triazole bond.

Two of the four TBDMS groups exhibit large thermal ellipsoids, indicative of disorder / thermal motion, all attempts to model this was unsuccessful – the largest areas on unassigned electron density were all in vicinity of these groups.

While solvent of crystallization (toluene) was clearly present in the unit cell they were heavily disordered and could not be refined; therefore, using the Olex2 solvent masking function the contribution of the disordered solvent (total electron count comparable to *ca.* 3 toluene molecules in the unit cell) was compensated for (analogous to the SQUEEZE function in PLATON). [195, 196, 197]

Table 4: Table of crystallographic data for compounds 83 and 92

	cone-5,11,17,23-tetra-nitro-25,26,27,28-propargylcalix[4]arene **83**	cone-5,11,17,23-tetra-(4-[3,5-bis(trifluoromethyl)benzene]-1H-1,2,3-triazole-1-yl)-25,26,27,28--TBDMS-propargylcalix[4]arene **92**
empirical formula	ca C_{43} H_{35} N_4 $O_{13¼}$	C_{104} H_{100} F_{24} N_{12} O_4 Si_4
formula weight	819.75	2150.31
temperature / K	140(1)	100(2)
crystal system	Monoclinic	triclinic
space group	$P2_1/n$	P-1
a / Å	11.5321(6)	12.2448(2)
b / Å	23.8990(14)	21.1239(3)
c / Å	14.6678(8)	23.5984(5)
α / °	90	80.210(2)
β / °	94.030(4)	80.212(2)
γ / °	90	75.892(2)
volume / $Å^3$	4032.5(4)	5780.6(2)
Z	4	2
ρ_{calc} / $mg.mm^{-3}$	1.350	1.235
μ / mm^{-1}	0.102	0.142
F(000)	1708	2224
crystal size / mm^3	0.40 × 0.17 × 0.035	0.126 × 0.063 × 0.038
radiation	Mo Kα (λ = 0.71073 Å)	Mo Kα (λ = 0.71075 Å)
2Θ range for data collection	5.77 to 43.00 °	3.462 to 50.054°
index ranges	−11 ≤ h ≤ 11, −24 ≤ k ≤ 24, −15 ≤ l ≤ 15	−14 ≤ h ≤ 14, −25 ≤ k ≤ 25, −28 ≤ l ≤ 27
reflections collected	40810	85652
independent reflections	4617 [R_{int} = 0.127, R_{sigma} = 0.0434]	20419 [R_{int} = 0.0489, R_{sigma} = 0.0434]
data / restraints / parameters	4617 / 0 / 589	20419 / 389 / 1644
goodness-of-fit on F^2	1.201	1.063
final R indexes [I≥2σ(I)]	R_1 = 0.0835, wR_2 = 0.1291	R_1 = 0.0931, wR_2 = 0.2613
final R indexes [all data]	R_1 = 0.1139, wR_2 = 0.1395	R_1 = 0.1245, wR_2 = 0.2809
largest diff. peak / hole /$e.A^{-3}$	0.23 / −0.27	0.95 / −1.28

References

References

1 G. Q. Lin, Y. M. Li and A. S. C. Chan, *Principles and Applications of Asymmetric Synthesis.*, John Wiley & Sons Inc, New York, 2002.

2 L. A. Nguyen, H. He and C. Pham-Huy, *Int. J. Biomed. Sci.*, 2006, **2**, 85–100.

3 T. Nagatsu and M. Sawada, *Parkinsonism Related Disorders*, 2009, **15**, S3–S8.

4 K. Lloyd, O. Hornykiewicz, A. K. Lloyd and O. Hornykiewicz, *Science*, 1970, **170**, 1212–1213.

5 H. Blaschko, *J. Physiol.*, 1942, **101**, 337–349.

6 W. Rehman, L. M. Arfons and H. M. Lazarus, *Ther. Adv. Hematol.*, 2011, **2**, 291–308.

7 M. E. Franks, G. R. Macpherson and W. D. Figg, *Lancet*, 2004, **363**, 1802–1811.

8 G. Blaschke, H. H.-P. Kraft and H. Markgraf, *Chem. Ber.*, 1980, **113**, 2318–2322.

9 A. Aitken and S. N. Kilenyi, *Asymmetric Synthesis*, Taylor & Francis, 1992.

10 T. Katsuki and K. B. Sharpless, *J. Am. Chem. Soc.*, 1980, **102**, 5974–5976.

11 M. Kirschner and J.-M. Kassaian, in *Ullmann's Encyclopedia of Industrial Chemistry*, John Wiley & Sons Inc, 2000, vol. 35, pp. 671–678.

12 R. C. Anderson and B. Fraser-Reid, *J. Org. Chem.*, 1985, **50**, 4781–4786.

13 M. M. Heravi, V. Zadsirjan and B. Farajpour, *RSC Adv.*, 2016, **6**, 30498–30551.

14 M. Christmann and S. Bräse, *Asymmetric Synthesis–The Essentials*, Wiley Online Library, 2006.

15 N. H. Anders, *J. Lipid Res.*, 1969, **10**, 316–319.

16 D. Enders and H. Eichenauer, *Angew. Chemie*, 1976, **88**, 579–581.

17 C. Semenza, S. De Pellegrin, I. Battel, M. Garzon, F. Meneghello, V. Chiarelli, E. J. Corey and D. Enders, *Tetrahedron Lett.*, 1976, **17**, 3–6.

18 D. Enders, H. Eichenauer, J. Melorose, R. Perroy and S. Careas, *Tetrahedron Lett.*, 1977, **18**, 191–194.

19 R. R. Peters, D. Enders, A. Job, C. F. Janeck, W. Bettray, R. R. Peters and D. Enders, *Tetrahedron*, 2002, **58**, 2253–2329.

20 D. Enders, G. Bachstädter, K. A. M. Kremer, M. Marsch, K. Harms and G. Boche, *Angew. Chem. Int. Ed.*, 1988, **27**, 1522–1524.

21 M. M. Midland, D. C. McDowell, R. L. Hatch and A. Tramontano, *J. Am. Chem. Soc.*, 1980, **102**, 867–869.

22 M. M. Midland, S. Greer, A. Tramontano and S. A. Zderic, *J. Am. Chem. Soc.*, 1979, **101**, 2352–2355.

23 M. M. Midland, in *Encyclopedia of Reagents for Organic Synthesis*, John Wiley & Sons Ltd, 2001, pp. 9–10.

24 R. Noyori, *Angew. Chem. Int. Ed.*, 2002, **41**, 2008–2022.

25 H. Takaya, K. Mashima, K. Koyano, M. Yagi, H. Kumobayashi, T. Taketomi, S. Akutagawa and R. Noyori, *J. Org. Chem.*, 1986, **51**, 629–635.

26 D. Cai, J. Payack, D. Bender, D. Hughes, T. Verhoeven and P. Reider, *Org. Synth.*, 1999, **76**, 6.

27 M. Kitamura, M. Tokunaga and R. Noyori, *J. Org. Chem.*, 1992, **57**, 4053–4054.

28 T. Ohta, H. Takaya, M. Kitamura, K. Nagai and R. Noyori, *J. Org. Chem.*, 1987, **52**, 3174–3176.

29 R. Noyori, M. Ohta, Y. Hsiao, M. Kitamura, T. Ohta and H. Takaya, *J. Am. Chem. Soc.*, 1986, **108**, 7117–7119.

30 A. G. Doyle and E. N. Jacobsen, *Chem. Rev.*, 2007, **107**, 5713–5743.

31 U. Eder, G. Sauer and R. Wiechert, *Angew. Chem. Int. Ed.*, 1971, **10**, 496–497.

32 Z. G. Hajos and D. R. Parrish, *J. Org. Chem.*, 1974, **39**, 1615–1621.

33 H. Gröger and J. Wilken, *Angew. Chem. Int. Ed.*, 2001, **40**, 529–532.

34 G. M. Whitesides and C.-H. Wong, *Angew. Chem. Int. Ed.*, 1985, **24**, 617–638.

35 W. Boland, C. Frößl, M. Lorenz, D. R. Tobergte and S. Curtis, *Synthesis*, 1991, **12**, 1049–

1072.

36 T. Hudlicky, H. F. Olivo and B. McKibben, *J. Am. Chem. Soc.*, 1994, **116**, 5108–5115.

37 G. Jian-Xin, L. Zu-Yi and L. Guo-Qiang, *Tetrahedron*, 1993, **49**, 5805–5816.

38 Z.-L. Wei, Z.-Y. Li and G.-Q. Lin, *Tetrahedron*, 1998, **54**, 13059–13072.

39 J. Oku and S. Inoue, *J. Chem. Soc. Chem. Commun.*, 1981, **5**, 229–230.

40 A. Mori, H. Ohno, H. Nitta, K. Tanaka, S. Inoue, D. R. Tobergte and S. Curtis, *Synlett*, 1991, **8**, 563–564.

41 K. Narasaka, T. Yamada, H. Minamikawa and C. Letters, *Chem. Lett.*, 1987, **16**, 2073–2076.

42 M. T. Reetz, F. Kunisch, P. Heitmann, J. Melorose, R. Perroy and S. Careas, *Tetrahedron Lett.*, 1986, **27**, 4721–4724.

43 F. Effenberger, T. Ziegler and S. Förster, *Angew. Chem. Int. Ed.*, 1987, **26**, 458–460.

44 N. Klempier, H. Griengl and M. Hayn, *Tetrahedron Lett.*, 1993, **34**, 4769–4772.

45 K. M. Koeller and C.-H. H. Wong, *Nature*, 2001, **409**, 232–240.

46 M. S. Levitt, R. F. Newton, S. M. Roberts and A. J. Willetts, *J. Chem. Soc. Chem. Commun.*, 1990, **8**, 619–620.

47 S. Forster, J. J. Roos, F. Effenberger, H. Wajant, A. Sprauer, S. Förster, J. J. Roos, F. Effenberger, H. Wajant and A. Sprauer, *Angew. Chem. Int. Ed.*, 1996, **35**, 437–439.

48 J. P. Barnier, L. Blanco, G. Rousseau, E. Guibe-Jampel and I. Fresse, *J. Org. Chem.*, 1993, **58**, 1570–1574.

49 K. Nakamura, T. Miyai, Y. Kawai, N. Nakajima and A. Ohno, *Tetrahedron Lett.*, 1990, **31**, 1159–1160.

50 H. Kolbe, *Justus Liebigs Ann. Chem.*, 1848, **64**, 339–341.

51 M. Orsini, M. Feroci, G. Sotgiu and A. Inesi, *Org. Biomol. Chem.*, 2005, **3**, 1202–1208.

52 M. Rafiee, *Synlett*, 2007, **3**, 503–504.

53 L. Horner and D. Degner, *Tetrahedron Lett.*, 1968, **9**, 5889–5892.

54 D. Seebach and H. A. Oei, *Angew. Chem. Int. Ed.*, 1975, **14**, 634–636.

55 S. Zhao, M. Horne, A. M. Bond and J. Zhang, *Green Chem.*, 2014, **16**, 2242–2251.

56 B.-L. Chen, Y. Xiao, X.-M. Xu, H.-P. Yang, H. Wang and J.-X. Lu, *Electrochim. Acta*, 2013, **107**, 320–326.

57 K. Zhang, H. Wang, S.-F. F. Zhao, D.-F. F. Niu and J.-X. X. Lu, *J. Electroanal. Chem.*, 2009, **630**, 35–41.

58 S. F. Zhao, M. X. Zhu, K. Zhang, H. Wang and J. X. Lu, *Tetrahedron Lett.*, 2011, **52**, 2702–2705.

59 A. K. Yadav and A. Singh, *Bull. Chem. Soc. Jpn.*, 2002, **75**, 587–588.

60 A. K. Yadav, M. Manju and P. R. Chhinpa, *Tetrahedron Asymmetry*, 2003, **14**, 1079–1081.

61 E. Kariv, H. A. Terni and E. Gileadi, *Electrochim. Acta*, 1973, **18**, 433–441.

62 N. Schoo and H.-J. Schäfer, *Liebigs Ann. Chem.*, 1993, **6**, 601–607.

63 M. Feroci, A. Inesi, M. Orsini and L. Palombi, *Org. Lett.*, 2002, **4**, 2617–2620.

64 T. H. Yan, C. W. Tan, H. C. Lee, H. C. Lo and T. Y. Huang, *J. Am. Chem. Soc.*, 1993, **115**, 2613–2621.

65 M. Feroci, M. Orsini, L. Palombi, G. Sotgiu, M. Colapietro and A. Inesi, *J. Org. Chem.*, 2004, **69**, 487–494.

66 M. M. Heravi and V. Zadsirjan, *Tetrahedron Asymmetry*, 2014, **25**, 1061–1090.

67 A. Deronzier and J. C. Moutet, *Coord. Chem. Rev.*, 1996, **147**, 339–371.

68 T. Nonaka, T. Fuchigami and S. Abe, *Chem. Lett.*, 1983, 1033–1036.

69 J. Kopilov, E. Kariv and L. L. Miller, *J. Am. Chem. Soc.*, 1977, **99**, 3450–3454.

70 B. F. Watkins, J. R. Behling, E. Kariv and L. L. Miller, *J. Am. Chem. Soc.*, 1975, **97**, 3549–3550.

71 S. Pleus and M. Schwientek, *Synth. Commun.*, 1997, **27**, 2917–2930.

72 M. Schwientek, S. Pleus and C. H. Hamann, *J. Electroanal. Chem.*, 1999, **461**, 94–101.

73 M. Salmon, *J. Electrochem. Soc*, 1985, **132**, 1897–1899.

74 J.-C. Moutet, L. Y. Cho, C. Duboc-Toia, S. Menage, E. C. Riesgo and R. P. Thummel, *New J. Chem.*, 1999, **23**, 939–944.

75 S. Chardon-Noblat, I. M. F. de Oliveira, J. Moutet and S. Tingry, *J. Mol. Catal. A Chem.*, 1995, **99**, 13–21.

76 J. Moutet, C. Duboc-Toia, S. Ménage and S. Tingry, *Adv. Mater.*, 1998, **10**, 665–667.

77 M. Fujihira, A. Yokozawa, H. Kinoshita and T. Osa, *Chem. Lett.*, 1982, **11**, 1089–1092.

78 J.-N. Rebilly and O. Reinaud, *Supramol. Chem.*, 2014, **26**, 454–479.

79 R. Cacciapaglia, S. Di Stefano, L. Mandolini and R. Salvio, *Supramol. Chem.*, 2013, **25**, 537–554.

80 A. Baeyer, *Berichte der Dtsch. Chem. Gesellschaft*, 1872, **5**, 280–282.

81 P. Tome and A. Baeyer, *Berichte der Dtsch. Chem. Gesellschaft*, 1872, **5**, 1094–1100.

82 L. Lederer, *J. für Prakt. Chemie*, 1894, **50**, 223–226.

83 O. Manasse, *Berichte der Dtsch. Chem. Gesellschaft*, 1894, **27**, 2409–2413.

84 J. H. Freeman, B. S. Hunter, P. Ritchie and E. J. Kingsley, *J. Appl. Polym. Sci.*, 1969, **13**, 1323–1324.

85 L. Baekeland, US Patent 942699, 1909.

86 C. D. Gutsche, *Calixarenes*, The Royal Society of Chemistry, 2008.

87 A. Zinke and E. Ziegler, *Berichte der Dtsch. Chem. Gesellschaft*, 1941, **74**, 1729.

88 A. Zinke and E. Ziegler, *Berichte der Dtsch. Chem. Gesellschaft*, 1944, **77**, 264–272.

89 A. Zinke, R. Kretz, E. Leggewie, K. Hössinger, G. Hoffmann, P. Weber v. Ostwalden, E. Wiesenberger and M. Sobotka, *Monatshefte für Chemie und verwandte Teile anderer Wissenschaften*, 1952, **83**, 1213–1227.

90 B. T. Hayes and R. F. Hunter, *J. Appl. Chem.*, 1958, **8**, 743–748.

91 C. D. Gutsche and R. Muthukrishnan, *J. Org. Chem.*, 1978, **43**, 4905–4906.

92 J. W. Cornforth, P. D'Arcy Hart, G. A. Nicholls, R. J. W. Rees and J. A. Stock, *Brit. J. Pharmacol.*, 1955, **10**, 73–86.

93 C. D. Gutsche, I. Muzaffer and D. Stewart, *J. Org. Chem.*, 1986, **1**, 742–745.

94 C. D. Gutsche, B. Dhawan, K. H. No and R. Muthukrishnan, *J. Am. Chem. Soc.*, 1981, **103**, 3782–3792.

95 D. R. Stewart and C. D. Gutsche, *Org. Prep. Proced. Int.*, 1993, **25**, 137–139.

96 M. Ferchichi, E. Jeanneau, J.-C. Sollier, F. Meganem, U. Darbost and I. Bonnamour, *CheM*, 2011, **1**, 27–35.

97 C. D. Gutsche, J. S. Rogers, D. Stewart and K.-A. See, *Pure Appl. Chem.*, 1990, **62**, 485–491.

98 F. Ullmann and K. Brittner, *Berichte der Dtsch. Chem. Gesellschaft*, 1909, **42**, 2539–2548.

99 C. D. Gutsche, *Acc. Chem. Res.*, 1983, **16**, 161–170.

100 C. D. Gutsche, B. Dhawan, J. A. Levine, K. Hyun No and L. J. Bauer, *Tetrahedron*, 1983, **39**, 409–426.

101 T. Harada, F. Ohseto and S. Shinkai, *Tetrahedron*, 1994, **50**, 13377–13394.

102 K. Iwamoto and S. Shinkai, *J. Org. Chem.*, 1992, **57**, 7066–7073.

103 A. Arduini, E. Ghidini, A. Pochini, R. Ungaro, G. D. Andreetti, G. Calestani and F. Ugozzoli, *J. Incl. Phenom.*, 1988, **6**, 119–134.

104 K. Iwamoto, K. Fujimoto, T. Matsuda and S. Shinkai, *Tetrahedron Lett.*, 1990, **31**, 7169–7172.

105 M. Coruzzi, G. D. Andreetti, V. Bocchi, A. Pochini and R. Ungaro, *J. Chem. Soc. Perkin Trans. 2*, 1982, **53**, 1133–1138.

106 C. D. Gutsche, B. Dhawan, K. H. No and R. Muthukrishnan, *J. Am. Chem. Soc.*, 1981, **103**, 3782–3792.

107 Y. Aoyama, Y. Tanaka, H. Toi and H. Ogoshi, *J. Am. Chem. Soc.*, 1988, **110**, 634–635.

108 F. R. P. Crisóstomo, A. Lledó, S. R. Shenoy, T. Iwasawa and J. Rebek, *J. Am. Chem. Soc.*, 2009, **131**, 7402–7410.

109 S. R. Shenoy, F. R. P. Crisóstomo, T. Iwasawa and J. Rebek, *J. Am. Chem. Soc.*, 2008, **130**, 5658–5659.

110 V. K. Gupta, R. Ludwig and S. Agarwal, *Anal. Chim. Acta*, 2005, **538**, 213–218.

111 G. McMahon, S. O. Malley, K. Nolan and D. Diamond, *Arkivoc*, 2003, **7**, 23–31.

112 D. Diamond and K. Nolan, *Anal. Chem.*, 2001, **73**, 22 A-29 A.

113 D. Diamond and M. A. McKervey, *Chem. Soc. Rev.*, 1996, **25**, 15–24.

114 S. Y. Li, Y. W. Xu, J. M. Liu and C. Y. Su, *Int. J. Mol. Sci.*, 2011, **12**, 429–455.

115 S. Shirakawa and S. Shimizu, *New J. Chem.*, 2010, **34**, 1217–1222.

116 P. R. Moses, L. Wier and R. W. Murray, *Anal. Chem.*, 1975, **47**, 1882–1886.

117 K. D. Snell and A. G. Keenan, *Chem. Soc. Rev.*, 1979, **8**, 259–282.

118 P. Abiman, G. G. Wildgoose and R. G. Compton, *Int. J. Electrochem. Sci.*, 2008, **3**, 104–117.

119 R. Jiang and S. Dong, *J. Electroanal. Chem.*, 1988, **246**, 101–117.

120 A. Eftekhari, *Talanta*, 2001, **55**, 395–402.

121 M. Boopathi, M. S. Won and Y. B. Shim, *Anal. Chim. Acta*, 2004, **512**, 191–197.

122 J. Papillon, E. Schulz, S. Gélinas, J. Lessard and M. Lemaire, *Synthetic Metals*, 1998, **96**, 155–160.

123 M. Vago, F. J. Williams and E. J. Calvo, *Electrochem. Commun.*, 2007, **9**, 2725–2728.

124 E. George, US Patent 3242059A, 1966.

125 T. F. O'Brien, T. V Bommaraju and F. Hine, *Handbook of Chlor-Alkali Technology*, Springer Science & Business Media, 2007.

126 Euro Chlor, http://www.eurochlor.org/the-chlorine-universe/how-is-chlorine-produced/the-membrane-cell-process.aspx, (acessed September 2016).

127 G. Gritzner and J. Kůta, *Electrochim. Acta*, 1984, **29**, 869–873.

128 R. G. Compton and C. E. Banks, *Understanding Voltammetry*, Imperial College Press, London, 2011.

129 A. Casnati, F. Sansone and R. Ungaro, *Acc. Chem. Res.*, 2003, **36**, 246–254.

130 N. Pirrincioglu, F. Zaman and A. Williams, *J. Chem. Soc. Perkin Trans. 2*, 1996, **1**, 2561–2562.

131 J. P. Buttress, D. P. Day, J. M. Courtney, E. J. Lawrence, D. L. Hughes, R. J. Blagg, A. Crossley, S. E. Matthews, C. Redshaw, P. C. Bulman Page and G. G. Wildgoose, *Langmuir*, 2016, **32**, 7806–7813.

132 A. Mattiuzzi, I. Jabin, C. Mangeney, C. Roux, O. Reinaud, L. Santos, J.-F. Bergamini, P. Hapiot and C. Lagrost, *Nat. Commun.*, 2012, **3**, 1130–1138.

133 M. V Sheridan, K. Lam and W. E. Geiger, *Angew. Chem. Int. Ed.*, 2013, **52**, 12897–12900.

134 A. Zinke and E. Ziegler, *Berichte der Dtsch. Chem. Gesellschaft*, 1941, **74**, 1729–1736.

135 C. D. Gutsche and M. Iqbal, *Org. Synth.*, 1990, **68**, 234–235.

136 C. D. Gutsche and J. A. J. Levine, *J. Am. Chem. Soc.*, 1982, **104**, 2652–2653.

137 C. D. Gutsche, M. Iqbal, K. S. Nam, K. See and I. Alam, *Pure Appl. Chem.*, 1988, **60**, 483–488.

138 M. V Sheridan, K. Lam and W. E. Geiger, *J. Am. Chem. Soc.*, 2013, **135**, 2939–2942.

139 S. Shinkai, K. Araki, T. Tsubaki, T. Arimura and O. Manabe, *J. Chem. Soc. Perkin Trans. 1*, 1987, 2297–2299.

140 C. D. Gutsche and K. C. Nam, *J. Am. Chem. Soc.*, 1988, **110**, 6153–6162.

141 S. K. Sharma, S. Kanamathareddy, C. D. Gutsche and A. G. Fallis, *Synthesis*, 1997, **11**, 1268–1272.

142 J. C. Duff and E. J. Bills, *J. Chem. Soc.*, 1932, 1987–1988.

143 G. Dyker, M. Mastalerz and I. M. Müller, *Eur. J. Org. Chem*, 2005, **17**, 3801–3812.

144 D. N. Reinhoudt, W. Verboom, A. Durie, R. J. M. Egberink and Z. Asfari, *J. Org. Chem.*,

1992, **57**, 1313–1316.

145 F. Bernardi, F. Cacace, G. de Petris, F. Pepi, I. Rossi, A. Troiani, de Petris G, F. Pepi, I. Rossi and A. Troiani, *Chem. – A Eur. J.*, 2000, **6**, 537–544.

146 V. Bocchi, D. Foina, A. Pochini, R. Ungaro and G. D. Andreetti, *Tetrahedron*, 1982, **38**, 373–378.

147 F. D. Bellamy and K. Ou, *Tetrahedron Lett.*, 1984, **25**, 839–842.

148 H. C. Kolb, M. G. Finn and K. B. Sharpless, *Angew. Chem. Int. Ed.*, 2001, **40**, 2004–2021.

149 J. H. Cho and B. M. Kim, *Tetrahedron Lett.*, 2002, **43**, 1273–1276.

150 A. G. Jarvis, A. C. Whitwood and I. J. S. Fairlamb, *Dalton Trans.*, 2011, **40**, 3695–3702.

151 M. Deiamar, R. Hitmi, J. Pinson and J. M. Saveant, *J. Am. Chem. Soc.*, 1992, **114**, 5884–5886.

152 C. Lagrost, J.-M. Noël, B. Sjöberg, R. Marsac, D. Zigah, J.-F. Bergamini, A. Wang, S. Rigaut and P. Hapiot, *Langmuir*, 2009, **25**, 12742–12749.

153 M. Pandurangappat, N. S. Lawrence and R. G. Compton, *Analyst*, 2002, **127**, 1568–1571.

154 D. R. Laws, J. Sheats, A. L. Rheingold and W. E. Geiger, *Langmuir*, 2010, **26**, 15010–15021.

155 Y. R. Leroux and P. Hapiot, *Chem. Mater.*, 2013, **25**, 489–495.

156 S. Y. Sayed, A. Bayat, M. Kondratenko, Y. Leroux, P. Hapiot and R. L. McCreery, *J. Am. Chem. Soc.*, 2013, **135**, 12972–12975.

157 J. E. B. Randles, *Trans. Faraday Soc.*, 1948, **44**, 327–338.

158 A. Sevcik, *Collect. Czech. Chem. Commun*, 1948, **13**, 349–377.

159 E. W. Weisstein, in *CRC Concise Encyclopedia of Mathematics*, Chapman & Hall/CRC, Boca Raton, 2003, pp. 430–431.

160 J. Klimentová and P. Vojtíšek, *J. Mol. Struct.*, 2007, **826**, 48–63.

161 G. G. Wildgoose, S. J. Wilkins, G. R. Williams, R. R. France, D. L. Carnahan, L. Jiang, T. G. J. Jones and R. G. Compton, *ChemPhysChem.*, 2005, **6**, 352–362.

162 B. Ortiz, C. Saby, G. Y. Y. Champagne and D. Bélanger, *J. Electroanal. Chem.*, 1998, **455**, 75–81.

163 C. G. R. Heald, G. G. Wildgoose, L. Jiang, T. G. J. Jones and R. G. Compton, *ChemPhysChem.*, 2004, **5**, 1794–1799.

164 D. P. Cormode, A. J. Evans, J. J. Davis and P. D. Beer, *Dalton Trans.*, 2010, **39**, 6532–6541.

165 J. P. Collman, N. K. Devaraj, T. P. A. Eberspacher and C. E. D. Chidsey, *Langmuir*, 2006, **22**, 2457–2464.

166 National Institute of Standards and Technology (NIST), http://srdata.nist.gov/xps/, (accessed October 2015).

167 A. S. C. Chan, T. T. Huang, J. H. Wagenknecht and R. E. Miller, *J. Org. Chem.*, 1995, **60**, 742–744.

168 R. Matthessen, J. Fransaer, K. Binnemans and D. E. De Vos, *Beilstein J. Org. Chem.*, 2014, **10**, 2484–2500.

169 S. F. Zhao, H. Wang, Y. C. Lan, X. Liu, J. X. Lu and J. Zhang, *J. Electroanal. Chem.*, 2012, **664**, 105–110.

170 O. Scialdone, C. Amatore, A. Galia and G. Filardo, *J. Electroanal. Chem.*, 2006, **592**, 163–174.

171 S. F. Zhao, M. Horne, A. M. Bonda and J. Zhang, *Phys. Chem. Chem. Phys.*, 2015, **17**, 19247–19254.

172 O. Scialdone, M. A. Sabatino, C. Belfiore, A. Galia, M. P. Paternostro and G. Filardo, *Electrochim. Acta*, 2006, **51**, 3500–3505.

173 C. Maugeri, M. A. Alisi, C. Apicella, L. Cellai, P. Dragone, E. Fioravanzo, S. Florio, G. Furlotti, G. Mangano, R. Ombrato, R. Luisi, R. Pompei, V. Rincicotti, V. Russo, M. Vitiello and N. Cazzolla, *Bioorg. Med. Chem.*, 2008, **16**, 3091–3107.

174 X. Ma and S. B. Herzon, *J. Org. Chem.*, 2016, **81**, 8673–8695.

175 S. Shirakawa, A. Moriyama and S. Shimizu, *Eur. J. Org. Chem*, 2008, **2008**, 5957–5964.

176 F. D'Souza, Y.-Y. Hsieh, H. Wickman and W. Kutner, *Electroanalysis*, 1997, **9**, 1093–1101.

177 a Ferancová and J. Labuda, *Fresenius J. Anal. Chem.*, 2001, **370**, 1–10.

178 W. Li, G. Jin, H. Chen and J. Kong, *Talanta*, 2009, **78**, 717–722.

179 F. Zhang, S. Gu, Y. Ding, Z. Zhang and L. Li, *Anal. Chim. Acta*, 2013, **770**, 53–61.

180 A. Ferancová, E. Korgová, J. Labudaa, J. Zima and J. Barek, *Electroanalysis*, 2002, **14**, 1668–1673.

181 A. Ferancová, E. Korgová, T. Buzinkaiová, W. Kutner, I. Štěpánek and J. Labuda, *Anal. Chim. Acta*, 2001, **447**, 47–54.

182 J. M. P. J. Garrido, V. Rahemi, F. Borges, C. M. A. Brett and E. M. P. J. Garrido, *Food Control*, 2016, **60**, 70–11.

183 Y. Wang, H. Chen, Y. Xiao, C. H. Ng, T. S. Oh, T. T. Y. Tan and S. C. Ng, *Nat. Protoc.*, 2011, **6**, 935–942.

184 F. Macaev and V. Boldescu, *Symmetry*, 2015, **7**, 1699–1720.

185 W. Zhao and Q. Zhong, *J. Incl. Phenom. Macrocycl. Chem.*, 2012, **72**, 1–14.

186 K. Kanagaraj and K. Pitchumani, *J. Org. Chem.*, 2013, **78**, 744–751.

187 L. Yong, *Chinese Chem. Lett.*, 2004, **15**, 400.

188 S. Simaan and S. E. Biali, *J. Org. Chem*, 2003, **68**, 3634–3639.

189 M. J. Chetcuti, A. M. J. Devoille, A. B. Othman, R. Souane, P. Thuéry and J. Vicens, *Dalton Trans.*, 2009, **16**, 2999–3008.

190 *CrysAlisPro, Oxford Diffraction /Agilent Technologies, Yarnton*, U.K.

191 L. J. Farrugia, *J. Appl. Crystallogr.*, 2012, **45**, 849–854.

192 G. M. Sheldrick, *Acta Crystallogr. Sect. A*, 2008, **64**, 112–122.

193 G. M. Sheldrick, *Acta Crystallogr. Sect. C*, 2015, **71**, 3–8.

194 S. J. Coles and P. A. Gale, *Chem. Sci.*, 2012, **3**, 683–689.

195 O. V. Dolomanov, L. J. Bourhis, R. J. Gildea, J. A. K. Howard and H. Puschmann, *J. Appl.*

Crystallogr., 2009, **42**, 339–341.

196 L. J. Bourhis, O. V. Dolomanov, R. J. Gildea, J. A. K. Howard and H. Puschmann, *Acta Crystallogr. Sect. A Found. Adv.*, 2015, **71**, 59–75.

197 A. L. Spek, *Acta Crystallogr. Sect. C*, 2015, **71**, 9–18.